

**U.S. DEPARTMENT OF COMMERCE
National Technical Information Service**

AD-A032 478

THE GENERATION AND RADIATION OF SUPERSONIC
JET NOISE
VOLUME I. SUMMARY

LOCKHEED-GEORGIA COMPANY, MARIETTA

SEPTEMBER 1976

AD A 032478

335113
AFAPL-TR-76-65
VOLUME I

~~12~~
NW

**THE GENERATION AND RADIATION OF SUPERSONIC JET
NOISE
VOLUME I SUMMARY**

**LOCKHEED-GEORGIA COMPANY
MARIETTA, GEORGIA 30063**

SEPTEMBER 1976

**TECHNICAL REPORT AFAPL-TR-76-65
FINAL REPORT FOR PERIOD 6 NOVEMBER 1972 - 6 NOVEMBER 1975**

Approved for public release; distribution u. limited

**DEPARTMENT OF TRANSPORTATION
OFFICE OF NOISE ABATEMENT
WASHINGTON, D.C.**

**AIR FORCE AERO-PROPULSION LABORATORY
AIR FORCE WRIGHT AERONAUTICAL LABORATORIES
AIR FORCE SYSTEMS COMMAND
WRIGHT PATTERSON AIR FORCE BASE, OHIO 45433**

REPRODUCED BY
**NATIONAL TECHNICAL
INFORMATION SERVICE**
U. S. DEPARTMENT OF COMMERCE

W
DDC
RECEIVED
NOV 24 1976
REGISTRY
A

NOTICE

When Government drawings, specifications, or other data are used for any purpose other than in connection with a definitely related Government procurement operation, the United States Government thereby incurs no responsibility nor any obligation whatsoever; and the fact that the Government may have formulated, furnished, or in any way supplied the said drawings, specifications, or other data, is not to be regarded by implication or otherwise as in any manner licensing the holder or any other person or corporation, or conveying any rights or permission to manufacture, use, or sell any patented invention that may in any way be related thereto.

This final report was prepared by the Lockheed-Georgia Company, Marietta, Georgia, under Contract F33615-73-C-2032. The effort was sponsored by the Air Force Aero-Propulsion Laboratory, Air Force Systems Command, Wright-Patterson AFB, Ohio and the Department of Transportation under Project 3066, Task 14, and Work Unit 08 with Mr. Paul A. Shahady (AFAPL/TBC) as Project Engineer. Dr. Gordon Banerian was the Project Manager for the Department of Transportation. Dr. Harry E. Plumblee of Lockheed-Georgia was technically responsible for the work.

This report has been reviewed by the Information Office, ASD/OIP, and releasable to the National Technical Information Service (NTIS). At NTIS, it will be available to the general public, including foreign nations.

This technical report has been reviewed and is approved for publication.


PAUL A. SHAHADY
Project Engineer
USAF


DR. GORDON BANERIAN
Project Manager
Department of Transportation

FOR THE COMMANDER


ROBERT E. HENDERSON
Manager, Combustion Technical Area

Copies of this report should not be returned unless return is required by security considerations, contractual obligations, or notice on a specific document.

UNCLASSIFIED

SECURITY CLASSIFICATION OF THIS PAGE (When Data Entered)

REPORT DOCUMENTATION PAGE		READ INSTRUCTIONS BEFORE COMPLETING FORM
1. REPORT NUMBER AFAPL-TR-76-65-Vol I ✓	2. GOVT ACCESSION NO.	3. RECIPIENT'S CATALOG NUMBER
4. TITLE (and Subtitle) THE GENERATION AND RADIATION OF SUPERSONIC JET NOISE. Volume I, Summary	5. TYPE OF REPORT & PERIOD COVERED FINAL TECHNICAL REPORT ✓ 6 NOV 72 - 6 NOV 75	
	6. PERFORMING ORG. REPORT NUMBER LG76ER0133 ✓	
7. AUTHOR(s) Harry E. Plumblee, Jr.	8. CONTRACT OR GRANT NUMBER(s) Contract F33615-73-C-2032 ✓	
9. PERFORMING ORGANIZATION NAME AND ADDRESS Lockheed-Georgia Company ✓ Marietta GA 30063	10. PROGRAM ELEMENT, PROJECT, TASK AREA & WORK UNIT NUMBERS PE 62203F, Proj 3066, Task 14, Work Unit 08	
11. CONTROLLING OFFICE NAME AND ADDRESS Air Force Aero-Propulsion Laboratory/TBC Wright-Patterson AFB OH 45433	12. REPORT DATE September 1976	
	13. NUMBER OF PAGES 129	
14. MONITORING AGENCY NAME & ADDRESS (if different from Controlling Office)	15. SECURITY CLASS. (of this report) Unclassified	
	15a. DECLASSIFICATION/DOWNGRADING SCHEDULE	
16. DISTRIBUTION STATEMENT (of this Report) Approved for Public Release; Distribution Unlimited.		
17. DISTRIBUTION STATEMENT (of the abstract entered in Block 20, if different from Report)		
18. SUPPLEMENTARY NOTES		
19. KEY WORDS (Continue on reverse side if necessary and identify by block number) Acoustics, Turbulence, Jet Noise, Laser Velocimetry, Supersonic Jets, Shock Noise		
20. ABSTRACT (Continue on reverse side if necessary and identify by block number) This report is published in four volumes. Volume I (this volume) summarizes the work accomplished. Volume II contains a detailed discussion of work accomplished since the publication of the interim report, and all the major conclusions reached during the program. Volume III is a data report which presents a detailed compilation of the turbulent mixing noise 1/3-octave spectra. Volume IV, another data report, contains the narrow-band spectra for broadband shock-associated noise.		

UNCLASSIFIED

SECURITY CLASSIFICATION OF THIS PAGE (When Data Entered)

UNCLASSIFIED

SECURITY CLASSIFICATION OF THIS PAGE (When Data Entered)

This volume contains a summary of all the work accomplished in the Phase II, Detailed Investigation, Contract No. F33615-73-C-2032, as well as a summary of items in the Phase I, Exploratory Program, Contract No. F33615-71-C-1663. There are three main sections. The first summarizes the problems with existing theories at the time the Phase I contract was initiated. The second outlines the criteria for a unified self-consistent theory of aerodynamic noise generation, and presents a brief derivation of Lilley's equation which is the basis for the theoretical studies in jet noise generation and radiation in the Phase II program. The third section summarizes the work accomplished in the Phase II contract. It covers turbulent mixing noise experiments; Lilley theory, numerical solutions, and comparisons with experiment; shock-associated noise experiments and comparison with Harper-Bourne-Fisher theory; large-scale turbulent structure and far-field noise theory; LV design and data comparisons with hot-wire results; and velocity measurements in supersonic jets, including comparison of noise scaling based on turbulence measurements, with 90° noise measurements.

ACCESSION BY	
NTIS	NTIS Section <input checked="" type="checkbox"/>
DDI	DDI Section <input type="checkbox"/>
UNANNOUNCED	<input type="checkbox"/>
JUSTIFICATION	
BY	
DISTRIBUTION/AVAILABILITY STATEMENT	
Doc.	Avail. and/or Sale
A	

UNCLASSIFIED

SECURITY CLASSIFICATION OF THIS PAGE (When Data Entered)

PREFACE

This report was prepared by the Lockheed-Georgia Company, Marietta, Georgia, for the Air Force Aero Propulsion Laboratory, Wright-Patterson Air Force Base under Contract F33615-73-C-2032. The report covers work done in the period 6 November 1972 through 6 November 1975. The work described herein is part of the Air Force Aero Propulsion Laboratory's joint program with the Department of Transportation to define and control the noise emission of aircraft propulsion systems.

Mr. Paul Shahady was the Air Force Aero Propulsion Laboratory's Project Engineer. The program is being conducted under Project 3066, Task 14. Dr. Gordon Banerian was the Project Manager for the Department of Transportation. Lockheed's Program Manager was Harry E. Plumblee, Jr.

Major contributors to the work performed under this contract and presented in this series of reports are: Robert H. Burrin, Peter D. Dean, Philip E. Doak, Michael J. Fisher, Sham S. Kapur, Jark C. Lau, Geoffrey M. Lilley, William T. Mayo, Donald M. Meadows, Christopher L. Morfey, Philip J. Morris, David M. Smith, H. K. "Bob" Tanna, Brian J. Tester, and M. Clay Whiffen.

The assistance of the following individuals is gratefully acknowledged: C. Benton Reid, who operated the test facilities and data acquisition systems; Edward C. Mills, who did the electronic design for the laser velocimeter circuitry discussed in this report; J. P. McKenna, who kept up with the budget and other administrative details; and last, but certainly not least, most gracious appreciation is extended to Barbara C. Reagan for her superb typing of all the manuscripts.

Gratitude is expressed to the University of Southampton for permitting Professor Philip E. Doak, Professor Geoffrey M. Lilley, Dr. Michael J. Fisher, and Dr. Christopher L. Morfey to participate in the performance of the research reported herein.

The author of this volume expresses sincere appreciation to all the individuals referred to above for helpful discussions during the writing of this summary volume. Also, special acknowledgement is due Robert H. Burrin for his assistance in assembling all the illustrations included in Volume I.

This report was submitted on 23 June 1976.

Publication of this report does not constitute Air Force approval of the report's findings or conclusions. It is published only for the exchange and stimulation of ideas.

CONTENTS

	<u>Page</u>
1 INTRODUCTION	1
2. REVIEW OF PREVIOUS WORK	4
2.1 Experimental Assessment of Lighthill's Formula for Isothermal Jet Noise	4
2.1.1 Practical Application of Lighthill Theory	4
2.1.2 The Analysis Method by Lush	6
2.2 Comments on Major Aerodynamic and Jet Noise Theories Available in 1972	13
2.2.1 Lighthill's Theory and Dimensional Analysis	15
2.2.2 Ribner's Contribution to Jet Noise Theory	19
2.2.3 Phillips' Theory	20
2.2.4 Conclusions of Critique of Analog Theories and Phillips' Theory and Requirements for a Consistent Theory of Jet Noise	21
3. THEORETICAL DEVELOPMENTS IN JET NOISE	23
3.1 Doak's Unified Theory of Aerodynamic Noise Generation	23
3.2 Lilley's Equation	28
4. SUMMARY OF RESULTS	30
4.1 Experimental Program	31
4.1.1 Jet Noise Experiments	31
4.1.2 Jet Flow Experiments	57
4.2 Turbulent Mixing Noise Theory and Comparison with Experiment	63
4.2.1 Monopole Source Solutions	64
4.2.2 Jet Noise Source Solutions	66
4.2.3 Lilley Data-Theory Comparison	67
4.3 Theory for Noise from Large-Scale Turbulent Structure	77
4.3.1 Method of Approach	81
4.3.2 The Turbulence Model	81
4.3.3 The Radiation Model	84
4.4 Shock-Associated Noise Theory	88
5. CONCLUSIONS	95
APPENDIX I - ANECHOIC JET NOISE TEST FACILITY CALIBRATION	99
APPENDIX II - THE LOCKHEED LASER VELOCIMETER	111
APPENDIX III - COMPARISON OF LV AND HOT-WIRE DATA	117
APPENDIX IV - LV-MICROPHONE AND LV-LV CORRELATION	123
REFERENCES	133

1. INTRODUCTION

The fundamentals of jet noise generation have been studied in great detail over the past twenty-five years. Lighthill's early work identified the basic jet noise generating mechanisms and provided the foundation for the numerous studies that followed. Much of the research following Lighthill's early work advanced the understanding of the jet noise generation process. However, in 1970, it was still not possible to theoretically (or even empirically) predict the complete characteristics of the noise field of a heated, supersonic jet, with even a faint degree of confidence. With the almost certain, even though delayed, introduction of supersonic passenger aircraft and the equally certain regulatory action against excessive noise from these aircraft, it appeared necessary to the U. S. Department of Transportation (DOT) and the USAF Aero Propulsion Laboratory (APL) that the noise generation and radiation mechanisms of supersonic jets must be better understood. In order to promote this understanding, a series of fundamental research contracts was initiated in mid-1971. These contracts were jointly funded by the DOT and the AF.

As a means of clarifying the history of this series of research investigations, a flow chart identifying the various contracts and technical publications which describe the contract results is shown in Figure 1.1. In the first phase of the AF/DOT program, three contractors participated in a problem definition study and state-of-the-art assessment. Lockheed's program produced a six-volume final report that included (i) a critical review of current jet noise theories, (ii) a description of Lilley's theory for jet noise generation, (iii) a set of detailed supersonic jet noise measurements over a limited temperature range to show both effects of temperature and quantitative deviations of existing theory from measurement, and (iv) an assessment of optical measurement techniques for establishing the flow characteristics in the free jet.

At the end of the Phase I program, contracts were established with Lockheed and G.E. to enter into a detailed program of fundamental theoretical and experimental studies of jet noise generating mechanisms and jet turbulence. During this Phase II program, in addition to a series of five oral briefings to interested governmental, university, and industrial observers, a number of publications and technical papers were produced which described progress in Lockheed's program of supersonic jet noise studies. This current report is part of a four-volume final report and serves as an overview summary of the significant findings from both Phase I and Phase II studies.

As a matter of current interest, immediately following the Phase II contract, Lockheed has begun a third program, with the goal of fitting all the results derived in the first two programs into a rather complete fundamental jet noise prediction analysis and associated computer programs.

In this volume of the Phase II final report, a summary of relevant results produced during the first two contracts will be given, with major emphasis on the Phase II results. However, the justifications produced during the Phase I program relevant to the problems with the Lighthill analogy theory and the requirements for an adequate theory for describing jet noise generation and radiation, as well as a derivation of the Lilley theory will also be included.

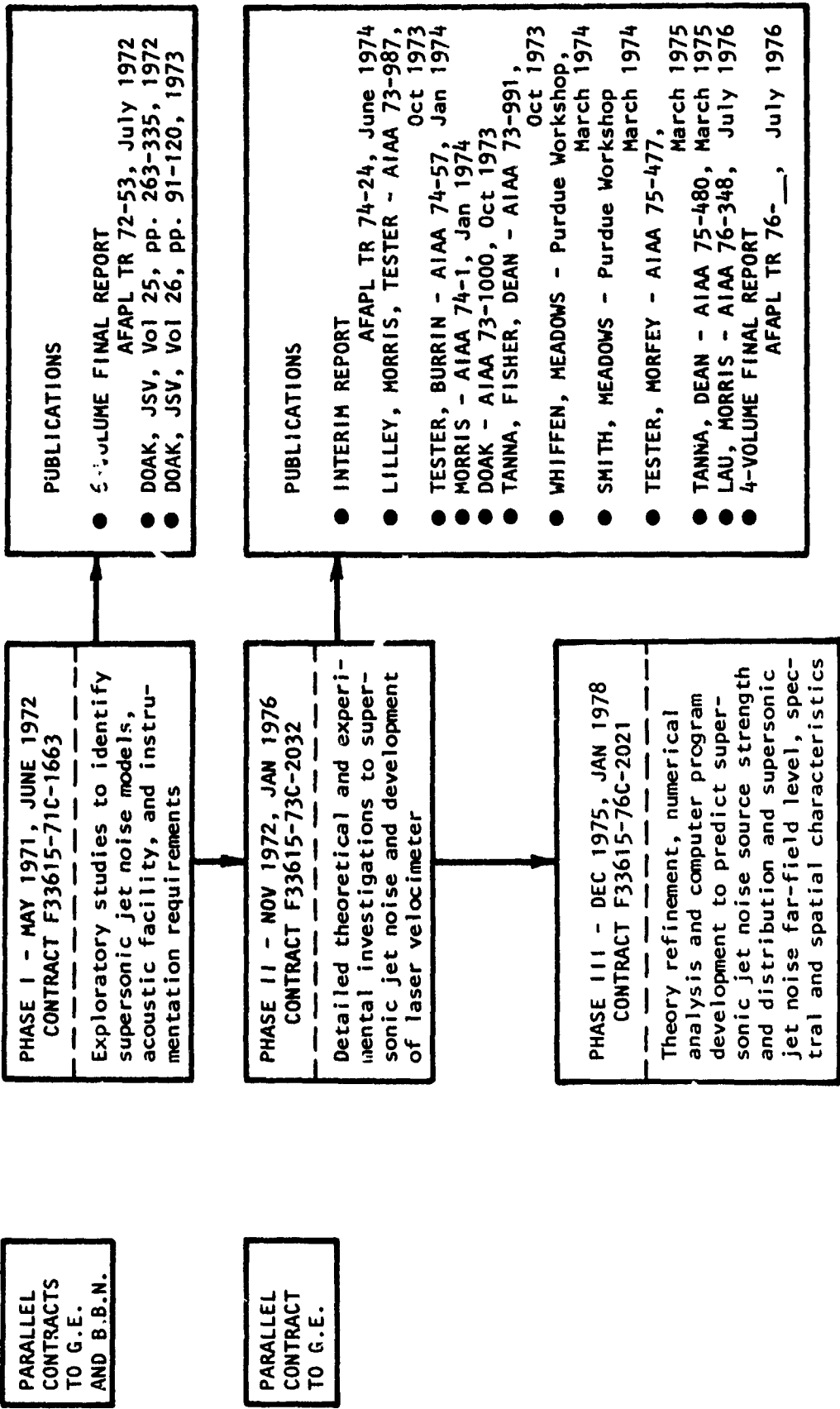


Figure 1.1 Outline of History of AF/DOT Supersonic Jet Noise Contracts

This summary report is accompanied by three other volumes. Referring to Figure 1.1, Volume II covers progress since the interim report. All the information contained in the papers referred to in the publication list is also contained in either the interim report or else in Volume II. Volume III is a compendium of turbulent mixing noise data and as such can be used as an independent source of accurate jet turbulent mixing noise data by other researchers. Volume IV contains similarly accurate data on shock-associated jet noise.

This brings the reader up to date on the history of the program. It will be necessary in the following to reference the various programs and the first contract will be called either the Phase I or else Exploratory Program. The second contract will be referred to as the Phase II program or Detailed Investigation.

This summary report will consist of three major sections. The first (Section 2) will outline the problems with theoretical work on jet noise existing prior to the Phase I contract. The second (Section 3) will outline the requirements for an adequate jet noise theory as developed during Phase I, and the third (Section 4) will summarize the results from the Phase II program. In addition, several appendices are included to discuss facility calibration, LV design and calibration, and other interesting information obtained during the LV measurement program.

2. REVIEW OF PREVIOUS WORK

In order to establish the requirements of a consistent approach for analyzing and theoretically modeling jet noise generation, the following subsections are presented which describe the earlier theories and their conceptual and mathematical difficulties and advantages, as well as comparisons of these theories with reliable experimental results.

2.1 EXPERIMENTAL ASSESSMENT OF Lighthill's FORMULA FOR ISOTHERMAL JET NOISE

The Lighthill theory of aerodynamic sound generation^{1,2}, in general, and jet noise generation, in particular, as well as notable extensions by Ribner³ and Ffowcs Williams⁴, have proved their worth in explaining many of the observed features of jet noise. However, detailed comparisons of jet noise characteristics such as those first discussed by Ribner³ and conducted in detail by Lush⁵, show serious areas of discrepancy between the "acoustic analogy" theory of Lighthill/Ribner/Ffowcs Williams and the very careful experimental results of Lush. Since this detailed and carefully conducted study by Lush⁵ formed the basis for evaluating current theory at the time the Phase I program began, it is useful to summarize Lush's findings and to use them as the primary justification for the approach taken in the current work.

While the Lighthill formulation of the problem of jet noise generation is mathematically exact, a penalty is paid for this exactness in terms of a source function, which cannot be identified exactly. Thus, practical usage has been limited to an approximate form of this source term without, in general, an assurance that important generation or transmission phenomena are not being ignored.

Lush shows clearly that practical application of the Lighthill formula* is in serious error for higher frequency jet noise at angles corresponding to maximum noise emission. Specifically, the formula overestimates considerably the high-frequency noise, particularly at angles close to the jet exhaust. His method indicates that these overestimations occur when the path length of the sound through the shear layer becomes comparable to or greater than the acoustic wavelength. Before discussing the details of Lush's comparison, a brief discussion is given of Lighthill's theory and approximations normally invoked for practical applications.

2.1.1 Practical Application of Lighthill Theory

The Lighthill theory¹ predicts the far-field intensity in the form

*We should differentiate clearly at this point between the Lighthill theory which may be exact and correct, and the Lighthill formula by which we infer the approximations necessary to the theory to render it in a form suitable for practical estimation procedures.

$$I = \frac{1}{16\pi^2 \rho a_0^5} \frac{1}{(1 - M_c \cos \theta)^6} \iint \frac{x_i x_j x_k x_l}{r^6} \frac{\partial^2 T_{ij}(\eta, t)}{\partial t^2} \frac{\partial^2 T_{ij}(\xi, t)}{\partial t^2} d\eta d\xi \quad (2-1)$$

where $T_{ij} = \rho v_i v_j + P_{ij} - a_0^2 \rho \delta_{ij}$.

For practical estimation purposes, the following assumptions are normally adopted:

- (a) T_{ij} may be approximated by the single term $\rho v_i v_j$.
- (b) The frequency weighting term implied by the time differentiation of T_{ij} scales on jet efflux velocity; that is, the turbulent field is jet Strouhal number dependent.
- (c) The fluctuating (turbulent) and mean velocities contained in T_{ij} are proportional to jet efflux velocity.
- (d) Both the shear layer width and turbulence scales are independent of jet efflux velocity, at least for conditions where the local-flow Mach number is everywhere less than unity.

There is, of course, strong experimental support for items (b), (c), and (d) from numerous investigations of turbulent flow fields and their insertion into the basic theory leads to the Lighthill formula

$$I(\theta) \propto \frac{f(\theta) V_J^8}{(1 - M_c \cos \theta)^5} D^2$$

where $f(\theta)$ is dependent on the type (i.e., longitudinal or lateral) of quadrupoles contributing.

While the Lighthill formula was generally accepted as more or less valid for subsonic jets, there were many worrying deviations noted in the literature between experiment and theory. Bushell⁶, in a very thorough study of model and full-scale engine data noted that the 8th power velocity dependence at high subsonic velocities was gradually reduced to something approaching 4th power dependence at low subsonic velocities. In his analysis of these results, he concludes that the observed deviations probably result from upstream disturbances and interactions with the nozzle. These problems have led to critical examinations of rig design and other potential jet noise sources, such as "lip noise."

In order to accurately determine the extent by which the Lighthill theory (and improvements by Ribner and Ffowcs Williams) actually deviated from carefully conducted experiments, Lush examined all the potential problems in jet rig design and jet noise testing and designed a rig for unheated jet tests which appeared to be free from the recognized problems. These test results were then compared by Lush with the Lighthill theory with a technique especially devised to highlight deviations between theory and experiment and furthermore, to reveal the physical reason for the disagreement. In the

following subsection, this work is outlined in reasonable detail, since it uniquely highlights one aspect of the problem with Lighthill's basic theory.

2.1.2 The Analysis Method by Lush

The basic analysis method adopted involves rewriting the Lighthill formula (as suggested by Lilley⁷ and discussed in detail by Ribner⁸) as,

$$I(\theta) = \frac{V_J^8}{(1 - M_C \cos\theta)^5} [K_1 + K_2 f(\theta)]$$

where K_1 is a constant of proportionality relevant to the set of randomly oriented quadrupole "sources" associated with self-noise; i.e., the turbulence-turbulence interaction term of T_{ij} . K_2 is a similar proportionality constant for the quadrupoles associated with the turbulence-mean shear interaction term and $f(\theta)$ is the directionality factor associated with these quadrupoles.

It should be noted here that, to predict the directionality of the noise for a given flow velocity, both the ratio K_2/K_1 and the form of $f(\theta)$ must be known. However, this difficulty is completely avoided if the variation of intensity with jet efflux velocity at a given angle to the jet axis is monitored.

The variation of noise intensity with jet efflux velocity for various angles to the jet axis is shown in Figure 2.1. It is apparent that, at 90° , the predicted V_J^8 dependence is obeyed with convincing accuracy. However, as the angle is reduced, comparison with theory becomes progressively worse, with theory overestimating measured values. To investigate this phenomena in more detail, a spectral comparison was conducted but as a function of a reduced, nondimensional frequency defined as

$$F = \frac{fD}{V_J} (1 - M_C \cos\theta) \quad (2-3)$$

where f is the observed acoustic frequency, D is the jet diameter, and V_J is the jet efflux velocity. The philosophy leading to the choice of this parameter is as follows. Consider a source being convected at Mach number M_C in a direction making an angle θ with a line joining the source to the observer. If the source frequency, observed in its moving reference frame, is f_s , then to the stationary observer the apparent frequency will be

$$f = \frac{f_s}{(1 - M_C \cos\theta)} \quad (2-4)$$

i.e., the well-known Doppler frequency shift effect.

Thus, the term $f(1 - M_C \cos\theta)$, in the equation defining our reduced non-dimensionalized frequency, F , corresponds to the actual source frequency. Due allowance is, therefore, made for the fact that a given convected source will appear to have various frequencies, depending on both the angle relative to the jet axis from which it is observed and its convection speed.

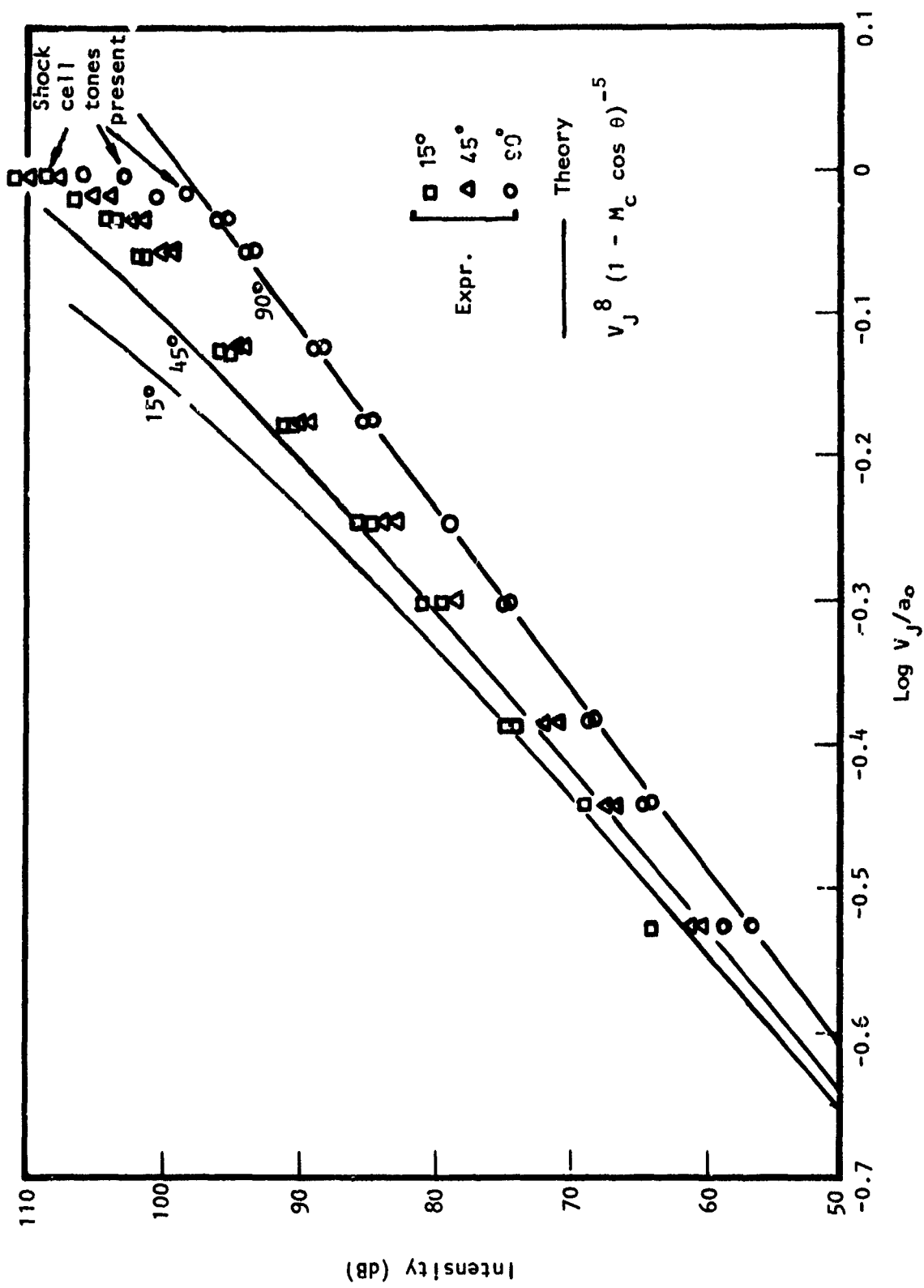


Figure 2.1 Velocity Dependence of Intensity at 15°, 45°, and 90° (From Ref. 5)

Finally, the source frequency f_s is nondimensionalized to form the Strouhal number $F = f_s D / V_j$. This nondimensional form is based on the observation that moving-axis turbulence frequencies, which determine source frequencies, scale on both jet diameter and jet efflux velocity. Thus, by monitoring acoustic levels for a given value of F , one is insured of monitoring the same sources irrespective of the jet velocity, their convection speed, or the angle from which they are viewed.

Thus, following the Lighthill formulation for such a given set of sources (i.e., $F = \text{const.}$), we would expect their intensity again to follow a law of the form [for small convection Mach number, where $\alpha^2 M_c^2 \ll (1 - M_c \cos \theta)^2$]

$$I(F = \text{const.}) \propto \frac{V_j^8}{(1 - M_c \cos \theta)^5} \quad (2-5)$$

To test the correctness of the Lighthill formula, Lush⁵ selected four values of F , namely 0.03, 0.10, 0.30, and 1.0. Results are again presented separately for each angle of the jet to avoid, as before, uncertainties associated with the relative contribution of the randomly oriented and preferentially oriented quadrupoles, respectively.

The results for the four values of F at 90° to the axis are shown in Figure 2.2. A convincing comparison of data with the anticipated "theoretical intensity" is apparent. Thus, for the 90° position, not only is the overall intensity predicted reasonably well, but also the variation of the individual "frequency" components.

However, similar analysis of results at 15° (Figure 2.3) produce a comparison of theory with experiment that is totally unsatisfactory, at least for the higher values of F . These, in fact, show an overall variation with jet efflux velocity appreciably less than V_j^8 . Clearly, extrapolation of the high-speed noise levels from the low-speed values according to the theoretical formula $V_j^8 (1 - M_c \cos \theta)^{-5}$ would result in large overestimates of these higher-frequency components, and these overestimates would become increasingly worse for higher speed.

A dramatic demonstration of the magnitude of these observed discrepancies can be made by considering noise spectra measured at 90° and 15° to the jet axis as shown in Figures 2-4 and 2-5, respectively. The Lighthill formulation would suggest that these spectra should be dependent on Strouhal number, with peak frequency proportional to jet efflux velocity. Indeed, at 90° (Figure 2.4) this is correct, and a convincing collapse of data can be obtained. However, for the 15° results, the peak frequency is essentially independent of jet velocity, again clearly showing the lack of high-frequency energy at these small angles.

Analysis of the results presented above indicated that, whenever the wavelength of the sound is large compared with the path length of sound through the turbulent flow field, predictions of the Lighthill formula are correctly obeyed. However, once this condition is violated, sound appeared to be produced with appreciably lower efficiency. Refraction is the effect most commonly used to explain this defect of sound energy near the jet exhaust axis.

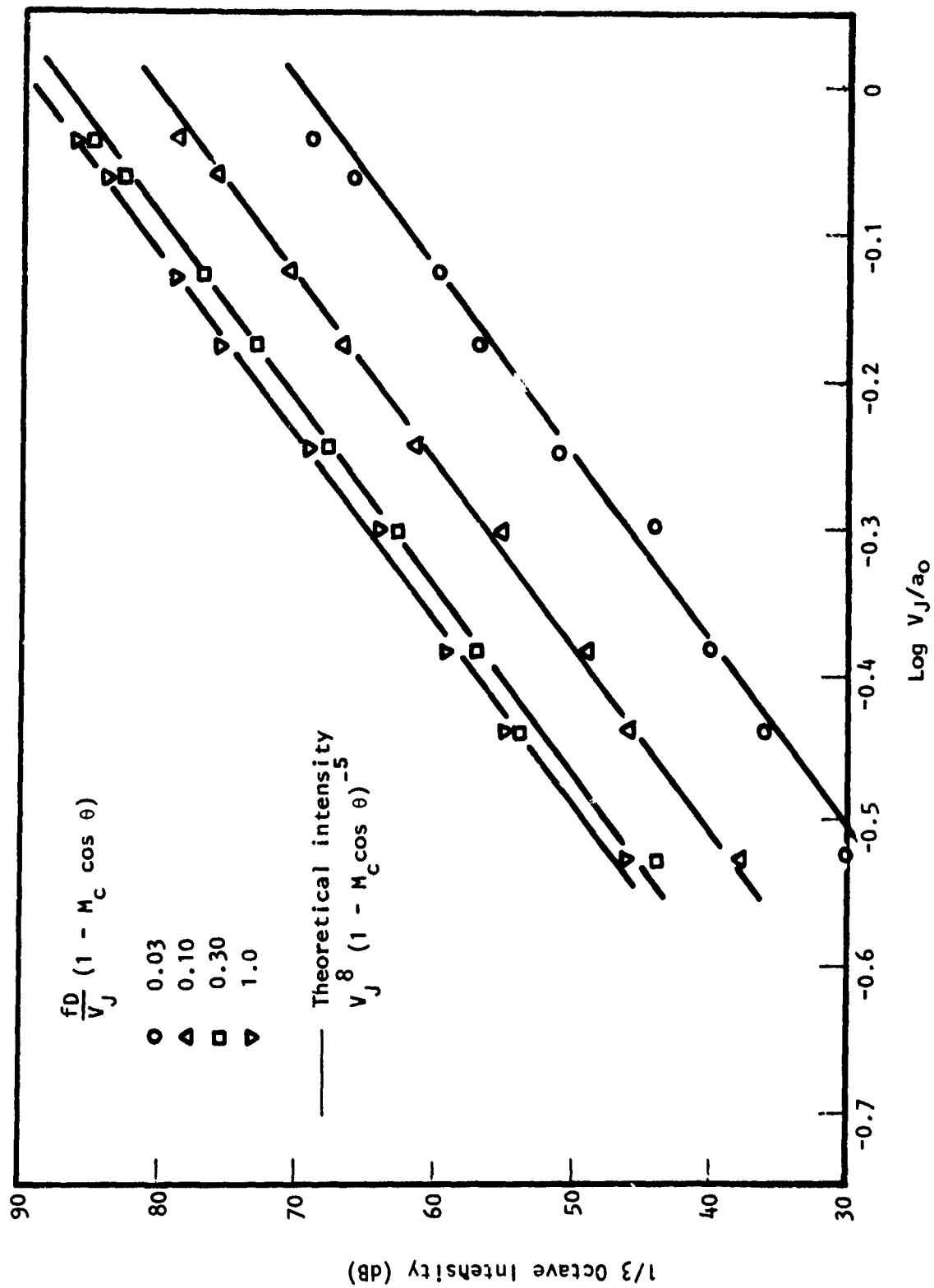


Figure 2.2 Velocity Dependence of 1/3-Octave Intensity at 90° (From Ref. 5)

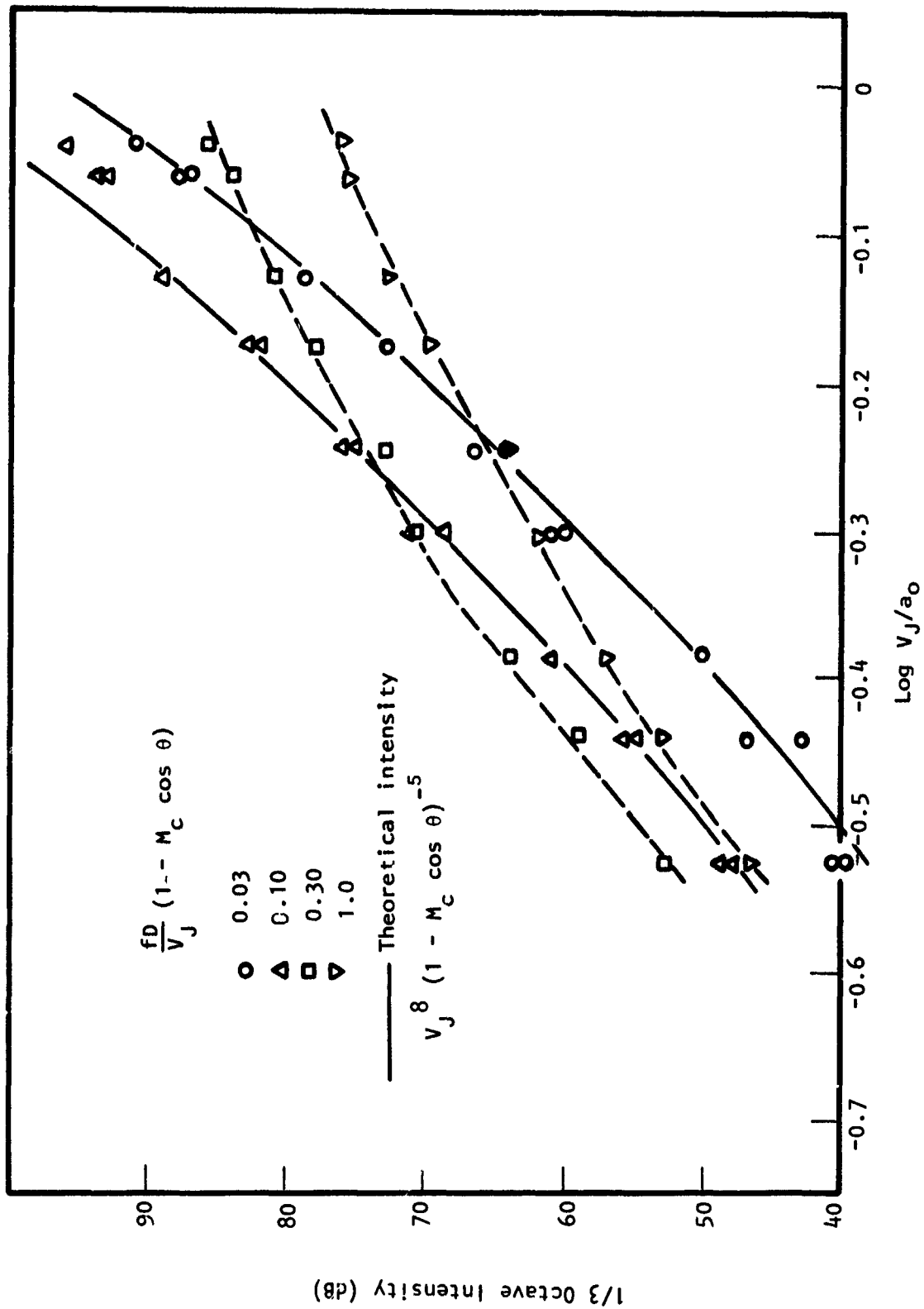


Figure 2.3 Velocity Dependence of 1/3-Octave Intensity at 15° (From Ref. 5)

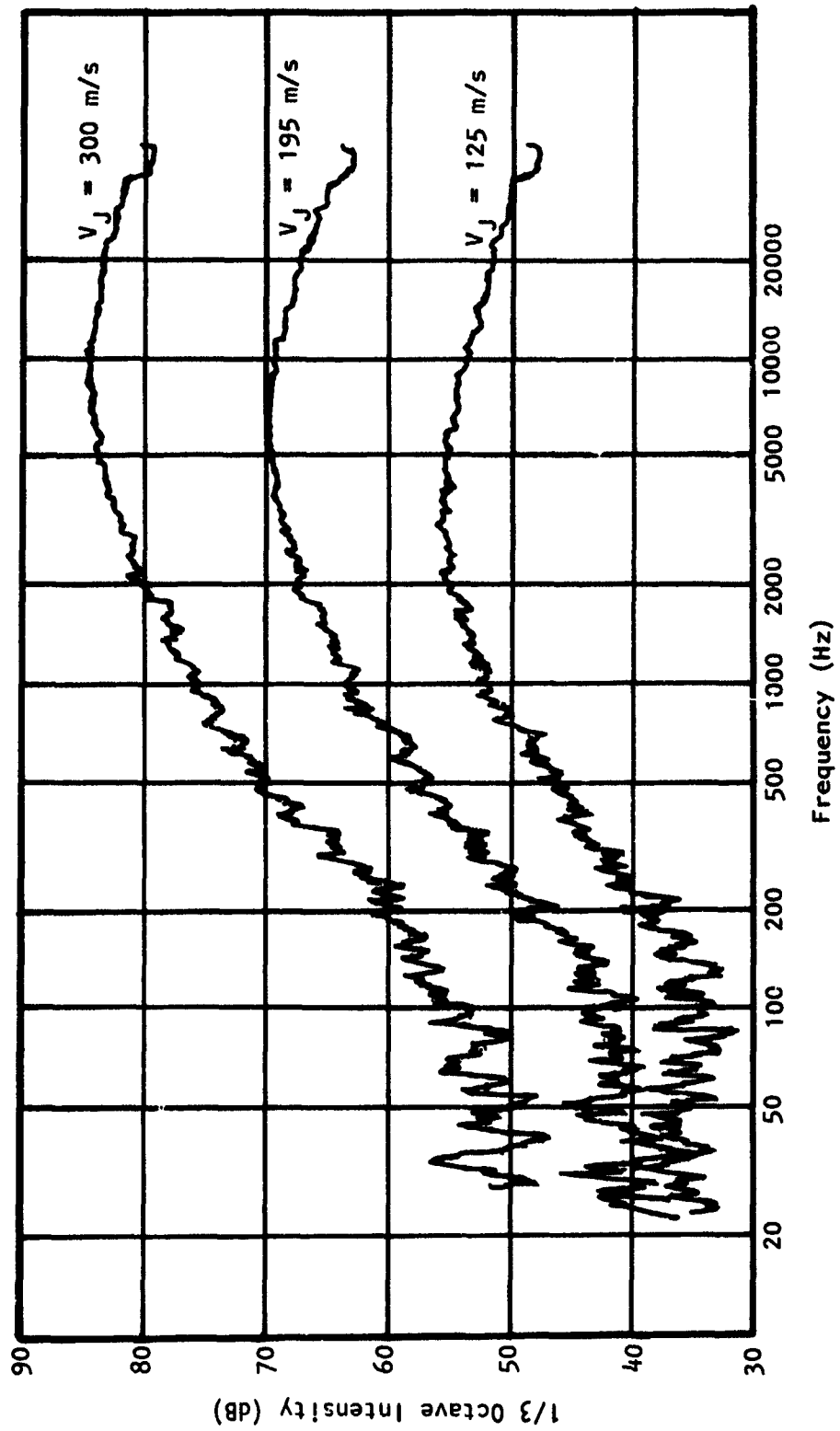


Figure 2.4 1/3-Octave Spectra at 90° for Various Jet Velocities (From Ref. 5)

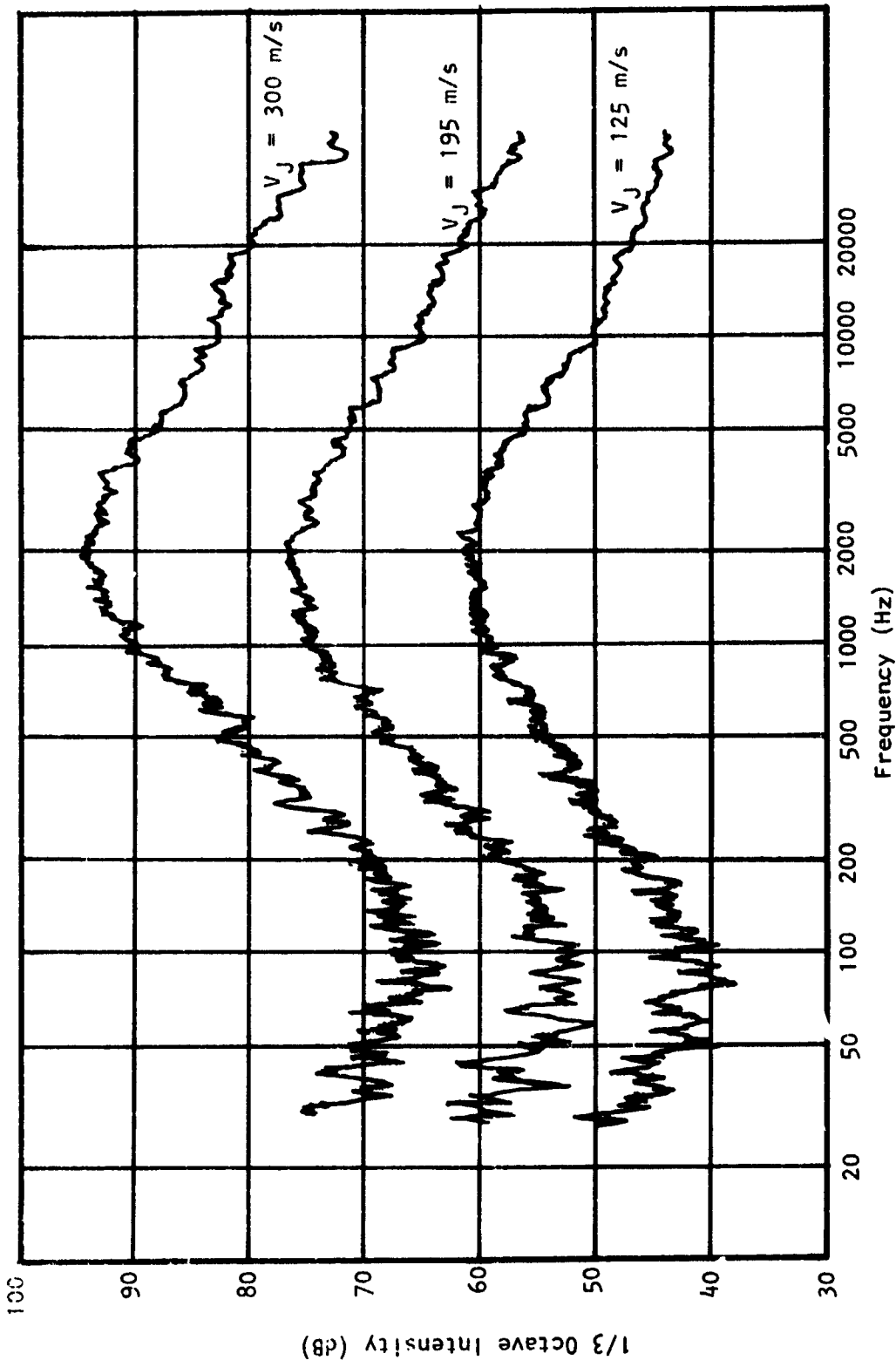


Figure 2.5 1/3-Octave Spectra at 15° for Various Jet Velocities (From Ref. 5)

However, if this is the only effect, then total power should obey the theoretical estimates, since the power once generated is merely redirected. The fact that this is not the case was also established by Lush, and his comparison is shown in Figure 2.6. It appears that the higher-frequency components exhibit a complete lack of convective amplification, which would help explain this reduction in source efficiency.

Finally, it is appropriate to consider the significance of these results to the noise of heated supersonic jets. First, further increase of speed above that considered by Lush (~1,000 fps) using hot unchoked jets will increase source frequencies so that an even more noticeable portion of the acoustic spectrum will fall into the range where acoustic wavelength is less than the path length through the turbulent flow. From these viewpoints, therefore, if better understanding of noise generated by pure turbulent mixing was to be achieved, irrespective of further complications of locally supersonic flow, shock waves, and other factors, a detailed theoretical model of noise generation by quadrupole sources contained in a shear layer of finite dimensions was required. This problem was ignored by Lighthill in favor of the simplified formulation by his analog theory.

Thus, in summary, the very careful comparison of jet noise experimental results with Lighthill's predictions produced major disagreements at high frequencies. Here, Lush speculated that both refraction and a reduction in source efficiency was contributing to the high frequency defect in sound level near the exhaust axis and the failure of total radiated sound power to match the theoretical value at high source frequency/high velocity combinations. Lush showed, in addition, a peculiar low frequency increase in noise (compared to the theory) at small angles and low frequencies.

This assessment of the several areas where the Lighthill theory failed, even for the case of unheated jets, led to a further examination of jet noise theories in general and the requirements of a new theory to make up for the observed discrepancies discussed above. The following section is a summary of this critique of the various competing theories at the time the Phase I program was initiated.

2.2 COMMENTS ON MAJOR AERODYNAMIC AND JET NOISE THEORIES AVAILABLE IN 1972

In this subsection, a critique by Doak⁹ of existing jet noise theories is summarized. Although Lighthill's equation has already been compared with experiment and was shown to be inadequate for detailed predictions of jet noise, it is presented in another context in this section to provide a basis for discussing competing theories at the time Doak's review was completed.

Reference has been made to "acoustic analogy" theories of aerodynamic noise. It is useful to state exactly the Lighthill definition of an acoustic analogy of jet noise. He discusses a method of identifying the aerodynamic sound sources in an equivalent, uniform acoustic medium at rest. The following is a direct quotation from Lighthill (Ref. 1, pp. 566-567):

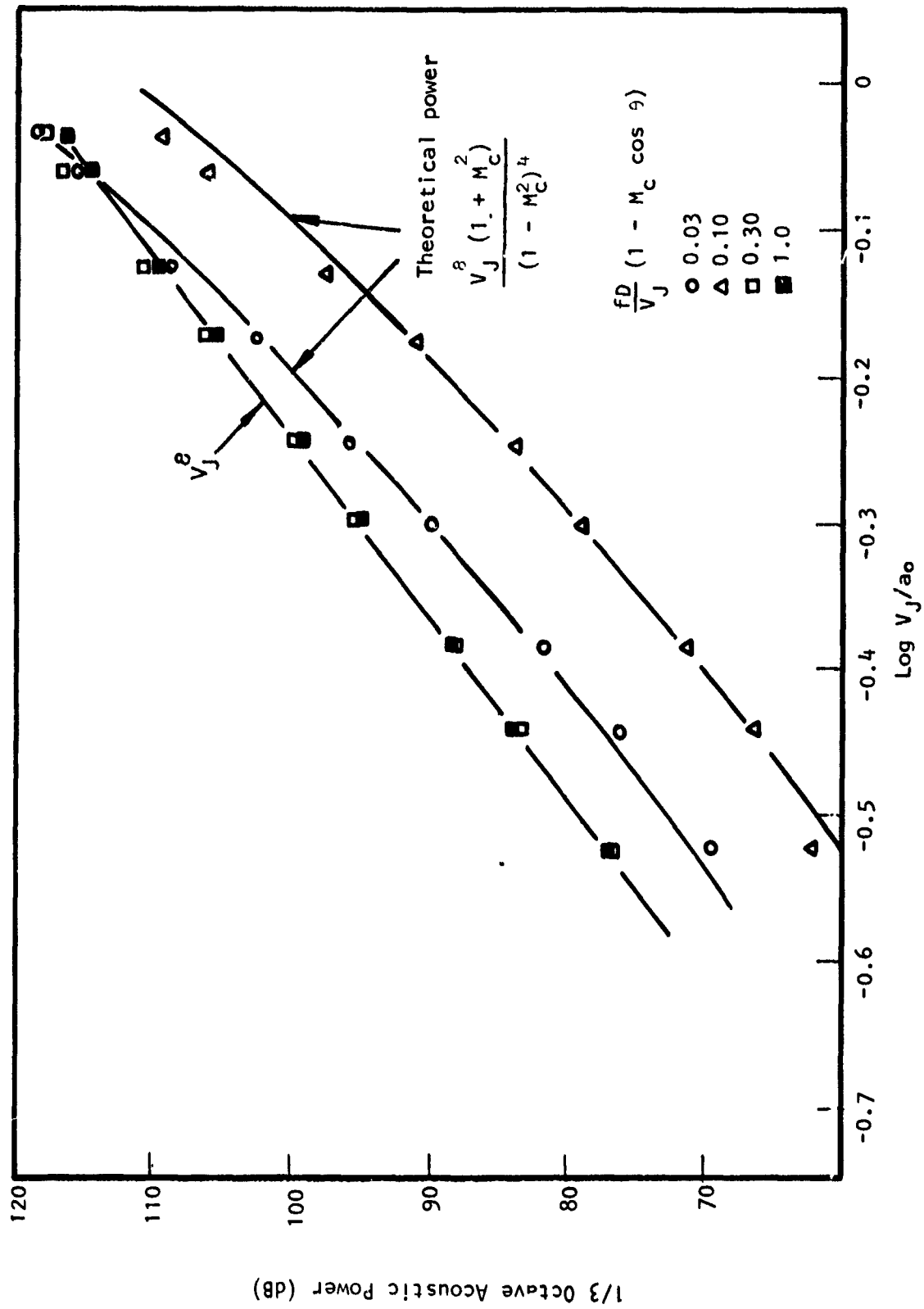


Figure 2.6 Velocity Dependence of 1/3-Octave Acoustic Power (From Ref. 5)

Considering a fluctuating fluid flow occupying a limited part of a very large volume of fluid of which the remainder is at rest, then the equations governing the fluctuations of density in the real fluid will be compared with those which would be appropriate to a uniform acoustic medium at rest, which coincided with the real fluid outside the region of flow. The difference between the two sets of equations will be considered as if it were the effect of a fluctuating external force field, known if the flow is known, acting on the said uniform acoustic medium at rest, and hence radiating sound in it according to the ordinary laws of acoustics.

This scheme has two advantages. First, since we are not concerned (see §1) with the back-reaction of the sound on the flow, it is appropriate to consider the sound as produced by the fluctuating flow after the manner of a forced oscillation. Secondly, it is best to take the free system, on which the forcing is considered to occur, as a uniform acoustic medium at rest, because otherwise, after the sound produced has been estimated, it would be necessary to consider the modifications due to its convection with the turbulent flow and propagation at a variable speed within it, which would be difficult to handle. But by the method just described, all the effects are replaced by equivalent forcing terms and incorporated in the hypothetical force field.

The underlined portions are incorporated to highlight the assumptions of Lighthill's theory, as he analyzed the difficulties of realistically accounting for the obvious interactions of sound with the flow both in the process of generation and propagation.

2.2.1 Lighthill's Theory and Dimensional Analysis

Lighthill's exact acoustic analogy equation for the mass density is

$$\frac{c_0^2}{\partial x_i^2} \frac{\partial^2 \rho}{\partial t^2} - \frac{\partial^2 \rho}{\partial t^2} = - \frac{\partial^2 T_{ij}}{\partial x_i \partial x_j} \quad (2-6)$$

where

$$T_{ij} = \rho v_i v_j + (p - c_0^2 \rho) \delta_{ij} - S_{ij} \quad (2-7)$$

and

$$S_{ij} = \mu \left[\frac{\partial v_i}{\partial x_j} + \frac{\partial v_j}{\partial x_i} - 2 \frac{\partial v_k}{\partial x_k} \delta_{ij} \right] + \left[\frac{4}{3} \mu + \epsilon \right] \frac{\partial v_k}{\partial x_k} \delta_{ij}. \quad (2-8)$$

The constant c_0 is mathematically arbitrary but in keeping with the philosophy behind the analogy; Lighthill regards it in his physical interpretation of the

theory as the speed of sound in a suitable reference medium. Lighthill assumed that the physical situation was one in which a disturbed, sound generating flow field would exist only within a limited volume of the fluid, outside of which would be fluid at rest, apart from "acoustic" disturbances propagating out from the source region. If the speed of sound in this outer fluid is taken as c_0 and if only acoustic disturbances exist there, the homogeneous part of Equation (2-6) should exactly describe the mass density fluctuations in this region. Thus, to justify application of the analog in a given situation, one needs to establish the existence, in that case, of a region of real surrounding fluid, having a uniform mean temperature corresponding to a sound speed c_0 , which is suitably quiescent. For an inviscid, non-heat-conducting fluid in the outer region, it can be shown that $\partial^2 T_{ij} / \partial x_i \partial x_j$ falls to zero faster than $(\partial^2 \rho / \partial t^2) - c_0^2 \nabla^2 \rho$, for low Mach numbers. Doak⁹ demonstrates by reference to the Rayleigh linearized equations that in the limit of a nearly quiescent medium, of Stokesian viscosity and thermal conductivity, the right-hand side of Lighthill's exact equation for aerodynamic sound generation, Equation (2-6), does not reduce to zero completely in comparison to the left-hand side. He shows, in fact, that the case of a Stokesian fluid, Equation (2-6), reduces in the limit of an ambient medium, to a homogeneous wave equation in pressure rather than density. Furthermore, he questions the wisdom of formulating an acoustic problem in terms of density rather than pressure, but concludes that both the density and "preferred" pressure formulations (Doak⁹, pp. 56-57) are conceptually valid within the limits of the analysis.

However, the main shortcoming of the "acoustic analogy" approach lies in the inability of the experimenter to accurately determine the effective sources. The terms $\partial^2 (\rho v_i v_j) / \partial x_i \partial x_j$ that represent, in the form of equivalent sources, convection of the sound waves that are generated elsewhere, are usually small compared with the dominant terms depending upon only the turbulent (i.e., solenoidal) velocity components. Therefore, hot-wire anemometer measurements of the equivalent source terms will usually not reveal these convection effects although, of course, the convection of the equivalent "turbulent quadrupole sources" themselves will be readily apparent. Hence, a prediction of the radiated sound field from the "acoustic analogy" equation in such circumstances will not include the physically real, and generally significant, effects of the convection of the sound waves themselves in the flow. This important limitation applies to all "analog" and some "true source" (to be defined in a following section) theories. However, it is important to stress that Lighthill's theory is exact and would provide the exact solution if the source terms could be completely described.

With this important reservation in mind, we may now examine how Lighthill's theory has been applied in the correlation of jet noise. From a very simple point of view, Lighthill¹⁰ was able to deduce that the sound energy radiated would be proportional to (in the absence of convection effects)

$$\frac{\bar{T}^2 \omega^4 V_J}{\rho_0 c_0^5}$$

where \bar{T}^2 represents a mean-square fluctuation of the quadrupole strength T_{ij} , ω is a typical frequency and V a typical eddy volume. Then by arguing that

Now in the mixing region, the fluctuations of terms like $\rho v_i v_j$ in the quadrupole strength T_{ij} are in proportion to $\rho_0 U_j^2$, changing little with x , but the typical frequency ω falls away like U/x , while the typical eddy volume V grows like x^3 . We should therefore expect the power output to vary as $\rho_0 V_j^8 / a_0^5 x$ per unit volume of mixing region. But since the volume per unit length increases with x , the sound emitted per unit length of jet should remain constant in this region, the total up to $x = 4d$ being proportional to

$$I/\text{unit length} \propto \frac{\rho_0 V_j^8 d^2}{c_0^5} \quad (2-9)$$

This is the well-known U_j^8 law of jet noise and careful measurements show that it is applicable over a particular subsonic velocity range. The convection effects mentioned above refer to the "convective amplification" due to the motion of the sources relative to the observer. This factor was correctly derived by Ffowcs Williams¹¹ and modified Equation (2-9) by the factor

$$(1 - M_c \cos \theta)^{-5} \quad (2-10)$$

where $M_c \cos \theta$ is the convection Mach number in the direction of emission based on the atmospheric speed of sound.

A well-known solution to Equation (2-6) is obtained¹ provided refraction, diffraction and the effects of solid boundaries are neglected. This is given as

$$\rho(x, t) = \frac{1}{4\pi c_0^2} \int d\eta \frac{(x_i - y_i)(x_j - y_j)}{(|\underline{x} - \underline{y}| - M \cdot (\underline{x} - \underline{y}))^3} \frac{\partial^2 T_{ij}}{\partial t^2}(\underline{\eta}, \tau) \quad (2-11)$$

where \underline{y} is the source position, \underline{x} is the receiver position, $c_0 M$ is the uniform speed of source

$$\tau = t - \frac{|\underline{x} - \underline{y}|}{c_0} \quad (2-12)$$

and $\underline{\eta}$ is the moving coordinate defined by

$$\underline{\eta} = \underline{y} - c_0 \int_0^\tau M(\tau') d\tau' \quad (2-13)$$

A fairly straightforward analysis, based on this solution leads to the results that the spectrum of radiated noise is Strouhal number dependent; that sources contributing to the peak of the spectrum are contained in a region near the end of the potential core; that the low-frequency noise is generated downstream of the potential core in the fully developed region with the spectrum shape being related to the square of the Strouhal number; and, that the high-frequency

noise is generated in the mixing region, with the spectrum shape inversely related to the square of the Strouhal number.

These scaling laws highlight the obvious importance of Lighthill's theory since without these estimates it would not be possible to estimate the noise to within an order of magnitude, as Lighthill stated in the following extraction from Reference 1:

This paper is concerned with the general problem: given a fluctuating fluid flow, to estimate the sound radiated from it. Part II will take up the question of turbulent flows proper, with special reference to the sound field of a turbulent jet, for which a comparison with experiment is possible.

The problem's utility may be questioned on the grounds that we never know a fluctuating fluid flow very accurately, and that therefore the sound produced in a given process could only be estimated very roughly. Indeed, one could hardly expect, even with the great advances in knowledge of turbulent flow which have lately been made, that such a theory could be used with confidence to predict acoustic intensities within a factor of much less than 10. But, on the other hand, one could certainly make no confident estimate even to within a factor of 1000 on existing knowledge, and further, the range of intensities in which one is interested is at least 10^{14} . Also, nothing is known at present concerning how different sorts of changes in a flow pattern may be expected to alter the sound produced, and this is a serious impediment to those experimenting in novel fields of aerodynamic sound production. Clearly, such knowledge can arise only from a process in two parts, the first considering what sort of fluctuating flow will be generated, and the second what sound the flow will produce.

The proposed method of attack, in which first the details of the flow are to be estimated, for aerodynamic principles not concerned with the acoustic propagation of fluctuations in the flow, and secondly the sound field is to be deduced, precludes the discussion of phenomena where there is a significant back-reaction of sound produced on the flow field itself. But such back-reaction can be expected unless there is such a resonator present to amplify the sound.

Actually it seems likely from the theory in its present form that quantitative estimates of the sound field will be obtainable (as will be seen in Part III) only for the sound radiated into free space; and thus they will neglect not only neighboring resonators, but also all effects of refraction, diffraction, absorption or scattering by solid boundaries. But the general result of these effects could often be sketched in subsequently,

in the light of existing knowledge. Again, the estimates refer only to the energy which actually escapes from the flow as sound, and to its directional distribution; thus, the departures from inverse square-law radiation which are to be expected within a very few wavelengths of the flow, due to a standing wave pattern will not appear in the estimates, although they are implicit in the general theory. As a final restriction the theory is effectively confined in its application to completely subsonic flow, and could hardly be used to analyze the change in character of the sound produced which is often observed on transition to supersonic flow at least if, as Cave-Brown-Cave suggests, it is due to high-frequency emission of shock waves.

2.2.2 Ribner's Contributions to Jet Noise Theory

Based on Lighthill's model, Ribner¹² deduced that the noise power emitted by a slice of the jet is essentially constant in the mixing region (x^0 law) and falls off extremely fast (x^{-7} law) in the fully developed jet. Ribner has made a number of significant contributions to our understanding of jet noise. His own "dilation theory"¹³ is really a reformulation of Lighthill's theory and as such suffers from the same limitations. However, Ribner's work on directivity and the quadrupole correlation governing the pattern of jet noise is useful. He proposed¹⁴ (following the original phraseology used by Lilley⁷) to separate the contributions of various quadrupoles into "shear noise" and "self noise." The former quadrupoles contribution being non-zero only when the mean flow is nonuniform (i.e. possesses shear), the latter quadrupoles being free of cross-coupling with the mean flow. Based on this separation the total noise power emitted from a unit volume at a point y was found to be

$$p(y, \theta) = \underset{\text{self}}{A} + \underset{\text{shear}}{B}(\cos^4 \theta + \cos^2 \theta) / 2 . \quad (2-14)$$

This results in what Ribner refers to as a "basic" quasi-ellipsoidal pattern of jet noise directivity.

Ribner however also recognized the importance of refraction on jet noise directivity and various workers at the University of Toronto, Institute of Aerospace Studies, have made experimental and theoretical analyses of refraction¹⁵⁻¹⁸. Based on these results, MacGregor et al¹⁹ derive the "basic" pattern from theory and experiment.

However, it will be shown that this approach for describing jet noise, though valid, is unnecessary and subject to excessive difficulty in describing the source. By reformulating the problem in terms of a convected wave equation with all refractive and convective terms on the left-hand side, the effects of refraction, diffraction, and convection are automatically included in the solution. Further theories similar to Lighthill's and Ribner's analog are available such as those of Bschorr²⁰, Meecham²¹, and Crow²².

These were also critically examined by Doak⁹ in his comprehensive review in the Phase I work.

2.2.3 Phillips' Theory

We will now consider the work by Phillips²³. We may classify Phillips theory as a "true source" theory in which an attempt is made to identify the sources of the acoustic radiation field in the real, moving, inhomogeneous fluid and not in an equivalent (and fictitious), uniform acoustic medium. Phillips' equation, a convected wave equation, may be written as

$$\frac{\partial}{\partial x_i} \left(c^2 \frac{\partial r}{\partial x_i} \right) - \frac{D^2 r}{Dt^2} = -\gamma \frac{\partial v_i}{\partial x_j} \frac{\partial v_j}{\partial x_i} - \frac{D^2 \sigma}{Dt^2} + \gamma \frac{\partial}{\partial x_i} \left\{ \frac{1}{\rho} \frac{\partial}{\partial x_j} \left[\mu \left(\frac{\partial v_i}{\partial x_j} - \frac{\partial v_j}{\partial x_i} - \frac{2}{3} \frac{\partial v_k}{\partial x_k} \delta_{ij} \right) \right] \right\} \quad (2-15)$$

where $r \equiv \ln p$; $\sigma \equiv \ln(p/\rho\gamma)$, $c^2 \equiv \gamma p/\rho$, and $\gamma \equiv c_p/c_v$.

Phillips' interpretation of his equation suffers from a fundamental oversight. He interprets Equation (2-15) as follows:

The terms on the left-hand side are those of a wave equation in a moving medium with a variable speed of sound, the partial time derivatives of the ordinary wave equation being replaced by derivatives following the motion. The first term on the right-hand side represents the generation of pressure fluctuations by the velocity fluctuations in the fluid while the remaining terms describe the effects of entropy fluctuations and fluid viscosity.

In fact, the left-hand side of Equation (2-15) does not have the full, correct differential operator appropriate for pressure disturbances "in a moving medium with a variable speed of sound." There are no terms in the operator expressing the effects on propagation of the pressure disturbances of any shear in the flow. These terms arise from what Phillips mistakenly identified as entirely a "source" term, namely

$$-\gamma \frac{\partial v_i}{\partial x_j} \frac{\partial v_j}{\partial x_i}$$

on the right-hand side of his equation. This term contains a shear refraction term which, in a strictly logical manner, should be included on the left-hand side of Equation (2-15). For a given Mach number, the shear refraction term is significant for wavelengths comparable to, or greater than, the shear layer thickness, as well as the tendency of shear refraction to be more important at higher Mach numbers. It is also possible to show that the shear refraction terms in the disturbed flow itself, relative to the leading source term of the material derivative of Equation (2-15) are of order (L_v^2/L_A^2) , where L_v is the length scale characteristic of the turbulent "eddies" and L_A is the acoustic wavelength. L_v/L_A is believed to be small, and hence the shear refraction

terms are normally swamped in the disturbed flow by the source terms. Thus, the experimenter is quite unable to provide the theoretician with the information that the latter needs about such convection and refraction terms in the form of "equivalent source" data.

However, if the "source terms" could be completely identified then, of course, Phillips' theory is *exact*. We might also point out that Phillips' solution does not describe the far-field noise since his solution represents an infinitely wide shear layer or the inner solution in a method of matched asymptotic expansions.

2.2.4 Conclusions of Critique of Analog Theories and Phillips' Theory and Requirements for a Consistent Theory of Jet Noise

The convection and/or refraction terms on the right-hand side of the acoustic analogy equation and Phillips' equation are linear in the derivatives of the dependent variable, pressure, for which the solution is required. Omission of these convection and/or refraction terms affects both the propagation characteristics with respect to frequency and directionality and the effectiveness with which a given forcing function can cause the medium to fluctuate as an effective source of acoustic radiation. Thus, *the analog theories do not take account of the effects of the presence of the flow on the intrinsic efficiency with which a given source can produce far-field radiant acoustic energy*. In general, the radiation impedance seen by a given acoustic source in a given acoustic environment depends upon all the properties and characteristics of the entire environment, both in the near and far fields.

Of course, in the acoustic analogy formulation, all equivalent sources are regarded as if embedded in an ideal "acoustic" medium, and hence, again, if these equivalent sources are all accurately determined, the predictions of the radiated sound field will be correct and the radiation impedance problem, being well understood for such an ideal "acoustic" medium, presents no difficulties. If, however, the equivalent propagation-type source terms are not included with sufficient accuracy in the source data, then not only may the distributions in angle and frequency of the radiated sound be in error, but also the total radiated sound power itself may be in error, because the homogeneous part of the acoustic analogy equation does not yield radiation impedances that are appropriately modified to make up for the omissions or inexactitudes of the relevant equivalent source terms.

Thus, even the order-of-magnitude accuracy, as well as the detailed accuracy, of predictions of radiated sound from the acoustic analogy equation can depend very critically upon equivalent source terms that are small and largely undetectable by available experimental methods, in comparison to the leading equivalent source terms due primarily to the "turbulent" (that is, vortical) velocity fluctuations in the disturbed flow. In this respect, the acoustic analogy approach is undoubtedly more liable to error, and more likely to lead to confusion and misinterpretation in the analysis of experimental results, than is the Phillips' equation approach, in which at least some of the convection and refraction terms due to mean velocity variation and thermal inhomogeneity in the disturbed flow can be more accurately taken into account in the predictions, and in which, as a consequence, the radiation impedance effects will be similarly included.

In the preceding discussion, it has been shown that the principal weakness in practice of all analog theories is that their predictions are too sensitive to the details of the equivalent source distributions which *cannot be identified and measured to the accuracy required*. Conceptually, therefore, for engineering purposes, the analog theories are unsatisfactory since they do not provide unequivocal identification of all the various separate and distinct factors that can influence the radiated sound. In particular the theories conceal, rather than reveal, the influence of convection and refraction of the sound itself by the disturbed flow.

Based on these observations, it is concluded that a more correct form of convected wave equation which would give better analysis and prediction of the generation and radiation of aerodynamic noise, must contain only terms of quadratic and higher order in the perturbation quantities, retained and placed on the right-hand side as a source function. The "true source" model proposed by Phillips did not meet this criterion due to the inclusion of a shear refraction term on the right-hand side of his equation.

This basic fact was recognized some time ago by Pridmore-Brown²⁴ and by Mungur and his co-workers^{25,26}, in analyzing the propagation of sound in flow ducts with sheared flow. Evidence from flow duct experiments²⁷ shows conclusively that the effects of *both* Phillips' convection terms *and* the shear refraction term are significant. Thus, in his review⁹, Doak concluded that because of the conclusive evidence concerning the shear refraction terms, none of the existing theoretical predictions of aerodynamic noise from either mixing regions or boundary layers, could be regarded as complete and correct. "At best all predictions are incomplete; at worst they are incorrect."

This review has laid the foundation for the requirements of an unambiguous, theoretical approach to the problem of defining aerodynamic noise generation, in general, and jet noise, in particular. In the following sections, a unified theory of aerodynamic noise generation and a theory for jet noise generation from a region of parallel transversely sheared flow which meets the requirements detailed above will be outlined.

3. THEORETICAL DEVELOPMENTS IN JET NOISE

As a part of the fundamental studies supported by the AFAPL and DOT on supersonic jet noise in Phase I, Doak⁹ developed a unified theory of aerodynamic noise generation and Lilley²⁸ completed his work on jet noise generation in a parallel transversely sheared heated flow and reported on his final theoretical result which is now termed the Lilley equation. In the following, a brief summary of Doak's discussion will be presented, including a discussion of the relevance of his method of identification of acoustic, thermal, and vortical components in noise generation and radiation. Following this, Lilley's equation will be derived and its adherence to the rules of identification introduced by Doak will be demonstrated.

3.1 DOAK'S UNIFIED THEORY OF AERODYNAMIC NOISE GENERATION

Doak²⁹ began his work on a unified theory of noise generation in the early 1960's when he published his work on inhomogeneous acoustic wave equations for continuous media. In this early work he developed the fundamental ideas "... relevant to the identification of the actual physical sources of internally generated sound and to the formulation of the theory in such a way that these can be convincingly related to physical quantities that are measurable in practice." He derived an inhomogeneous convected wave equation in terms of mass density fluctuation for sound generation in a continuous medium, however, this derivation suffered from many of the problems with which Phillips²³ also was faced. This result had linear terms on the right-hand side in the $\rho_{\infty}(\partial v_i/\partial x_j)(\partial v_j/\partial x_i)$... type terms and thus was not suitable for properly separating generation from propagation.

However, in his work during the Phase I studies, Doak⁹ fully realized the significance of the distinction between source and acoustic terms in considering aerodynamic noise generation as outlined in the previous section. In order that the impact of Doak's thinking not be diluted, the present section will include the relevant extractions from his work on the importance of clear identification of source terms and propagation or diffusion terms.

On the type of dependent field variable to use, it is stated:

The first step towards achieving the "separate" understanding of 'all the phenomena of compressible, rotational flow,' that Crow has suggested as necessary for the problem of aerodynamic sound (see Ref. 22, p. 43), obviously must be to identify the various phenomena. Having previously arrived at general conclusions similar to those expressed by Crow, Doak had studied some aspects of this problem of identification²⁹⁻³¹, and had later come to the conclusion^{32,33} that a satisfactory identification could not be achieved if pressure, mass density and particle velocity were regarded as the primary, dependent field variables. Principal among the considerations leading to this conclusion was the fact that the Pridmore-Brown shear refraction term^{24-26,28,34} could not be isolated and unambiguously identified except in the special case of a flow with a purely transverse shear (see the discussions of Lilley's theory²⁷ in reference 9), when

particle velocity was used as a primary dependent field variable. A thorough study of the mathematical difficulties involved in eliminating certain field variables in favor of others, from the basic transport equations, showed that this lack of generality of the Pridmore-Brown shear refraction term could be traced in part to the fact that, when the particle velocity is separated into its unique irrotational and solenoidal components, neither the mean of the irrotational component nor that of the solenoidal component is necessarily zero. This has the consequence that, through the equation of mass transport, the mass density appears to have a direct dependence upon both the irrotational and solenoidal components of the particle velocity. This consequence, in turn, plays a significant role in preventing the elimination of any two of the three scalar field variables (pressure, mass density and the scalar velocity potential) from $\rho v_j v_j$, or its derivatives, in favor of the third. Thus, one cannot obtain an inhomogeneous partial differential equation for any scalar quantity, in terms of quantities associated with the solenoidal particle velocity field, which could be assumed to be known more or less independently.

It appears that the best that can be done, with the particle velocity as a field variable, is to produce successive approximation schemes, like those of Chu and Kovasznay³⁵, or of Morfey³⁶, or to obtain formulations valid to second order like that of Lilley²⁸, whereas the aim is to produce a generally valid system of coupled partial differential equations for the "acoustic," "turbulent" and "thermal" components of the motion, which reduce to the Stokes-Kirchoff-Rayleigh system in the limit of small amplitudes and small gradients. Phillips' equation and the generalized Rayleigh equations⁹ suffer from exactly the same difficulty, which for these equations appears principally as the insoluble problem of eliminating, in the general case, two of the three scalar field variables from Phillips' supposed "source" term, $(\partial v_i / \partial x_j)(\partial v_j / \partial x_i)$.

The clear implication of such unsuccessful exercises of elimination of scalar variables, especially in view of the fact that some of the difficulties arose in the relationships imposed by the mass transport equation, was that another vector field variable, other than the particle velocity, should be tried, and that it should be a variable that produced an as-simple-as-possible form of the mass transport equation. Obviously, therefore, the linear momentum density was a possible choice of dependent vector field variable, in place of the particle velocity.

He then goes on to justify his scheme for identifying the separate "acoustic," "thermal," and "vortical" components of motion.

First, there is a single, simple, obvious and by itself wholly sufficient reason why an identification scheme is necessary, on conceptual grounds. This is that the question 'How is sound generated in a disturbed flow?' is completely meaningless unless one knows what "sound" is "in" the disturbed flow. The acoustic analogy theories are framed on the premise that this question cannot be answered, in practice, because conditions inside the

disturbed flow are too complicated. With these theories, even at best, only association of an external sound field with each particular disturbed flow is possible and the question of how this external field is generated can be answered only by an "as if" analogy. Such an association is not generally possible because of the practical difficulties in obtaining independent estimates of certain equivalent source terms.

Second, there is a practical, as well as conceptual reason why an identification scheme is necessary. Accurate observation by measurements of the complicated conditions inside a disturbed flow is very difficult and costly in both time and equipment. Ultimately, irrelevant measurements of "equivalent" quantities, rather than of the essential quantities, are therefore particularly wasteful.

Third, a theory that is not a unified theory is no theory at all, but merely a collection of rules. As the observation by Crow implies, aerodynamic sound generation is an intrinsic part of the whole problem of compressible, rotational, fluctuating fluid flow, and must be considered as such. It must, therefore, eventually be formulated as a part of this whole problem. The science of magnetism could conceivably still be wholly and "more easily" described, as it once was, in terms of actual and/or equivalent magnetic dipoles as sources, with the Biot-Savart Law consigned to oblivion, but if this philosophy had been adopted in the past, there would now be no science of electromagnetism.

Fourth, and finally, even if it is acknowledged that an identification scheme is necessary, it might be argued that nothing better than the generalized Rayleigh equations is either needed or desirable. After all, these equations can be interpreted, for the desired purpose of identification, through a successive approximation scheme involving unambiguously identifiable higher-order interactions, such as that of Chu and Kovasznay³⁵. In this case, of course, the generalized Rayleigh form of Phillips' equation, would be that taken as generally "identifying" the "acoustic" type of motion. As long as nothing better can be found, it would certainly be best to adopt the generalized Rayleigh equations for this purpose, and to develop appropriate approximate formalisms from them, for particular classes of applications. This, in fact, is what Phillips²³, Lilley²⁸, and others working from Phillips equation have done, or attempted to do. Nevertheless, it is abundantly clear, from the many detailed comments made previously in this review (about, for example, the shear refraction term difficulties, the cumbersomeness of successive approximation methods, and the elimination and specific identification problems mentioned in the first three paragraphs of this section), that the generalized Rayleigh equations do not provide a logically satisfactory identification scheme in the general case, and that certain of the nonlinear terms in these equations give rise to special difficulties of interpretation and reduction in specific practical applications. Thus, if something better than the generalized Rayleigh equations can be found, there is certainly scope for its use.

Following this, Doak⁹ outlines his choice of primary field variables and justifies that choice:

As primary dependent field variables for a Stokesian fluid (or other continuum), Doak chooses the pressure, p , the mass density, ρ , and the linear momentum density, ρv_i . The linear momentum density is separated into its unique solenoidal and irrotational parts:

$$\rho v_i \equiv B_i - \partial\psi/\partial x_i \quad (3-1)$$

where

$$B_i \equiv \text{curl}_i (A) \quad (3-2)$$

so that

$$\partial B_i / \partial x_i \equiv 0. \quad (3-3)$$

A_i and ψ are thus, respectively, the vector and scalar potentials of the linear momentum density. As a vector field variable, the linear momentum density has certain a priori advantages over the particle velocity. First is the well-known fact that the linear momentum of any system of particles can be changed only by the action of external forces. As far as the system itself is concerned, it is therefore a conserved quantity, irrespective of the nature of the internal interaction forces. Second, the linear momentum density is to some extent more directly measurable than particle velocity. For example, a hot-wire anemometer is known to more nearly measure linear momentum density than particle velocity.

A point to be made in passing is that this particular advantage is no longer a very strong reason, since as will be discussed later in this summary, we have developed a laser velocimeter for measuring the components of fluctuating velocity in supersonic heated flows.

In concluding his remarks concerning the selection of field variables, Doak states:

Thus, with the auxiliary condition that B_i is purely solenoidal, there are three primary scalar field variables (p , ρ and ψ) and one primary vector field variable (B_i). In respect to the objectives of an identification scheme, the advantages of these field variables are at once apparent from the mass transport equation, which becomes simply (and exactly)

$$\frac{\partial^2 \psi}{\partial x_i^2} = \frac{\partial \rho}{\partial t}, \quad (3-4)$$

a Poisson equation for the scalar potential ψ in terms of the rate of change of mass density as a source term.

Finally, Doak names his new field variables:

...The scalar potential, ψ , of the linear momentum density can be regarded, for identification purposes, as depending only upon the fluctuating mass density (and vice versa) and not at all explicitly, upon either the solenoidal linear momentum density, B_i , or the pressure, p . To thus identify these quantities, ψ and ρ' , Doak has called them pyknodynamic, meaning 'associated with time-varying mass density' (by analogy to 'electrodynamic,' which of course means 'associated with varying electrical charge density')³². Since $\partial\psi/\partial x_i$ is thus, by definition, the pyknodynamic part of the linear momentum density, so B_i must, by logical consequence of this, be called the pyknostatic part of the linear momentum density.

These variables are used to derive a wave-type equation which Doak says leads to:

Natural and physically meaningful identifications of 'acoustic' and 'thermal' parts of the fluctuating mass density, scalar potential and pyknodynamic pressure. The resulting equations permit elimination of the 'acoustic' parts of the pressure and mass density in favor of the 'acoustic' part of the scalar potential, for which a fourth order inhomogeneous partial differential equation can be obtained [equation (43) of reference 33].

Also he has shown that under somewhat more general conditions, a fifth order inhomogeneous partial differential equation for the total fluctuating scalar potential can be obtained [equation (25) of reference 33].

Thus, taken together, the studies of Doak^{32,33} and Crow²² provide very strong evidence that, for the entire range of subsonic and supersonic jet flows, (a) only the "turbulent" and "thermal" fluctuations can be regarded as contributing to the generation of aerodynamic sound and (b) the convection and refraction of the sound by the disturbed flow must be taken into account explicitly.

In a later development, Doak³⁷ showed that his theory, in the limit of a transversely sheared, parallel flow, reduced to a generalized analog of the Landahl-Lilley equation.

Of Lilley's equation, he unequivocally stated⁹:

It has to be concluded that none of the existing theoretical predictions of aerodynamic noise from either mixing regions or boundary layers, excepting only that of Lilley²⁸ can be regarded at present as complete and correct. At best all other predictions are incomplete; at worst they are incorrect. For full emphasis of this point, it has to be added that 'all other' in this context means 'absolutely all other' predictions of the generation and radiation of aerodynamic noise from jet mixing regions and boundary layers, and includes the predictions of Lighthill, Ribner, Powell, Phillips, Ffowcs Williams, Crow, Pao and Lawson, and all predictions made by others using the basic formulations of these authors. In Schubert's work¹⁸ also,

because of his assumption of a relatively low Mach number and his adoption of Obukhov's 'quasi-potential,' it turns out that the shear refraction effects have not been completely taken into account. Lilley's recent work²⁸ is the only formulation of an aerodynamic noise generation and radiation problem in which the shear refraction terms have been properly recognized and included.

Thus, while Doak's theory was not reduced to numerical solution during this program, it provided the foundation for a unified theory of supersonic jet noise generation and furthermore formed the very fundamental yardstick for the evaluation of other jet noise theories.

It has been briefly remarked that Lilley's equation was the foundation of our analytical and numerical results in the detailed study of supersonic jet noise. Thus, to set the stage for work to follow, the derivation of Lilley's equation will be outlined.

3.2 LILLEY'S EQUATION

A derivation of Lilley's convected wave equation is accomplished in the following manner²⁸. For an inviscid, ideal, non-thermally conducting gas

$$\left. \begin{aligned} \frac{1}{\rho} \frac{D\rho}{Dt} + \frac{\partial v_k}{\partial x_k} &= 0 && \text{(mass balance)} \\ \frac{Dv_i}{Dt} + \frac{1}{\rho} \frac{\partial p}{\partial x_i} &= 0 && \text{(linear momentum balance)} \\ \frac{1}{\rho} \frac{Dp}{Dt} - \frac{\gamma}{\rho} \frac{D\rho}{Dt} &= 0 && \text{(energy balance - isentropy condition).} \end{aligned} \right\} \quad (3-5)$$

With the aid of the definitions

$$\begin{aligned} r &\equiv \log p/p_\infty \\ a^2 &\equiv \gamma p/\rho \quad \text{(local isentropic sound speed)} \end{aligned}$$

where p_∞ is a constant, reference pressure, these three equations can be combined into two equations in r , a_∞ and v_i :

$$\frac{Dr}{Dt} + \gamma \frac{\partial v_k}{\partial x_k} = 0, \quad (3-6)$$

$$a^2 \frac{\partial r}{\partial x_i} + \gamma \frac{Dv_i}{Dt} = 0. \quad (3-7)$$

Taking the divergence of the second of these two equations and subtracting from it the material derivative of Equation (3-6) gives Phillips' equation²³:

$$\frac{\partial}{\partial x_i} \left(a^2 \frac{\partial r}{\partial x_i} \right) - \frac{D^2 r}{Dt} = -\gamma \frac{\partial v_i}{\partial x_j} \frac{\partial v_j}{\partial x_i} . \quad (3-8)$$

It can be shown that the material derivative of Equation (3-8) produces [upon making use of (3-7)]:

$$\frac{D}{Dt} \frac{\partial}{\partial x_i} \left(a^2 \frac{\partial r}{\partial x_i} \right) - \frac{D^3 r}{Dt^3} - 2 \frac{\partial v_j}{\partial x_i} \frac{\partial}{\partial x_j} \left(a^2 \frac{\partial r}{\partial x_i} \right) = 2\gamma \frac{\partial v_i}{\partial x_j} \frac{\partial v_j}{\partial x_k} \frac{\partial v_k}{\partial x_i} \quad (3-9)$$

Consider now the perturbation situation assumed by Lilley, namely

$$r = \log \frac{p}{p_\infty} = \log \frac{(p_\infty + p')}{p_\infty} \approx p'/p_\infty = r' \quad (3-10)$$

(i.e., the mean pressure is uniform and the pressure fluctuations are relatively small);

$$v_i = (\bar{v}_1(x_2) + v_1', v_2', v_3') \quad (3-11)$$

where the fluctuating velocity components are small compared to the speed of sound;

$$a^2 = \bar{a}^2(x_2) + a^{2'} \approx \bar{a}^2(x_2) + \bar{a}^2(x) \left[\frac{p'}{p_\infty} - \frac{\rho'}{\rho} \right] . \quad (3-12)$$

For these assumptions, Equation (3-9) becomes

$$\begin{aligned} \frac{D^3 r'}{Dt^3} - \frac{D}{Dt} \frac{\partial}{\partial x_i} \left(\bar{a}^2 \frac{\partial r'}{\partial x_i} \right) + 2 \frac{\partial \bar{v}_1}{\partial x_2}(x_2) \frac{\partial}{\partial x_1} \left(\bar{a}^2 \frac{\partial r'}{\partial x_2} \right) = \\ - 6\gamma \frac{\partial \bar{v}_1(x_2)}{\partial x_2} \frac{\partial v_2'}{\partial x_k} \frac{\partial v_k'}{\partial x_1} \\ - 2\gamma \frac{\partial v_i'}{\partial x_j} \frac{\partial v_j'}{\partial x_k} \frac{\partial v_k'}{\partial x_i} + \text{higher order terms.} \end{aligned} \quad (3-13)$$

This is the usual general form of Lilley's equation and it completely satisfies the requirements of having all linear acoustic/mean flow and acoustic/mean temperature interaction terms on the left-hand side, while the remainder of the terms on the right-hand side are quadratic or higher order in the fluctuation quantities.

4. SUMMARY OF RESULTS

The review material and theoretical development presented in Sections 2 and 3 portrays the situation at the beginning of the Phase II contract, which was a complete theoretical and experimental investigation of the generation and radiation of supersonic jet noise. The initial theoretical approach had been selected in the Phase I conceptual studies and the experimental problems which had to be dealt with were determined. These problem areas had to be solved to achieve the goal of providing accurate data (i) for verification of the theory, once numerical solution had been accomplished, and (ii) to provide a basis for analytical model development, as necessary.

The specific program objectives were:

(1) the study of solutions to and limitations of and development of extensions to Lilley's theory of jet noise generation; this study would consist of (a) the further development of a deterministic large-scale model of turbulence as a source of jet noise, (b) the study of numerical solutions of Lilley's theory for assumed jet noise source distributions, and (c) the study of numerical solutions of Lilley's theory for jet noise source distributions computed from the deterministic turbulence model;

(2) the development of and qualification of anechoic facilities suitable for measurement of far-field, high-temperature supersonic jet noise without significant interference with the noise generation and radiation process;

(3) the acquisition and analysis of data from jet noise and turbulence experiments necessary for validation of the theoretical models and predictions; in addition, these experiments were to provide the basis for new theoretical models as required; and

(4) the development of optical instrumentation for providing the necessary turbulence data, in this case a laser velocimeter for the measurement of turbulence velocity intensity, scale, spectra and convection speeds, as well as mean flow velocity. In addition, the instrument must provide cross-spectra and cross-correlation information from orthogonal turbulence components at a point.

At the end of the Phase I "conceptual study" program, the state-of-the-art theory had been established. It was also established at that time that several problems existed with regard to experimental observations. The published jet noise experimental data suffered from several problems which fell in the following categories:

- o Facility contamination - The majority of published data appeared to suffer from some form of this problem. Contamination resulted from (i) free-field interference which ranged from reflections from wedges in ill-designed anechoic rooms to ground reflections in outside facilities, (ii) jet mixing interference such as insufficient entrainment air or wake impingement in anechoic rooms, and (iii) upstream noise and turbulence in jet rigs leading to erroneous far-field noise scaling laws.

- o Inadequate envelope of jet operating conditions - There was no single data source which covered the desired span of exit velocity and temperature. There were many ad hoc tests which covered selected portions of the data range, but as a result of suspected facility contamination, many of these were questionable to some degree.
- o Separation of effects - All of the supersonic jet noise data published contained both shock-associated noise as well as turbulent mixing noise. There had been no attempt to separate the effects by testing with properly designed convergent-divergent nozzles. We had designed and manufactured three con-div nozzles in the Phase I program and had conducted preliminary tests in an available anechoic room, but were faced with some of the facility contamination problems discussed above.

In addition to the jet noise data problems, there was no instrumentation available for measuring turbulence characteristics in a high temperature supersonic flow. The Laser Velocimeter (LV) had been identified as the most promising instrument for accomplishing this and the development of an LV, which measured components of mean and turbulent velocity and turbulent spectra in this high temperature supersonic flow environment, was a goal during this program.

In this section the experimental program will be discussed, including reference to facility or instrument validation. Following this will be a summary of the results obtained in the theoretical and numerical studies.

4.1 EXPERIMENTAL PROGRAM

This subsection will include descriptions of the results from both the noise and the jet flow experiments. Complete descriptions of these results are given in the interim report and Volume II of this final report.

4.1.1 Jet Noise Experiments

The jet noise program was conducted in two phases. In the first phase, the turbulent mixing noise was carefully examined. In order to accomplish this, in addition to extraordinary care in the facility design and calibration, a set of three carefully designed and precisely machined convergent-divergent nozzles were tested at their design operating conditions (as determined optically from Schlieren photographs) in order to eliminate the noise of shocked jet flow. The shock-associated jet mixing noise was studied by conducting tests at conditions equivalent to the turbulent mixing noise test conditions, but with a convergent nozzle, incorporating screech suppression. Thus, the shock-associated noise contained only the broad-band component associated with turbulence-shock cell interaction.

Before conducting the noise tests, the facility was subjected to extensive calibration testing. These calibrations consisted of inverse square law tests in the anechoic free-field environment, ambient noise tests, instrumentation noise tests, jet rig internal noise tests, and jet noise near-field/far-field determination. These results are summarized in Appendix I.

4.1.1.1 Turbulent mixing noise experiments[†]

Results from jet noise experiments have been published in the past by a large number of investigators. However, one of the most useful studies was that conducted by Lush⁵, in which the characteristics of turbulent mixing noise from *unheated* jets operated at *subsonic* exhaust velocities were examined experimentally in great depth. The inadequacies of the freely-convecting quadrupole theories¹⁻⁴, which do not account for the changes in radiation efficiency due to the shrouding of the sound sources in a jet flow by the mean flow environment, were highlighted by Lush (as discussed in detail in Section 2 of this report) over his restricted regime of jet operating conditions. As we now know, these differences between Lighthill theory and experiment are a result of acoustical mean flow interactions, and the detailed differences must be carefully documented in addition to providing data for detailed comparison with Lilley theory solutions.

In order to study these acoustic/mean-flow interaction effects quantitatively at all jet operating conditions of interest, it was vital to obtain turbulent mixing noise data of high accuracy over extensive ranges of jet velocity and exhaust temperature and to experimentally isolate the effects of velocity and temperature.

In order to accomplish this, the range of interest of the jet noise control parameters at the exhaust (velocity and temperature) was determined and a map of the various interrelated parameters (i.e., pressure ratio, density, Mach number, stagnation temperature) was constructed. This is shown in Figure 4.1. Since jet static temperature and jet velocity are the noise control parameters, a test plan was devised with independent variations of each of these. In the turbulent noise tests, it was necessary to minimize shock noise contamination. Thus, three convergent-divergent nozzles were designed by the method of characteristics, constructed from Inconel and tested to find the actual operating point. These nozzles are represented by the Mach 1.4, 1.7, and 2.0 lines in Figure 4.1. The convergent nozzle was used for all tests up to pressure ratios of 1.89. Note also that the variation of specific heat ratio, γ , with stagnation temperature was incorporated in the design of the test diagram, as γ varies from 1.40 at ambient temperature to 1.31 at 2000°F.

It is convenient to discuss the experimental results first at 90°, in order to minimize the added complications of flow acoustic interactions, and then to show the effects at other angles. There are three interesting velocity ranges in which to examine the temperature effects on spectra at 90°. These three ranges are illustrated in Figure 4.2 which shows the velocity dependence of overall noise at 90° for four values of jet temperature. The isothermal case ($T_j/T_o = 1$) shows the expected 8th power velocity dependence (actually 7.5 powers, to be discussed later). However, as the temperature is increased, two apparently different effects are observed. At high velocity, the noise is reduced as expected from dimensional analysis based on Lighthill's theory. However, at low velocity, an increase in temperature causes an increase in noise

[†]This section summarizes the results of jet noise experiments conducted during the Phase II program. More complete discussions of these tests and the data are found in References 38, 39, and 40 and Volume II, Section 2 of this report. A complete listing of the turbulent mixing noise data is included in Volume IV.

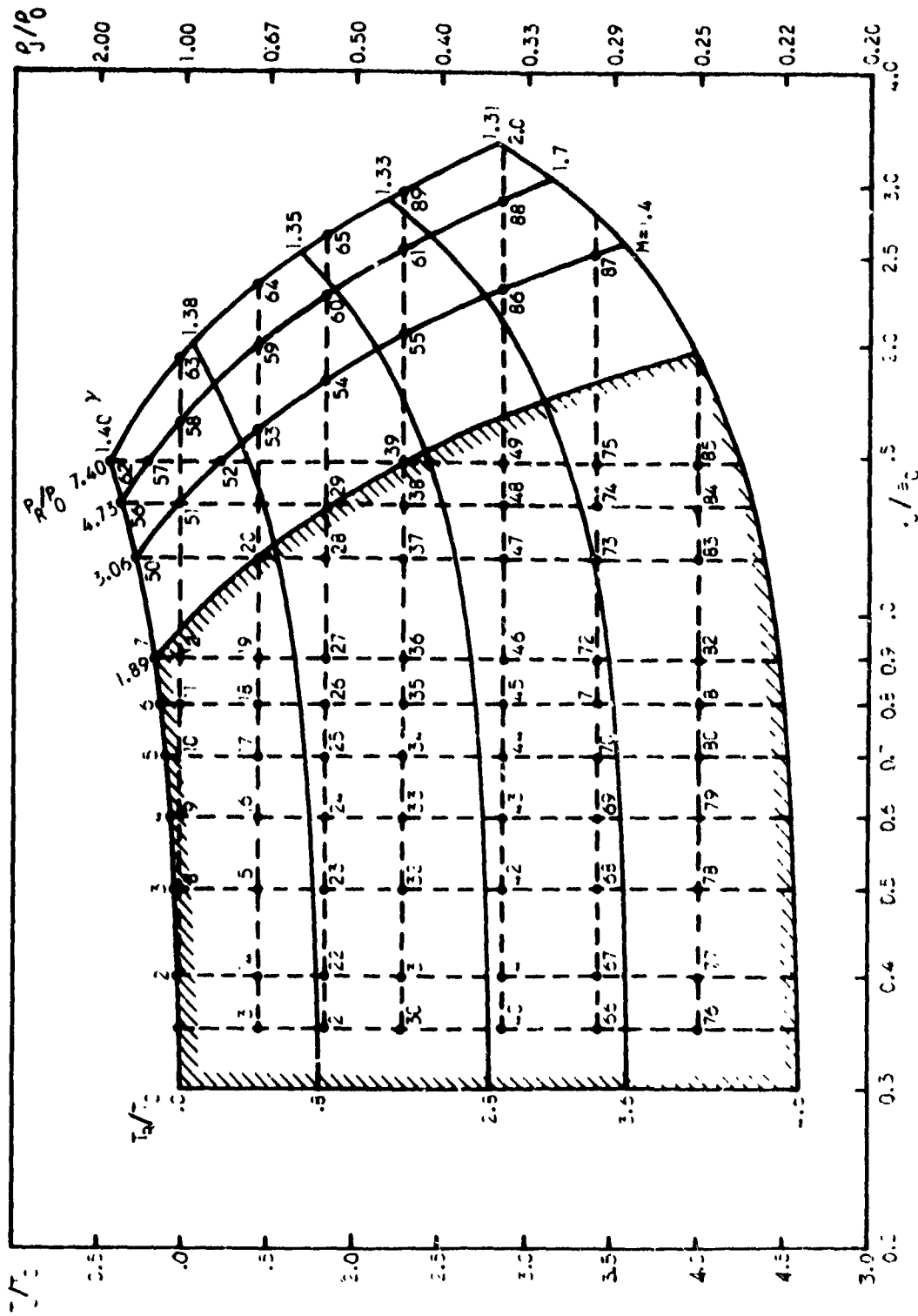


Figure 4.1 Experimental Program Chart

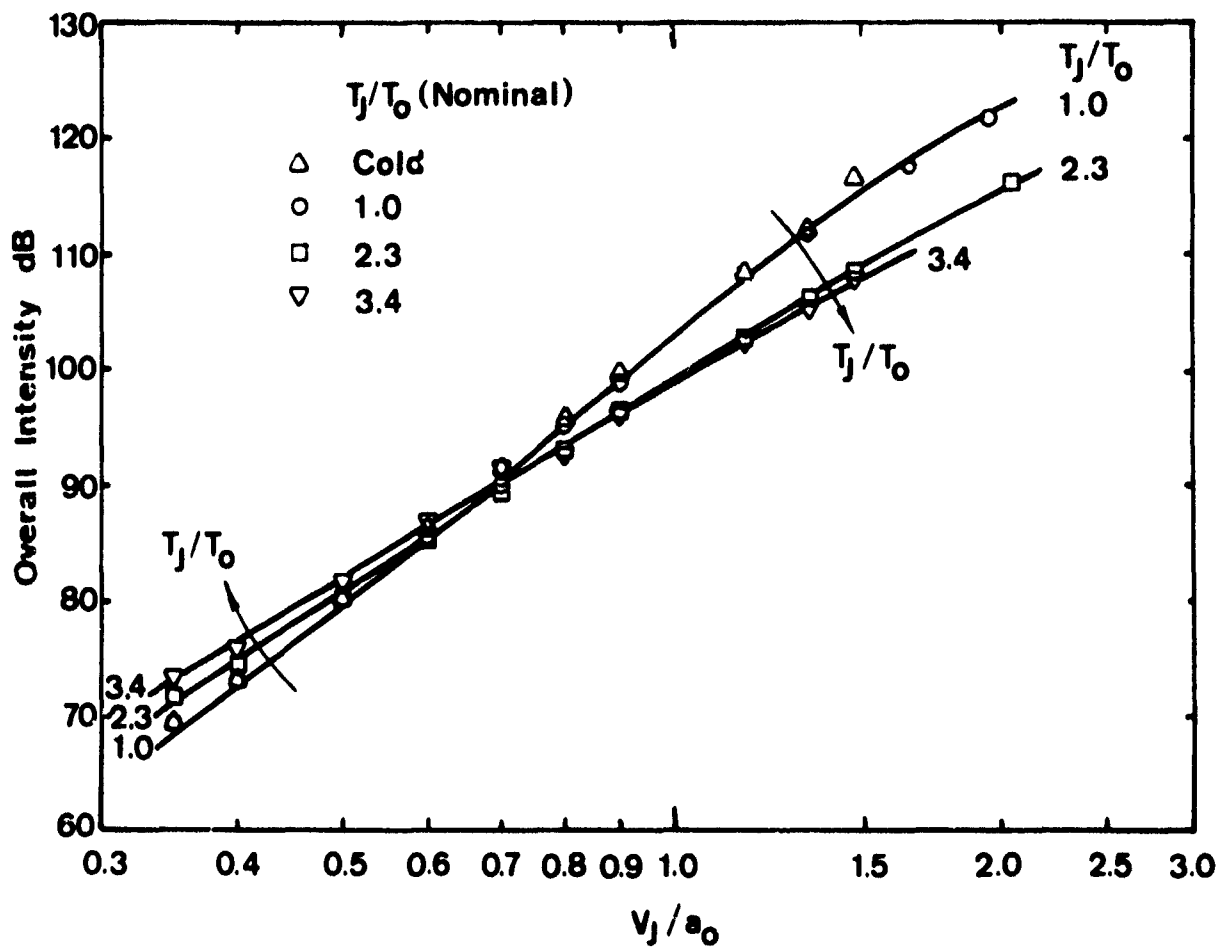


Figure 4.2 Effect of T_j/T_o on Velocity Dependence of Overall Intensity: $\theta = 90^\circ$

leading to speculation of the existence of an additional noise source. A detailed examination of the spectra for velocities below, at and above the reversal of temperature effects reveals other clues concerning the origin of the observed effect.

Figure 4.3 shows a comparison of measured spectra at low speed, $V_J/a_0 = 0.4$, for the isothermal jet (test point 2, see Figure 4.1) and at a high temperature (TP 41). The isothermal jet shows the characteristic broadband spectrum while the effect of elevated temperature clearly is to provide a significant noise increase, particularly in the lower frequencies.

Results for a medium velocity, $V_J/a_0 = 0.8$, are shown in Figure 4.4. Here all measurements on the constant velocity line between TP 6 and TP 45 have been included. At first sight it is tempting to conclude that the lower frequency portion of the spectrum is independent of temperature, while clearly the higher frequencies decrease progressively with increased temperature. However, a careful review of the data at a series of velocities in this region, indicated that this is an oversimplified view. As can be seen from Figure 4.4, the levels at these lower frequencies first decrease as one proceeds from TP 6 to TP 18 and then begin to increase again as the temperature is further increased.

Finally, at high velocity, it is observed that the spectrum decreases uniformly with increased temperature as shown in Figure 4.5. As can be seen from Figure 4.1, this data for $V_J/a_0 = 1.47$, covering the vertical line from TP 62 to TP 49, yields a large range of jet efflux temperature (i.e., T_J/T_0 varies by a factor of 5 between the lowest and the highest values). In the high frequency range, above 10 kHz, the spectrum for TP 52 actually crosses that for the lower temperature, TP 57. It was thought at first that this was indicative of shock-associated noise, due perhaps to poor "on-design" operation of this particular $M = 1.40$ nozzle. However, a systematic study of other data indicated that this uncharacteristic high-frequency contribution occurred irrespective of the velocity line considered and always was associated with the test point on that line for which the jet efflux temperature was closest to the ambient temperature; i.e., the rate of decrease of spectral level above 10 kHz was always at a minimum for the isothermal jet. When the jet temperature was different from the ambient, irrespective of the direction of this difference, a more rapid decrease was observed.

From these experimental data, one can speculate on scaling laws. In the early part of the Phase II program, a semi-empirical scaling law model was postulated in order to explain the measured results quantitatively. This scaling law model consisted of two noise sources. The first was "Reynolds shear stress noise," and the second was referred to as the "temperature fluctuation noise." The starting point for this model was an equation for sound pressure,

$$p = K_1 \left(\frac{\rho_S}{\rho_0} \right) \left(\frac{V_J}{a_0} \right)^2 \left(\frac{V_J}{a_0} \right)^n + K_2 \left(\frac{\Delta T}{T_J} \right) \left(\frac{V_J}{a_0} \right)^2. \quad (4-1)$$

The first term represents "Reynolds shear stress noise" that dominates at high V_J/a_0 , whereas the second term represents "temperature fluctuation noise" that dominates at low V_J/a_0 and high T_J/T_0 jet operation. It also will be noted that, for the moment, the power law dependence on velocity of the Reynolds

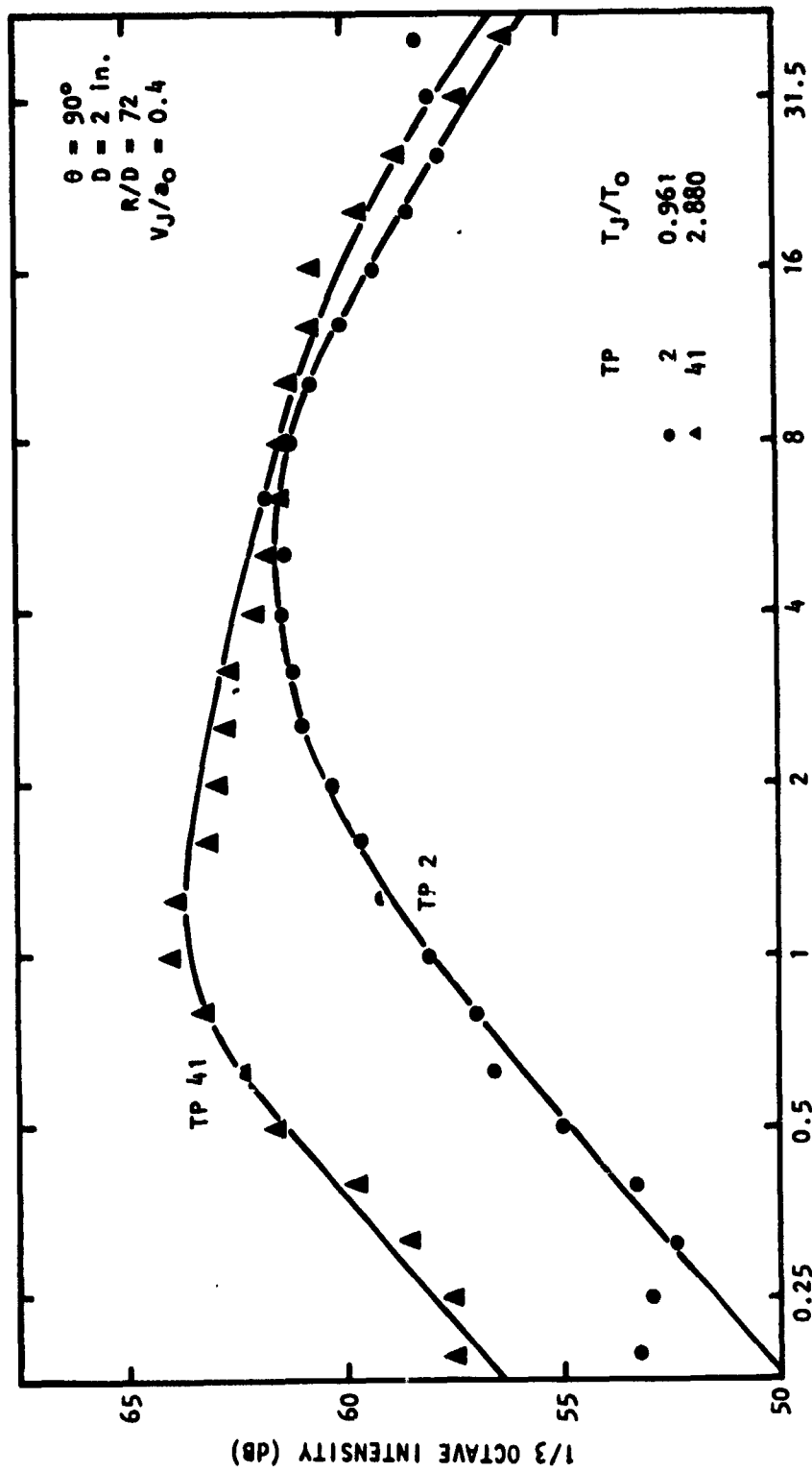


Figure 4.3 Effect of Temperature on Jet Noise at Low Velocity ($V_J/a_0 = 0.4$)

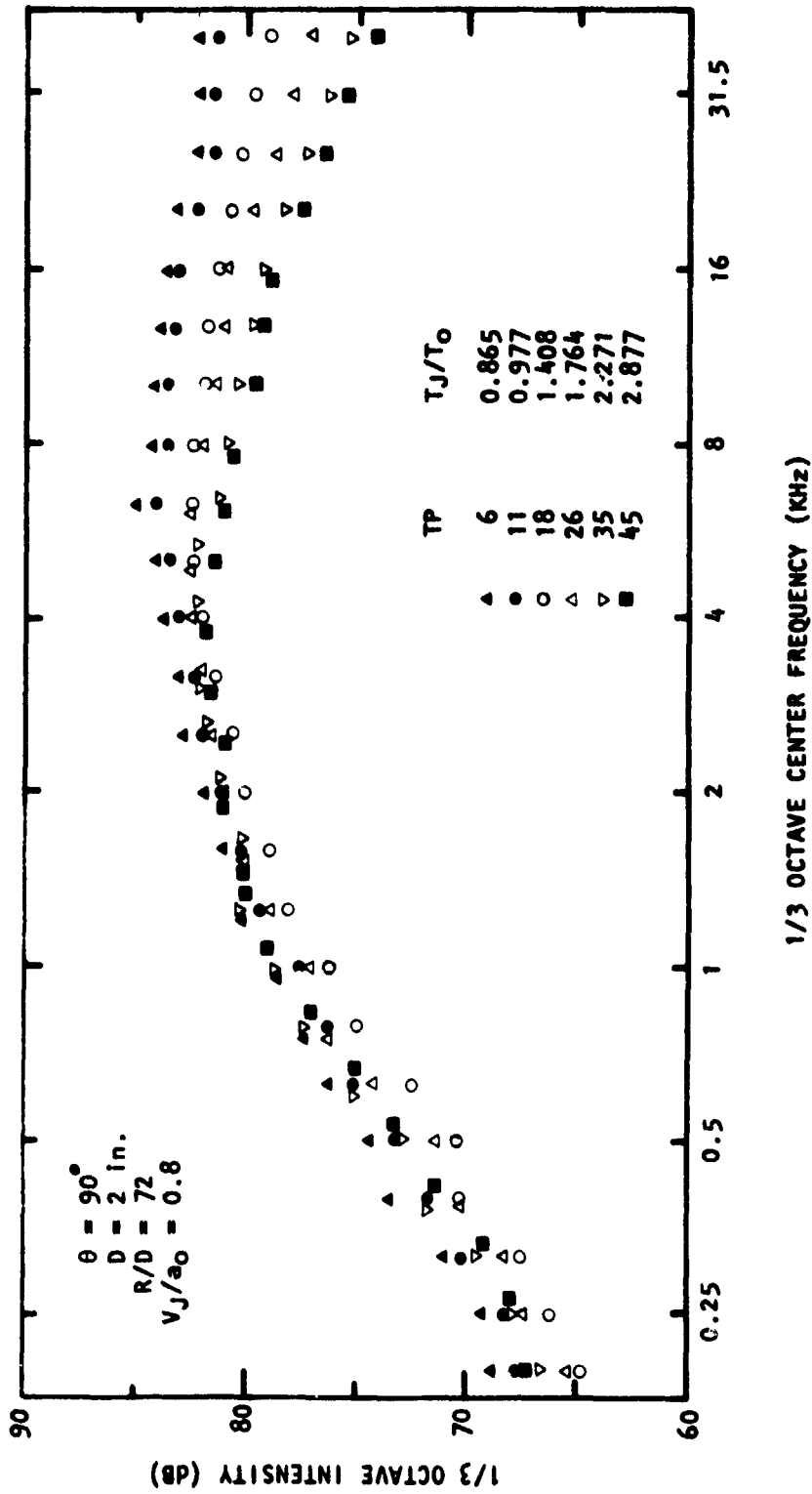
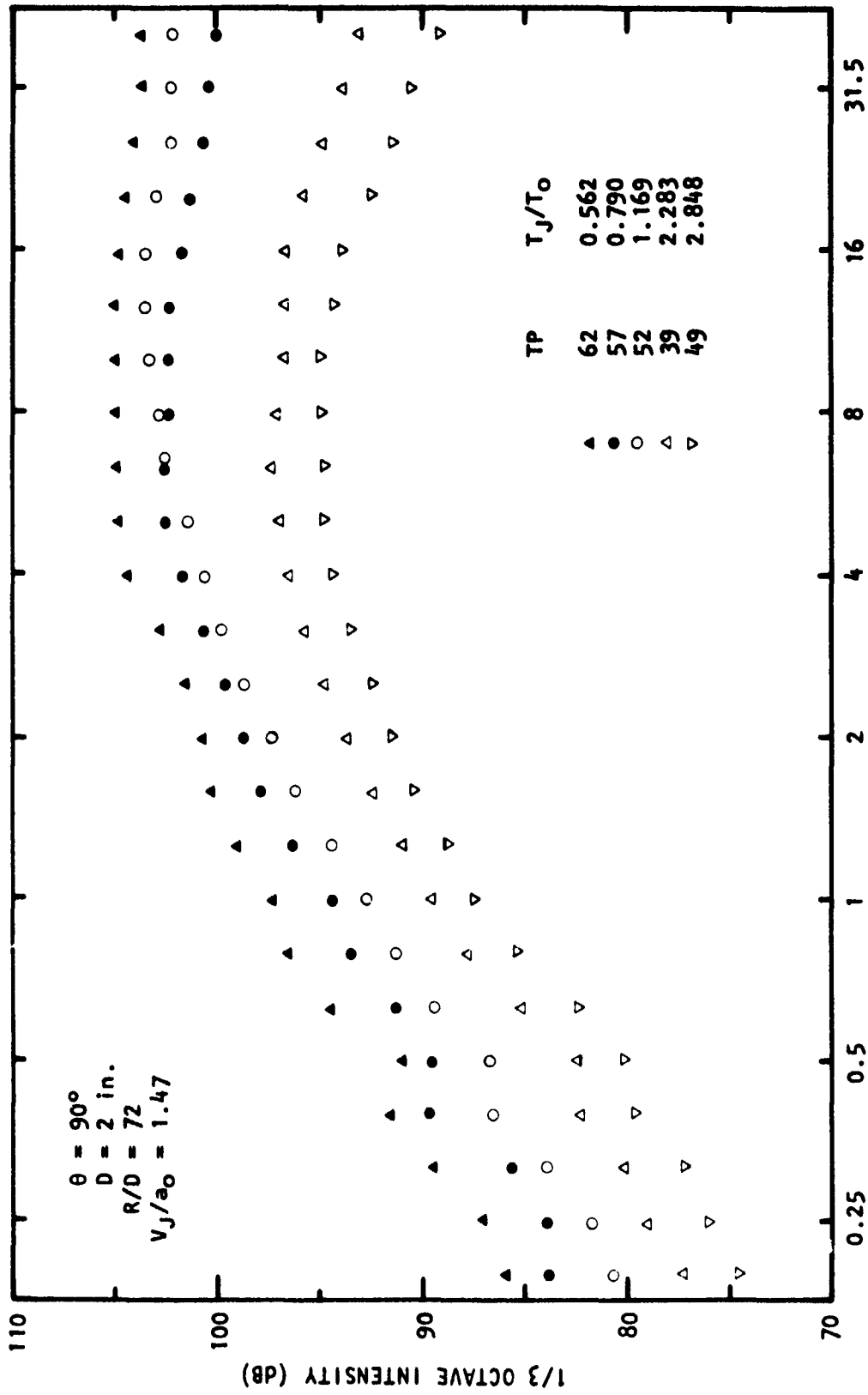


Figure 4.4 Effect of Temperature on Jet Noise at Medium Velocity
 $(V_J/a_0 = 0.8)$



1/3 OCTAVE CENTER FREQUENCY (KHZ)

Figure 4.5 Effect of Temperature on Jet Noise at High Velocity
 $(V_J/a_0 = 1.47)$

shear stress term has been left to be determined. The $(V_J/a_0)^2$ portion of the dependence arises from the second time derivative on the assumption of the Strouhal number dependence of the acoustic radiation. The value of n , however, depends essentially on the variation of mean square turbulence level with velocity.

The postulated model indicates that the velocity dependence of the Reynolds shear stress contribution should be obtained from data for which the jet efflux temperature is equal to the ambient. In this case the second term on the right-hand side of the above equation is precisely zero. The velocity dependence therefore was obtained from spectra measured along the horizontal line of Figure 4.1, joining test points 1 and 63. After considerable examination of the data, it was found that the intensity for the isothermal case scaled best with 7.5 powers of velocity. This suggests that the turbulence intensity does not scale linearly with mean velocity and, in fact, suggests a turbulence scaling of $\sqrt{v'^2} \propto V_J^{0.875}$. This implies that the normally accepted peak turbulence level of 14.5% (from available hot-wire measurements) at velocities of the order $V_J/a_0 = 0.5$ might decrease to about 12% at $V_J/a_0 = 2.0$. This point will be discussed in more detail later, when high velocity turbulence measurements with the Lockheed-Georgia Laser Velocimeter (LV) are presented, which qualitatively support the observation above from the 90° acoustic data.

It was also possible to establish a temperature scaling factor. This was determined to be of the form suggested above by examining the data at a constant velocity ratio for variation in jet temperature.

The somewhat surprising aspect of this data examination was that the scaling law model compared favorably with the measurements only when the two noise sources were assumed to be completely correlated in the statistical sense. The final form of the scaling law for noise radiation at 90° was found to be

$$S(\omega) = \overline{a^2} + 2\sqrt{\overline{a^2}}\sqrt{\overline{b^2}} + \overline{b^2}$$

where

$$\overline{a^2} = S_m(\omega_s) \left(\frac{T_s}{T_0}\right)^{-2} \left(\frac{V_J}{a_0}\right)^{7.5}$$

$$\overline{b^2} = S_T(\omega_s) \left(\frac{2\Delta T}{T_J}\right) \left(\frac{V_J}{a_0}\right)^4$$

and where $S_m(\omega_s)$ and $S_T(\omega_s)$ are the master shear stress noise and master temperature fluctuation noise spectra, respectively, and are given in Figure 4.6. T_s is the source region temperature, ΔT is the temperature difference $T_J - T_0$, and $\omega/\omega_s = V_J/a_0$ (for scaling purposes). An example of the validity and usefulness of the scaling law model is shown in Figure 4.7, where a comparison between the measured and predicted overall SPL's for all data at 90° is presented.

It is emphasized that although the semi-empirical scaling law model summarized above was found to be accurate for the prediction of noise at 90° to the jet axis, and indeed can be used for prediction purposes in the future, the theoretical work conducted subsequently during the Phase II program (and

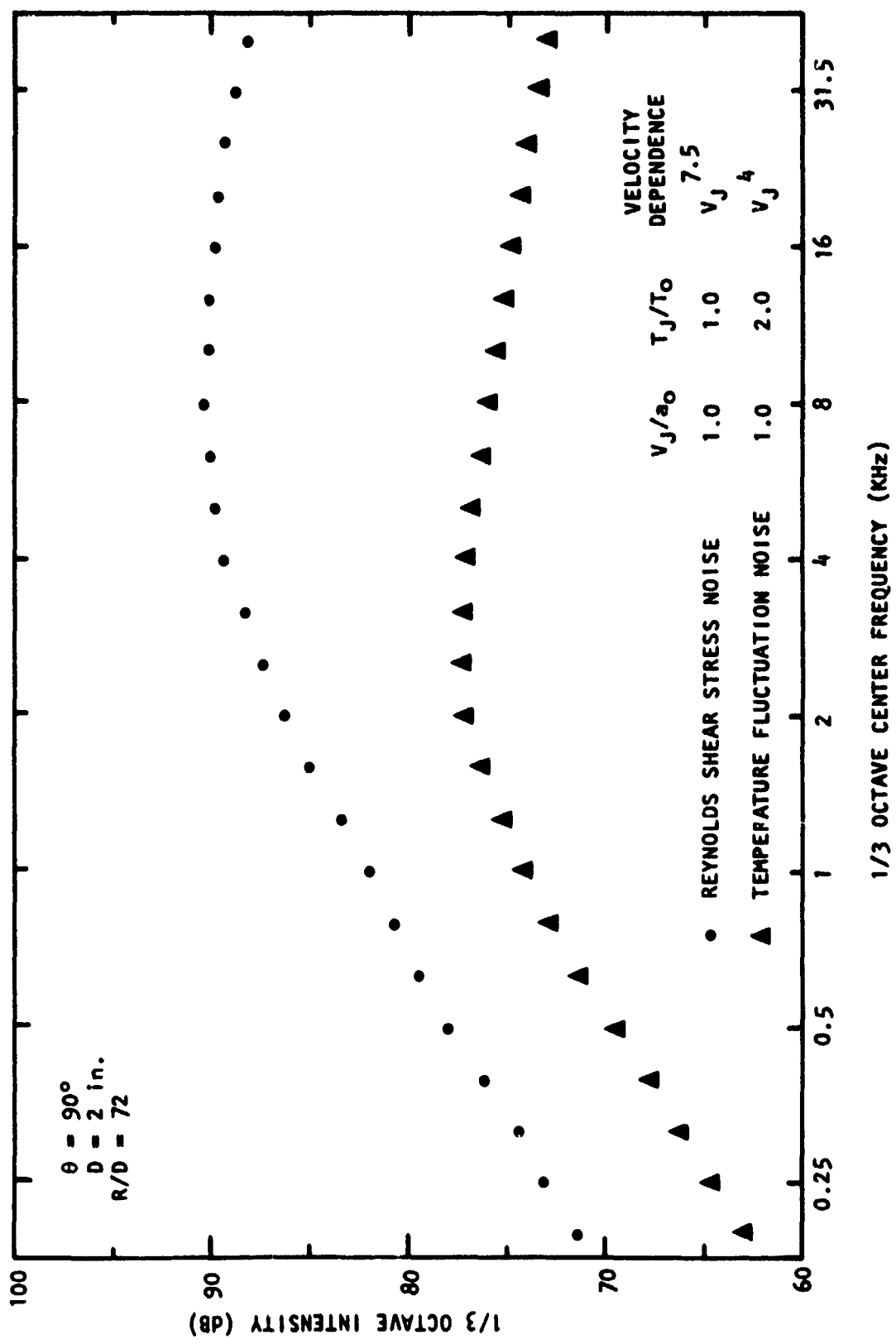


Figure 4.6 Master Spectra for Reynolds Shear Stress Noise and Temperature Fluctuation Noise, $\theta = 90^\circ$

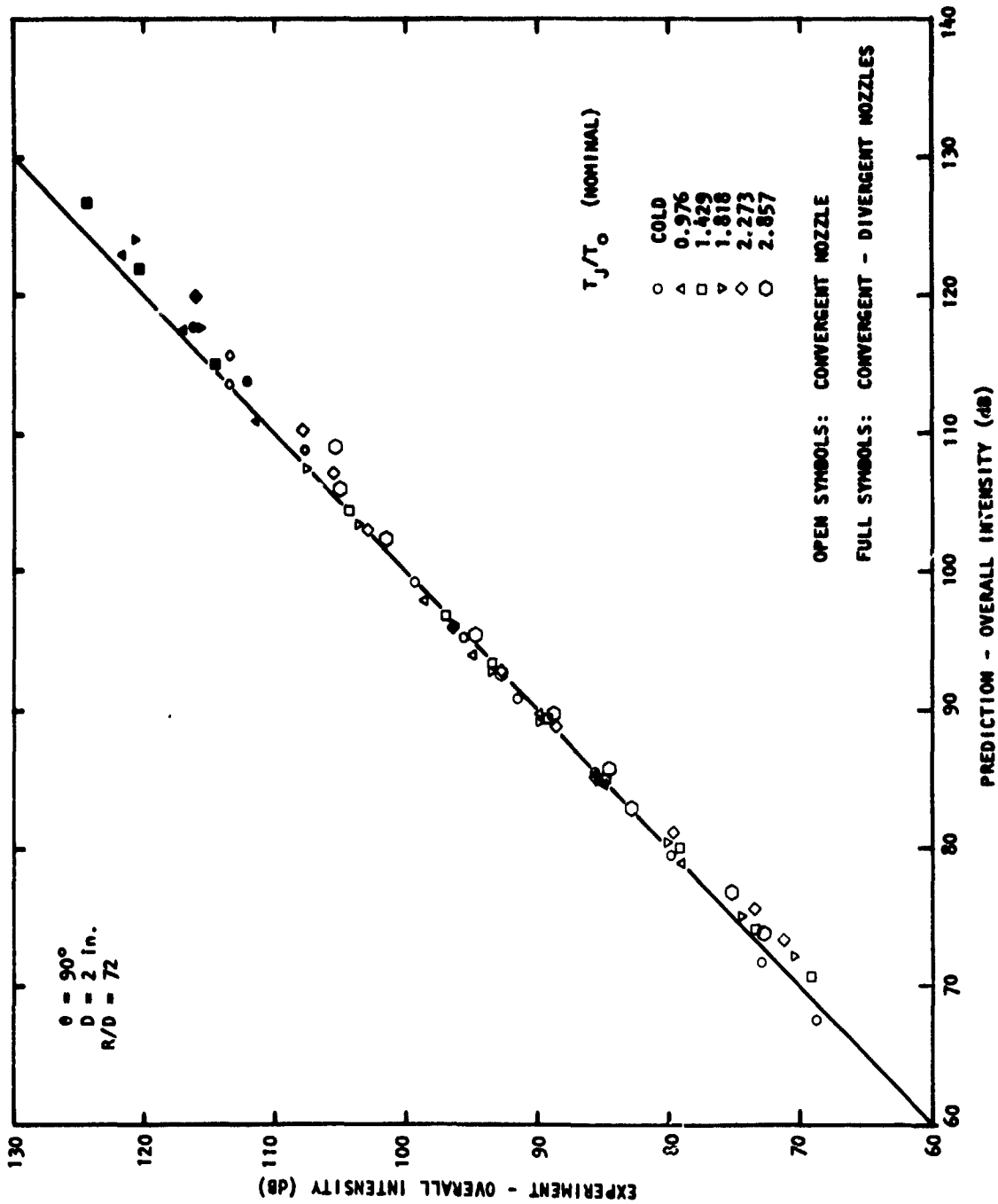


Figure 4.7 Comparison of Measured Overall Intensity at $\theta = 90^\circ$ with Prediction Model

discussed later in this section) provides more physically realistic for the temperature effects at 90° .

In order to examine the effects of temperature at other angles, it is useful to examine the directivity of overall intensity, shown in Figures 4.8 through 4.10 to gain an overall impression. At low velocity ($V_j/a_0 = 0.5$, it can be seen that the effect of heating observed previously at $\theta = 90^\circ$ holds at all angles; that is, the noise increases with heating. The directivities for $T_j/T_0 = 1$ and 3.4 are virtually parallel. On the other hand, at the medium jet velocity ratio of 0.9, the effect of heating is to produce a decrease in noise level. It is interesting to note that in Figure 4.9 over the range of T_j/T_0 considered here, there is no effect in the vicinity of $\theta = 40^\circ$, and as θ increases or decreases from 40° , there is a progressive reduction in overall intensity with heating. Finally, at $V_j/a_0 = 1.47$ (Figure 4.10), the reductions become very large indeed, especially near the jet axis.

The major effects of temperature on the noise spectrum and the variation of these effects throughout the speed range are illustrated in the vicinity of the peak radiation angle at $\theta = 45^\circ$ in Figures 4.11 through 4.13.

At low jet velocity ($V_j/a_0 = 0.5$, Figure 4.11), the effect of elevated temperature is to provide a significant noise increase at the lower frequencies, and a significant noise reduction at the higher frequencies. As the jet velocity increases, the noise increase at lower frequencies becomes less dramatic, and at high velocities ($V_j/a_0 = 1.47$, Figure 4.13), the noise levels at these frequencies in fact decrease with jet heating. In contrast, the effect at higher frequencies does not reverse as one proceeds from low to high V_j/a_0 ; the reductions in spectrum levels at these higher frequencies increase in magnitude as V_j/a_0 increases throughout the speed range.

At all velocities considered, the effects of jet heating described above alter the peak frequencies in a consistent manner; the peak frequencies decrease as the jet exit temperature ratio increases from unity. This suggests that it may be possible to scale the peak frequencies as a function of temperature.

As discussed in Section 2, it is imperative for comparison with theoretical results to extract directivity information from the jet noise data for constant *source* frequency. This was done in considerable detail for all the data taken. Those results will be shown, as appropriate, when comparing theory with experiment in Section 4.2.

4.1.1.2 Shock-associated noise

This experimental study[†] deals in particular, with the broadband component of shock-associated noise. To put the problem in perspective, when a convergent nozzle is operated at subcritical pressure ratio or when a convergent-divergent nozzle is operated at design pressure ratio, the acoustic spectrum

[†]These results are described in detail in Volume II, Section 7 and complete tabulations of the data are given in Volume IV.

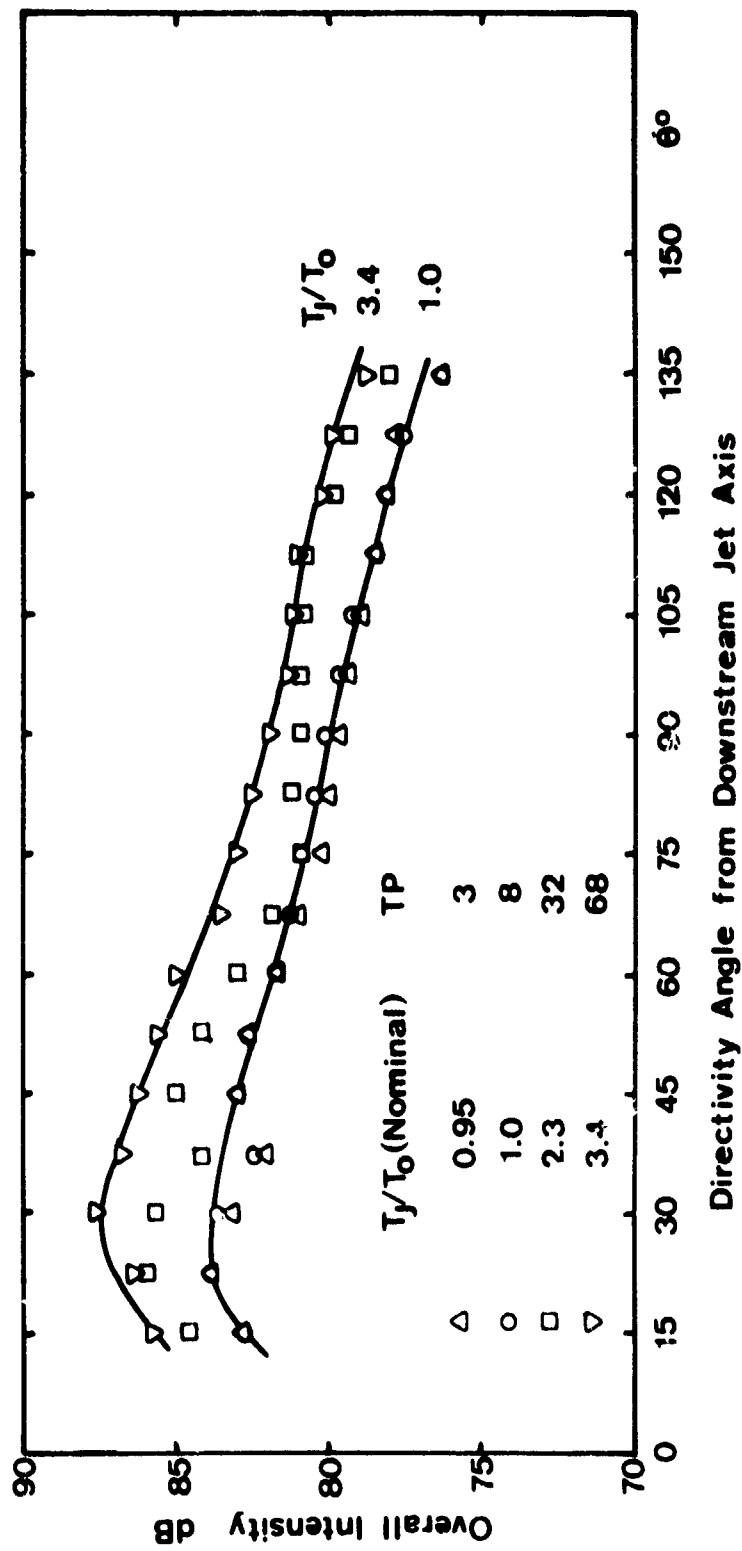


Figure 4.8 Effect of T_j/T_o on Directivity of Overall Intensity: $V_j/a_o = 0.5$

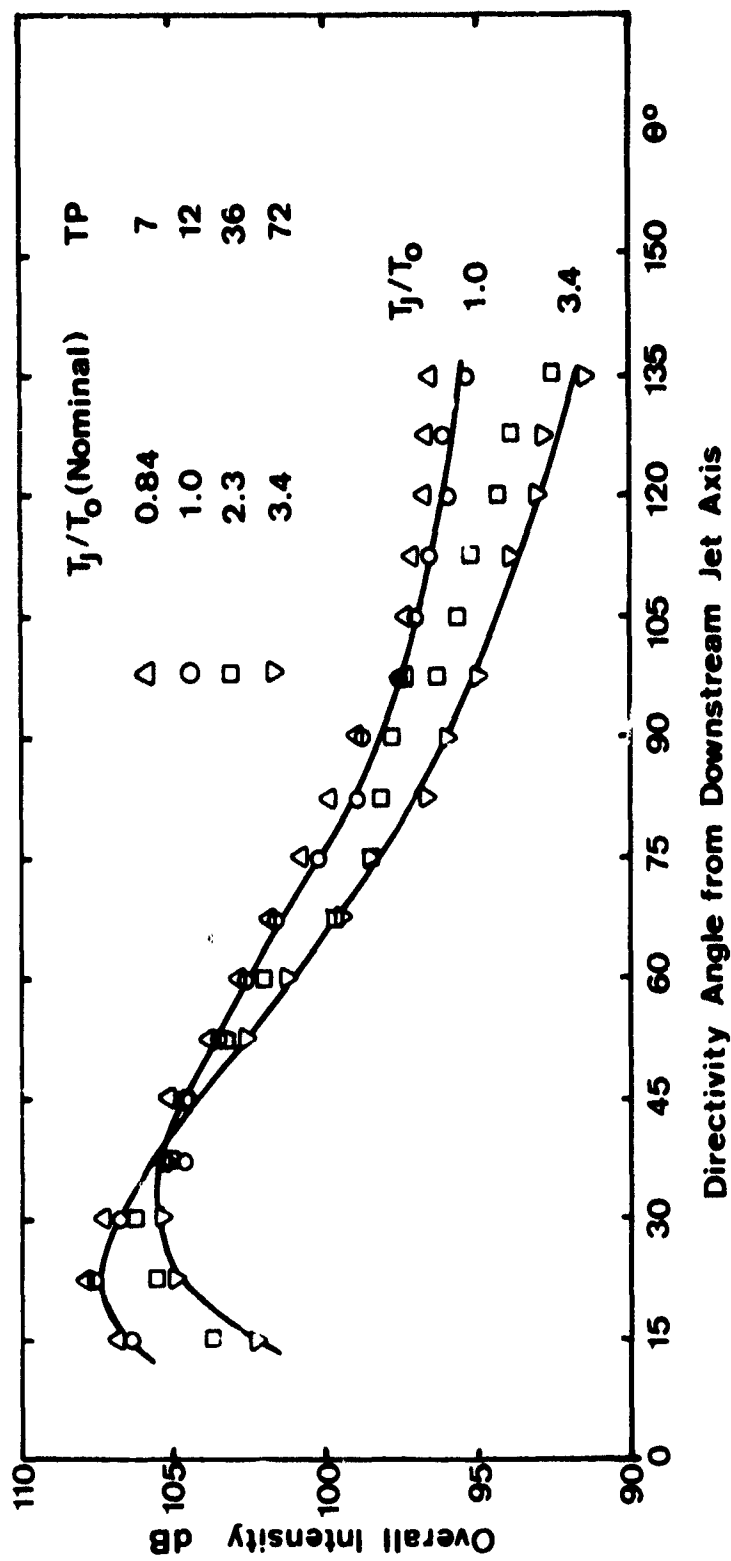


Figure 4.9 Effect of T_j/T_o on Directivity of Overall Intensity: $V_j/a_o = 0.9$

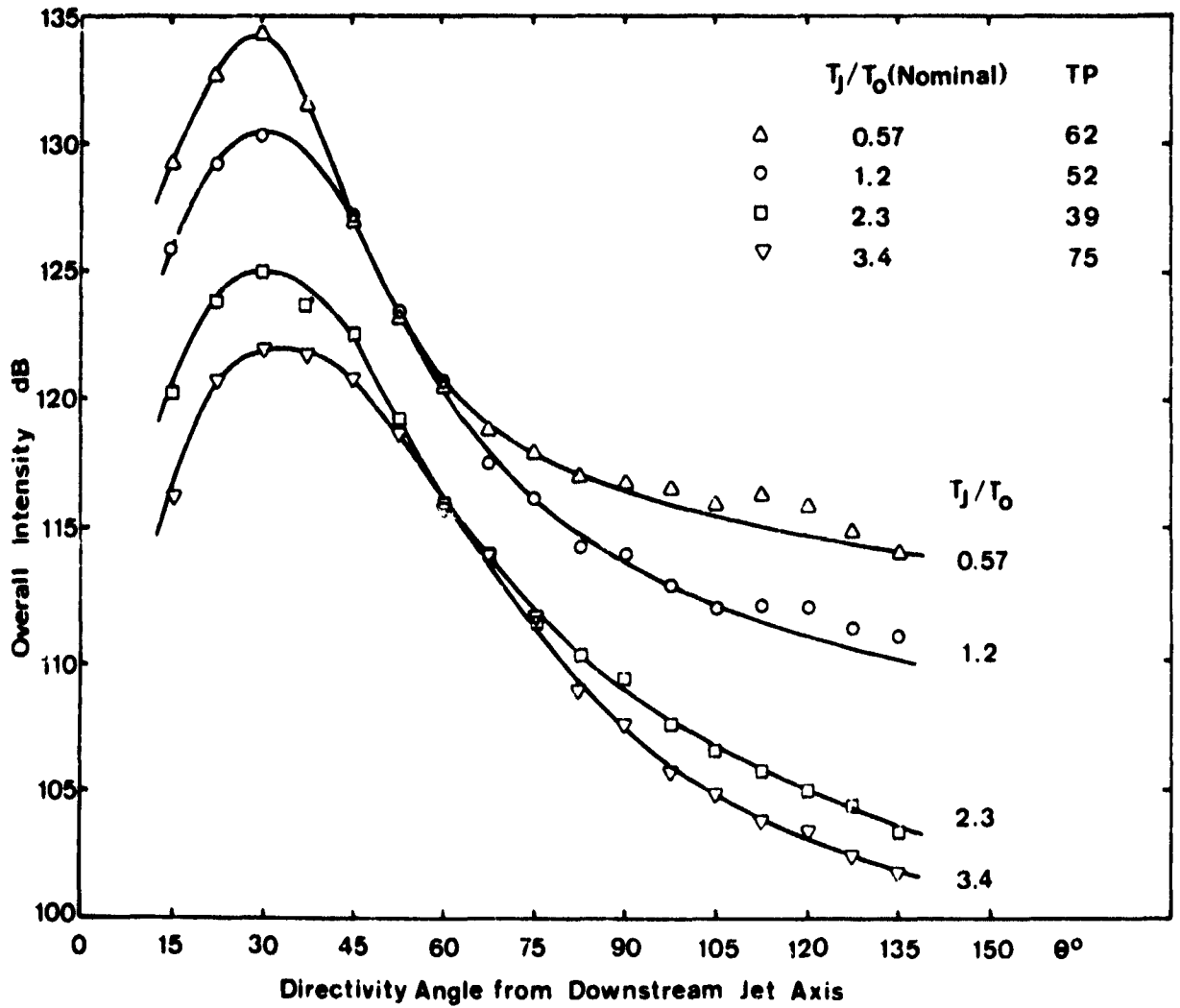


Figure 4.10 Effect of T_j/T_o on Directivity of Overall Intensity: $V_j/a_o = 1.47$

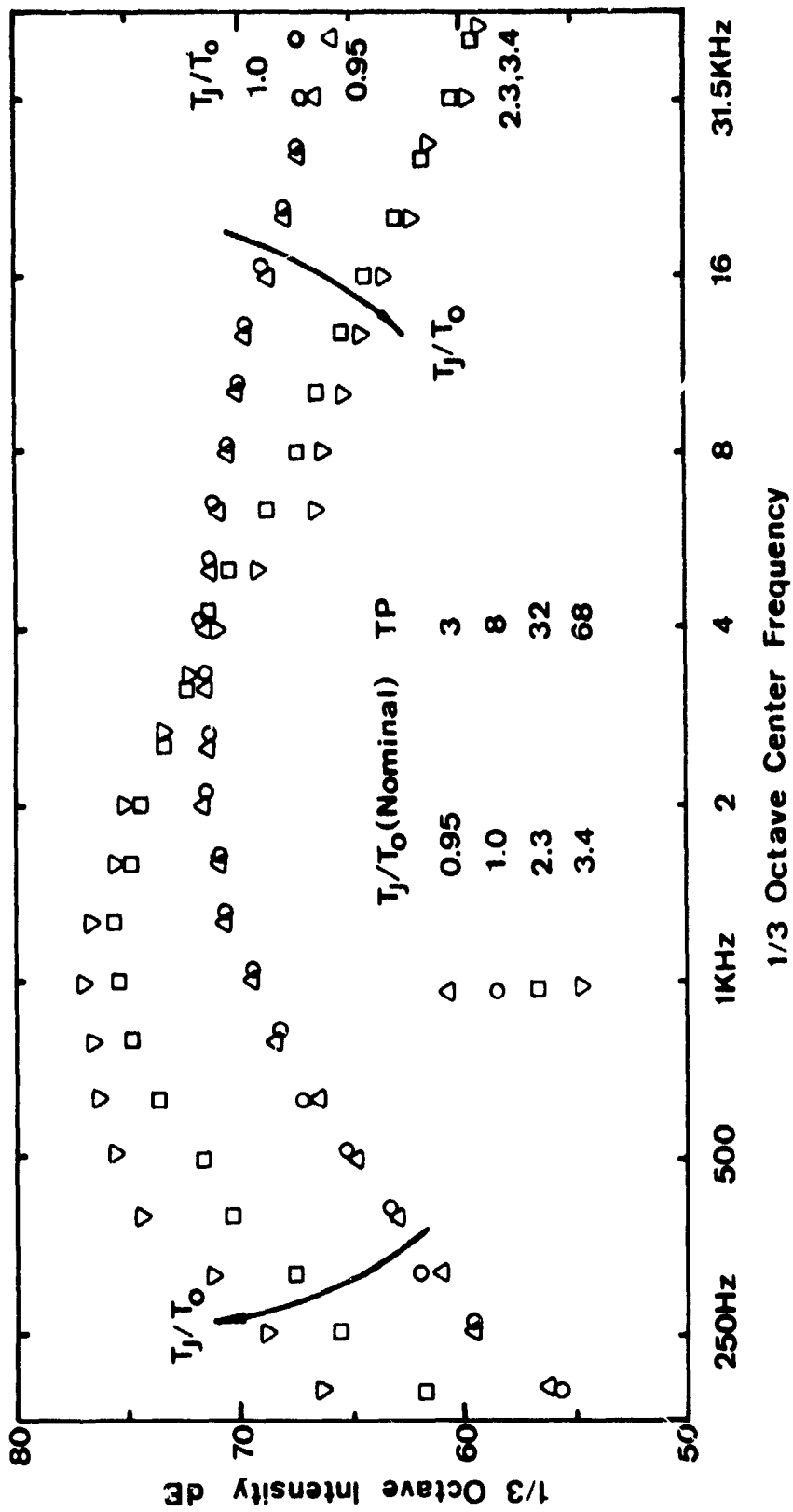


Figure 4.11 Effect of T_j/T_o on 1/3-Octave Spectra at Low Jet Velocity:
 $\theta = 45^\circ$, $V_j/a_o = 0.5$

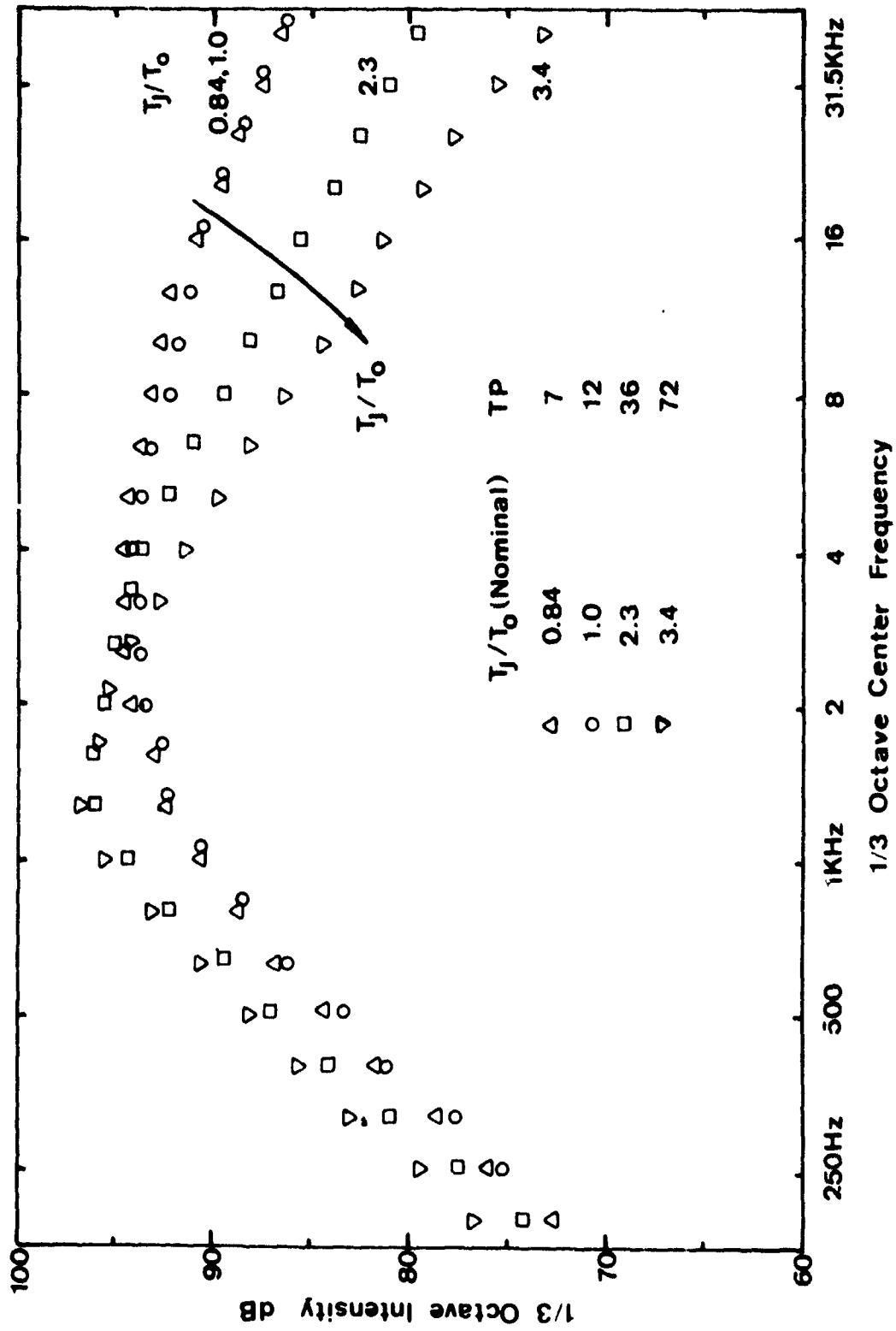


Figure 4.12 Effect of T_j/T_0 on 1/3-Octave Spectra at Medium Jet Velocity:
 $\theta = 45^\circ$, $V_j/a_0 = 0.9$

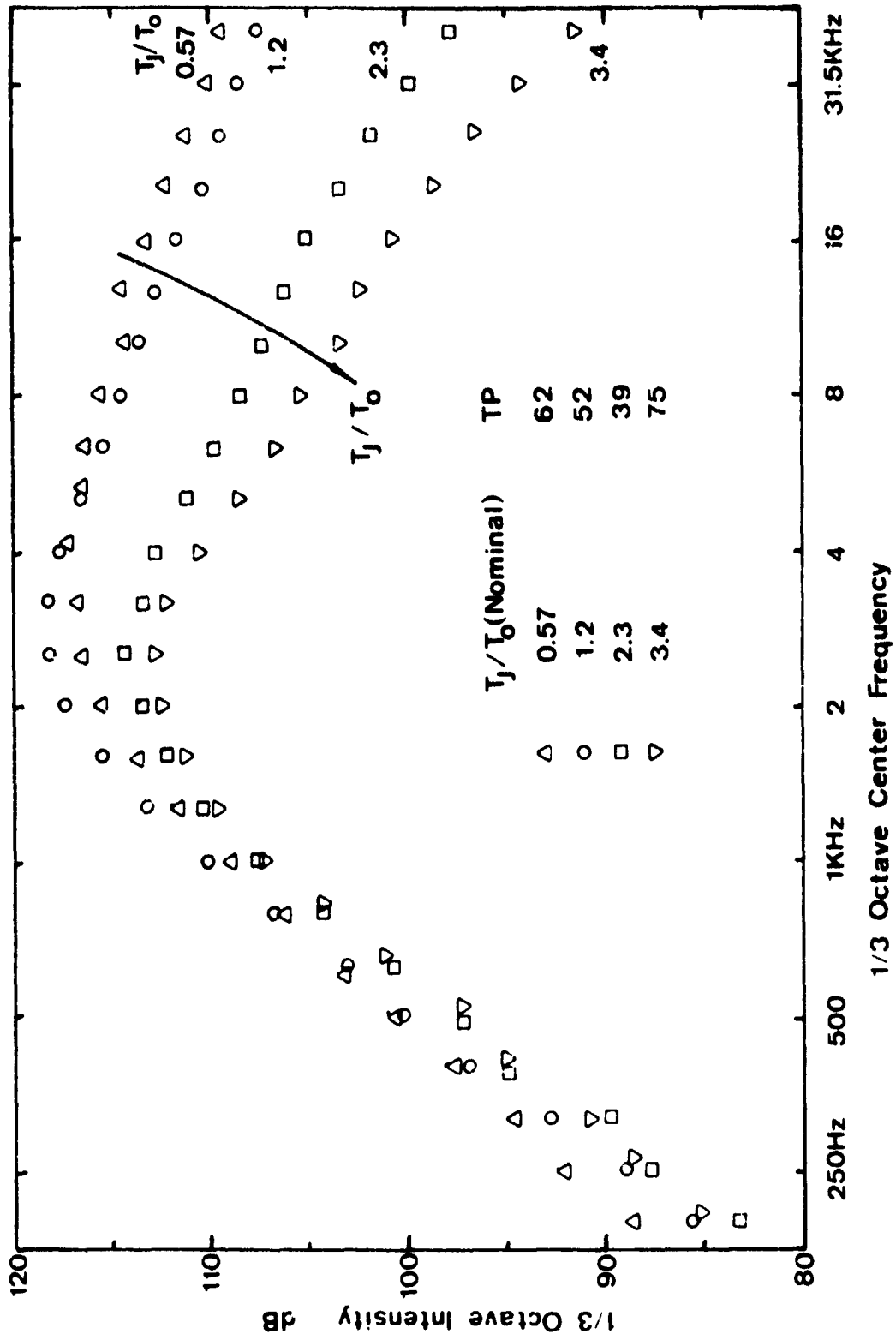


Figure 4.13 Effect of T_j/T_0 on 1/3-Octave Spectra at High Jet Velocity:
 $\theta = 45^\circ$, $V_j/a_0 = 1.47$

is broad and smooth, and consists of turbulent mixing noise. On the other hand, when a convergent nozzle is operated at supercritical pressure ratio (under-expanded) or when a convergent-divergent nozzle is operated at off-design Mach number (under-expanded or over-expanded), the resulting acoustic spectrum contains an extra noise contribution, due to the presence of shock structure in the jet flow, in addition to the basic turbulent mixing noise. The shock-related noise can be divided into two distinct types, each having its own characteristic properties. The first component is discrete in nature, usually with several harmonics, and is often referred to as the "screech" component. The second component is broadband in nature with a well-defined peak frequency. The former has been studied fairly extensively in the past, whereas the broadband shock-associated noise component has not been examined in great detail. In the present study, it is this broadband component that is investigated; and in order to examine its trends and dependencies accurately, the contribution from the screech component to the total sound field is suppressed without altering the turbulent mixing noise characteristics to any significant extent.

From early work, it is well known that shock-associated noise is primarily dependent on pressure ratio and is virtually independent of jet temperature, whereas turbulent mixing noise is controlled by velocity rather than pressure ratio. Thus, it can be concluded that shock-associated noise will be most significant in low-temperature, high velocity jets. Furthermore, it is also known that shock-associated noise is more or less omni-directional and would thus be expected to dominate at angles where turbulent mixing noise is minimum, that is, in the forward arc.

In order to quantitatively establish the characteristics of broadband shock-associated noise, it was necessary to formulate a test plan comparable to that described for turbulent mixing noise. In previous experimental investigations, it was observed that the intensity of shock-associated noise varied as

$$I \propto \beta^4, \text{ where } \beta = (M_J^2 - 1)^{\frac{1}{2}}.$$

Thus, as in the turbulent mixing noise tests, it is necessary to establish the exact variation of intensity with the control parameter. This led to the construction of a test diagram similar to Figure 4.1, as shown in Figure 4.14. In addition to the parameters of interest, T_J/T_0 and β , lines of constant velocity ratio, V_J/a_0 , and constant stagnation temperature, T_R/T_0 are shown, based on isotropic relationships. Correspondence between the shock-associated noise tests and the turbulent mixing noise tests occurs at β values of 0.94, 1.34, and 1.70, which corresponds to the design conditions for the Mach 1.4, 1.7 and 2.0 con-div nozzles. In addition, the temperature conditions chosen are those used for the turbulent mixing noise tests. Thus, for many of the test points, the pure turbulent mixing noise data can be compared directly with the shock-associated noise spectra.

To continue the preliminary assessment of the significance of broadband, shock-associated noise, the effects of temperature and velocity ratio are shown at three representative angles in Figure 4.15. In this chart, the turbulent mixing noise from subsonic jets and supersonic jets operating at the design pressure ratios is used as the reference and is displayed by the solid line and open-circles, whereas the shock noise from a convergent nozzle is shown by the solid symbols. This clearly shows the dominance of shock noise at large angles

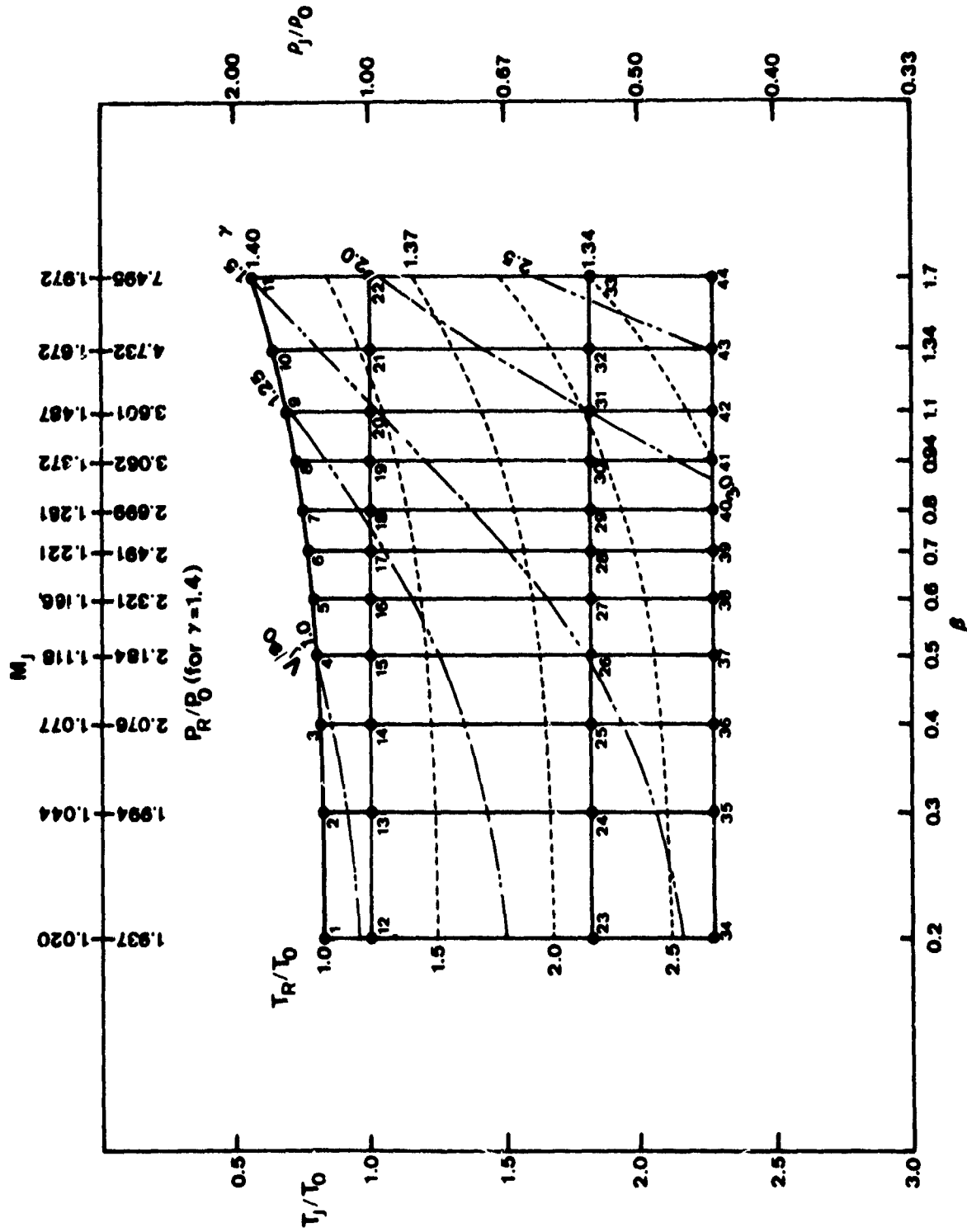


Figure 4.14 Experimental Program Chart for Shock-Associated Noise

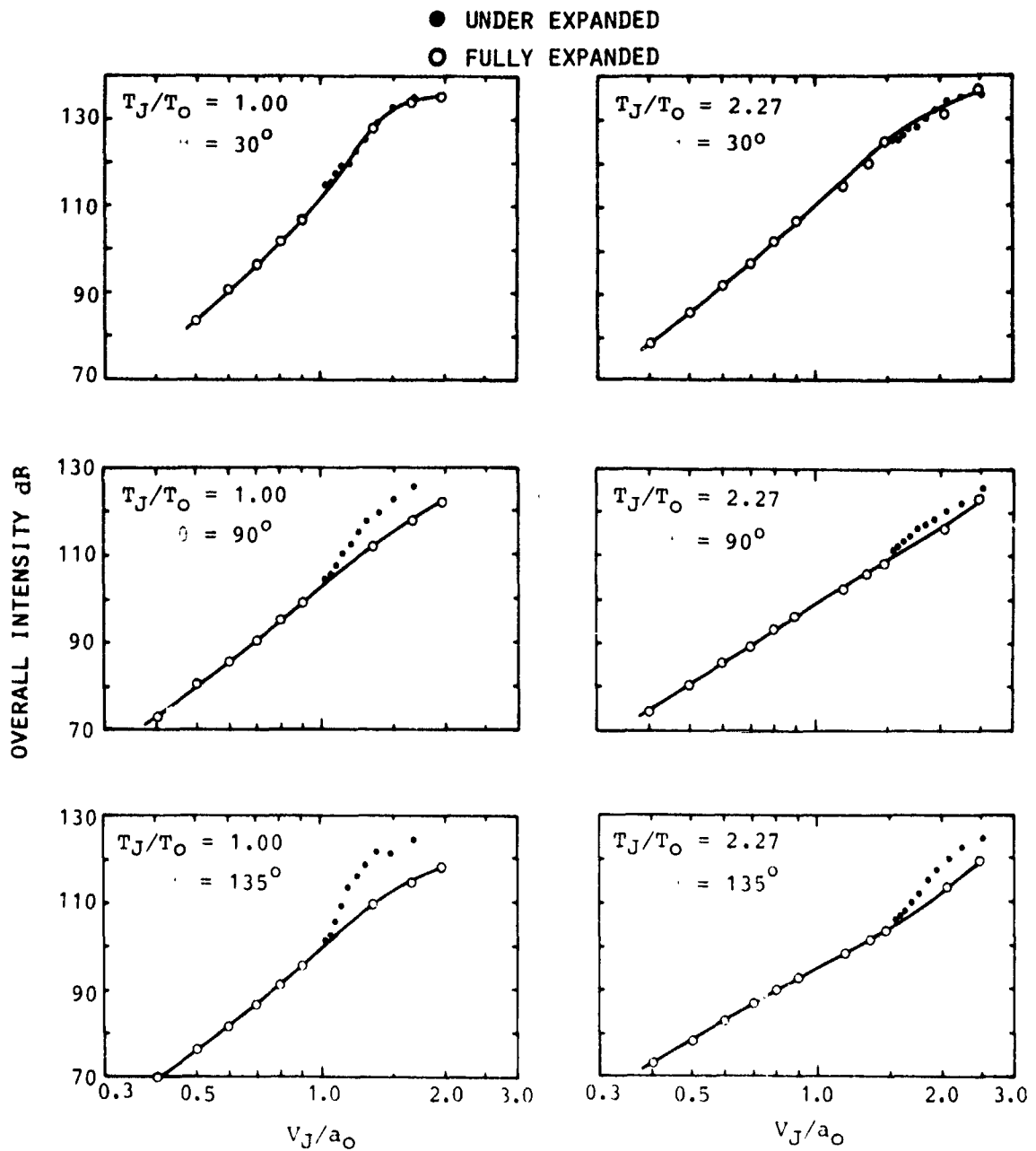


Figure 4.15 Overall Characteristics of Shock-Associated Noise

to the jet axis for super-critical pressure ratios. As temperature is increased, the significance of shock noise decreases for a given velocity ratio.

As a means of both testing the validity of the previously observed β scaling and further confirming the relative orders of magnitude of shock-associated noise and turbulent mixing noise, the noise from the convergent nozzle test is compared with turbulent mixing noise in Figure 4.16 for four different values of jet temperature ratio. The combined noise from the convergent nozzle tests for low values of β (just above choking) has approximately the same intensity value as the pure turbulent mixing noise, with this turbulent mixing noise dominance increasing with increasing temperature (corresponding to a velocity increase for fixed β). Once the shock-associated noise assumes dominance, β^4 scaling is observed up to $\beta \approx 1$ ($M = 1.4$). Temperature appears to have only a minor effect on overall shock-associated noise intensity at 135° to the jet axis.

Finally, the variation of shock-associated noise with observer angle θ is examined in Figure 4.17, where the results from under-expanded and fully-expanded jets for $\beta = 0.94$ are compared at four values of T_J/T_0 . For the unheated case ($T_J/T_0 = 0.73$), the shock-associated noise dominates over the turbulent mixing noise levels at all angles greater than the peak angle. As the jet efflux temperature is increased, the turbulent mixing noise contribution increases, while the shock noise remains essentially unaltered. The relative significance of shock-associated noise therefore diminishes as T_J/T_0 increases, and at the highest temperature considered ($T_J/T_0 = 2.27$), the directivity in the rear arc is primarily controlled by the mixing noise, whereas in the forward arc the total noise levels are dominated by shock-associated noise. For all values of T_J/T_0 , the directivities from under-expanded jets in the forward arc are essentially flat, indicating that the sound radiated by the presence of shocks in a jet flow is fairly omni-directional.

The spectral characteristics of broadband shock-associated noise are illustrated in Figure 4.18, which shows narrow-band spectra of both pure turbulent mixing noise from a C-D nozzle operating at its design pressure ratio and combined turbulent mixing/shock-associated noise from a convergent nozzle operating at the same pressure ratio. It is observed that the shock noise contribution does not modify the spectrum in the low frequency range, but at frequencies above the peak frequency the shock noise dominance is maintained.

If the shock noise spectra are examined for a systematic variation with emission angle, a rather interesting feature is observed. Figure 4.19 shows the $1/3$ -octave spectra for the isothermal jet at a Mach number of 1.37 ($\beta = 0.94$) for a representative range of angles. For clarity the $1/3$ -octave spectra at various angles are plotted on a sliding vertical scale, and the peak frequencies are joined by a broken curve. It can be seen that the peak frequency of shock-associated noise decreases as the observer angle (relative to the downstream jet axis) increases. It appears that the peak frequency exhibits a Doppler shift phenomenon, at least in a qualitative manner.

This is confirmed by examining the data at all test conditions, which supports the model, postulated by Harper-Bourne and Fisher⁴¹, of a moving source interacting with the stationary shock pattern as the noise generation mechanism.

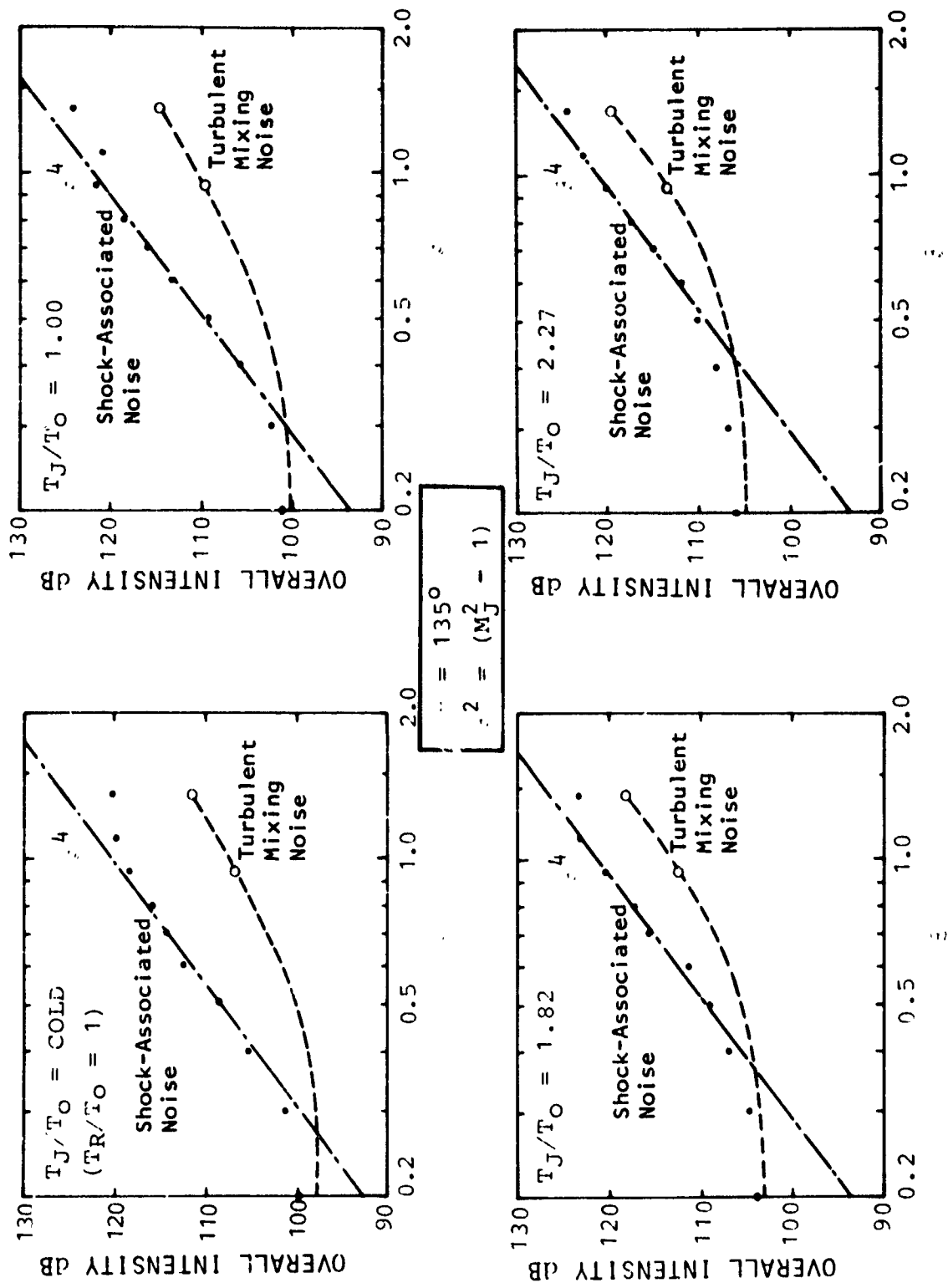


Figure 4.16 Overall Intensity Scaling

$\hat{b} = 0.94$
 $M_J = 1.372$

● UNDER EXPANDED
 ○ FULLY EXPANDED

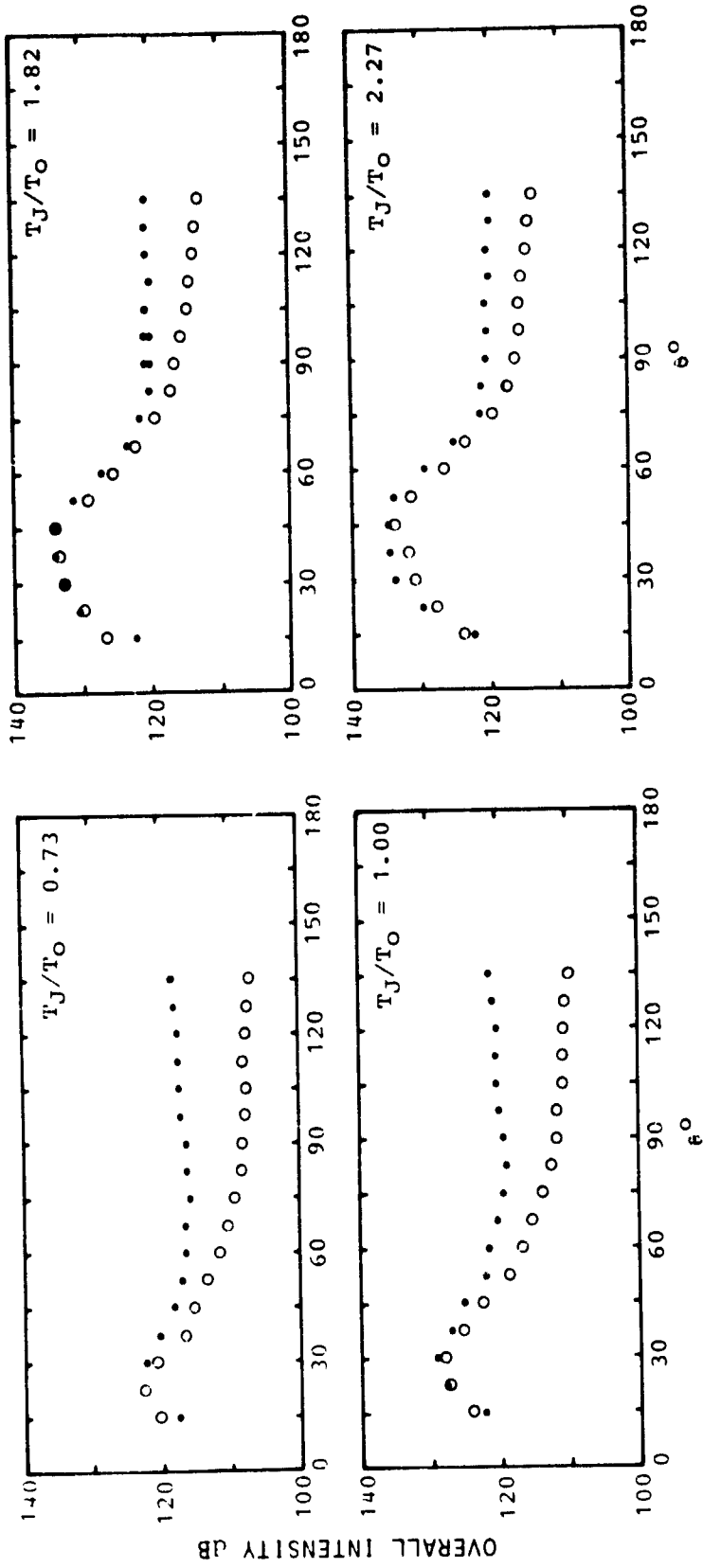


Figure 4.17 Directivity of Overall Intensity

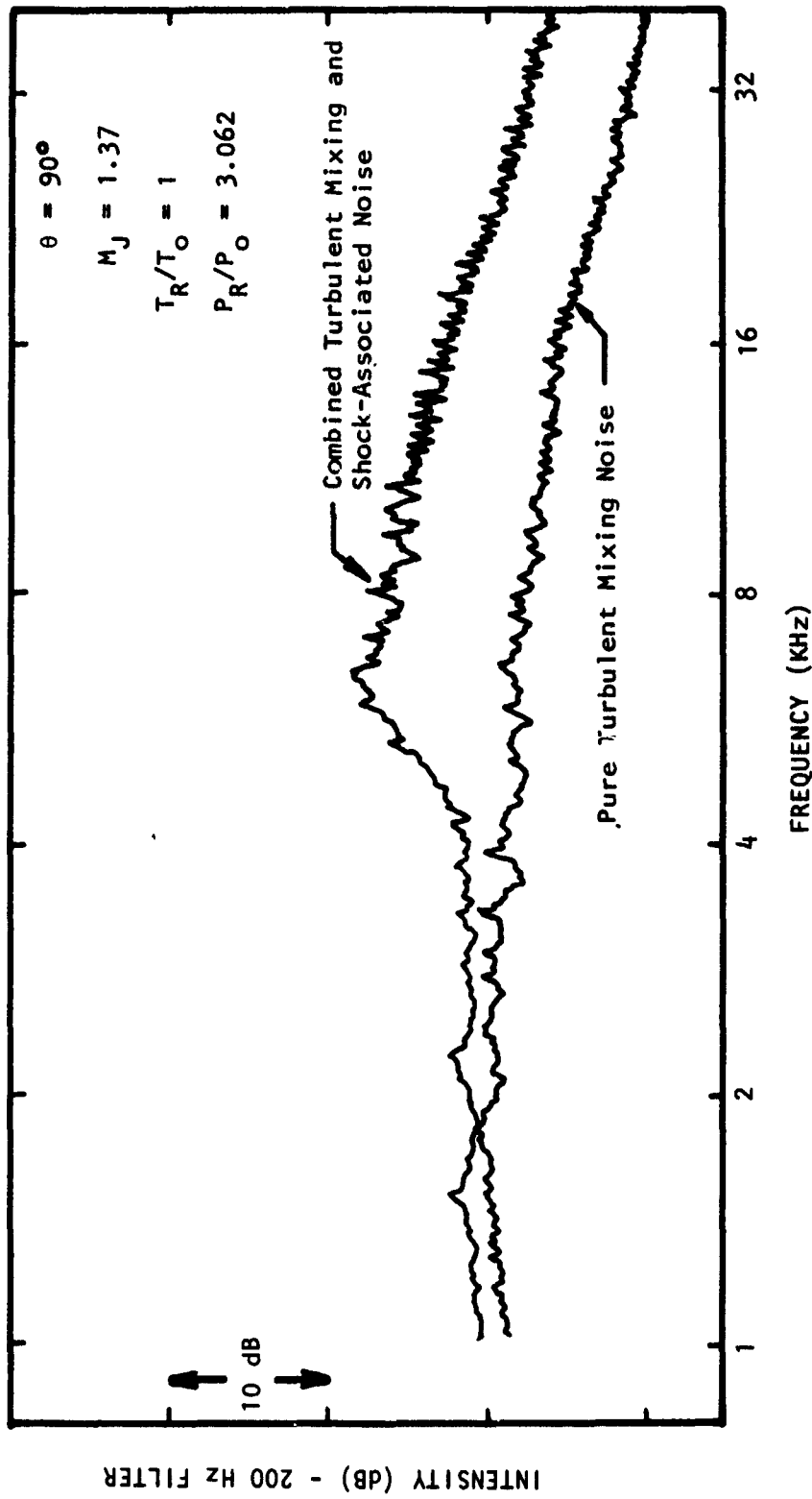


Figure 4.18 Comparison of Pure Turbulent Mixing Noise Spectrum and Spectrum Containing Broadband Shock-Associated Noise

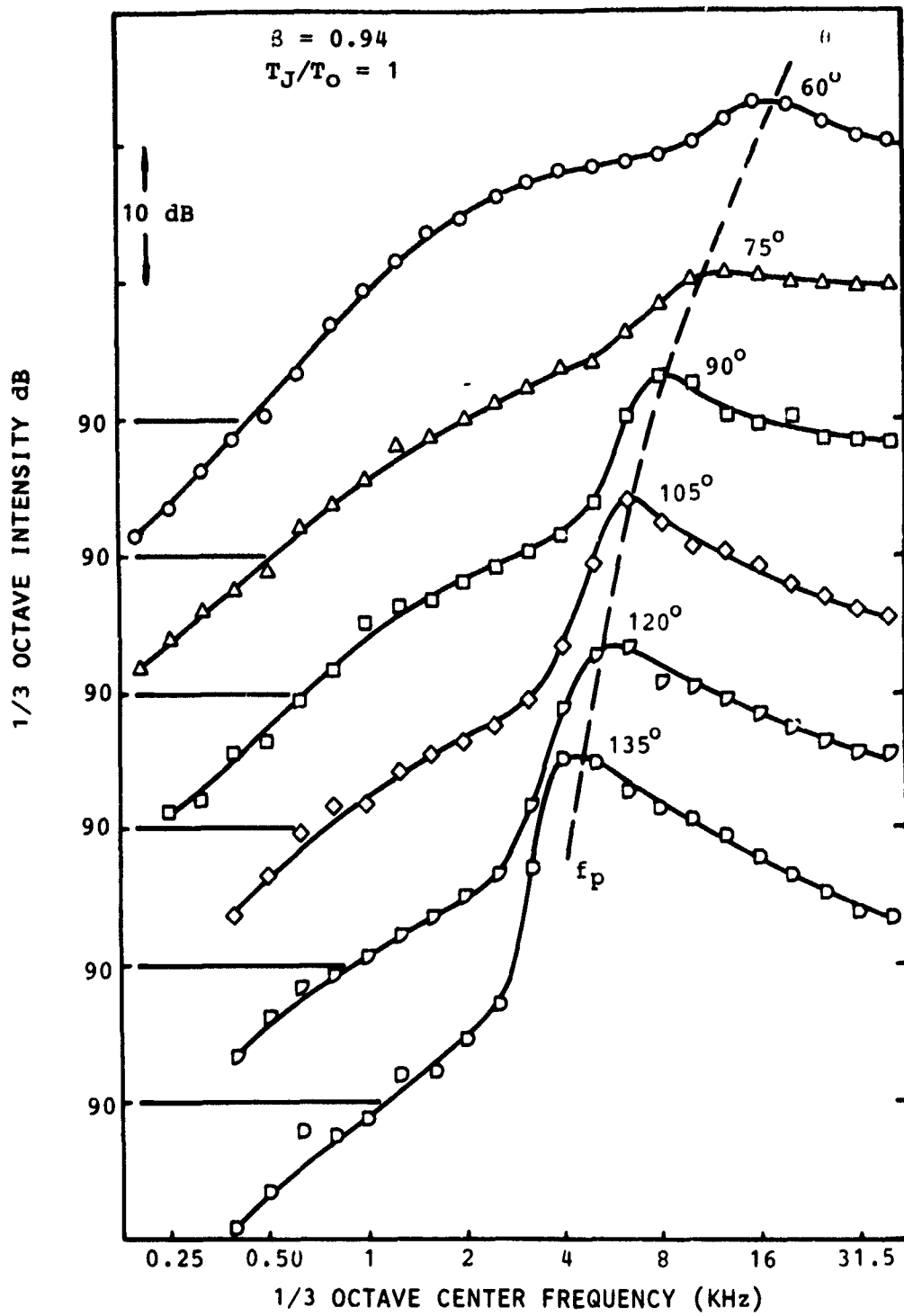


Figure 4.19 Variation of Peak Frequency with Angle

Further examination of the frequency spectra revealed that the peak frequency also scales on velocity, Mach number and diameter according to the following relationship derived by Harper-Bourne and Fisher, $f_p \propto V_J/8D$.

The complete set of test results is presented in Volume IV of this report and complete analysis of the results is given in Volume II.

4.1.2 Jet Flow Experiments

Once it was accepted that the Lilley theory and equation for a unidirectional parallel radially-sheared flow was an acceptable model for studying both jet noise generation and the acoustic/mean flow interactions involved in propagating the sound from the source region to the far field, it became crucial to have an accurate description of all the jet flow quantities, with particular emphasis on the velocity. A vast body of data existed on low velocity jets from hot-wire measurements, but turbulence measurements in particular were not available for jets at supersonic velocity and/or high temperature. The development of the Laser Velocimeter during this contract made it possible to obtain a limited amount of information on mean velocity and turbulence intensity and spectra near the end of the contract.

The Laser Velocimeter is described in Appendix II[†] and the calibration (or qualification) of the LV based on comparisons with hot-wire measurements are given in Appendix III. In the following discussion, a summary of results from measurements in high velocity jets and some basic scaling laws are given.^{††}

4.1.2.1 Jet flow measurements

The measurements in the jet were conducted under four jet flow conditions:

	<u>Jet Mach Number, M_J</u>	<u>Jet to Ambient Temp., T_J/T_0</u>
1	0.28	1.00
2	0.90	1.00
3	1.37	1.00
4	0.90	2.32

(The absolute velocity of the jets in Cases 3 and 4 is the same.)

Radial and centerline distributions of the basic quantities (e.g. mean velocity, and turbulence intensity) were obtained for these variations in Mach number and temperatures leading to new insight into effects of these on the jet structure.

Radial distributions of the mean velocity exhibited dynamic similarity for a given Mach number when plotted in terms of U/V_J and η^* [defined by

[†]The instrument developed by Lockheed-Georgia is described in detail in Reference 38 and Volume II, Section 5.

^{††}These data are described in detail in Reference 61 and Volume II, Section 6.

$(r - r_{0.5})/x$].* The axial distance to which similarity could be achieved depended on the jet Mach number, and varied from eight to sixteen diameters downstream in the range of Mach numbers encountered. This distance correlated directly with the potential core length and on the basis of the present results, was estimated to be twice the potential core length.

Radial distributions of the turbulence intensities and the covariance $u'v'$ normalized by V_J and V_J^2 , respectively, did not collapse. However, the radial turbulence distributions appeared to vary consistently with changing jet flow conditions, and the distributions were such that the peak occurred near $\eta^* = 0$ at all axial locations where similarity existed in the mean velocity distributions. The peak turbulence value generally tended to decrease with both increasing downstream distance and Mach number. At Mach 0.28 and $x/D = 2.0$, the peak intensity of the axial velocity fluctuations normalized by V_J was about 18%, and the radial component was about 14%, and the peak value of the covariance was about $16 \times 10^{-3} V_J^2$. Figure 4.20 shows a summary of the peak values of these turbulence characteristics as a function of the axial station and the Mach number.

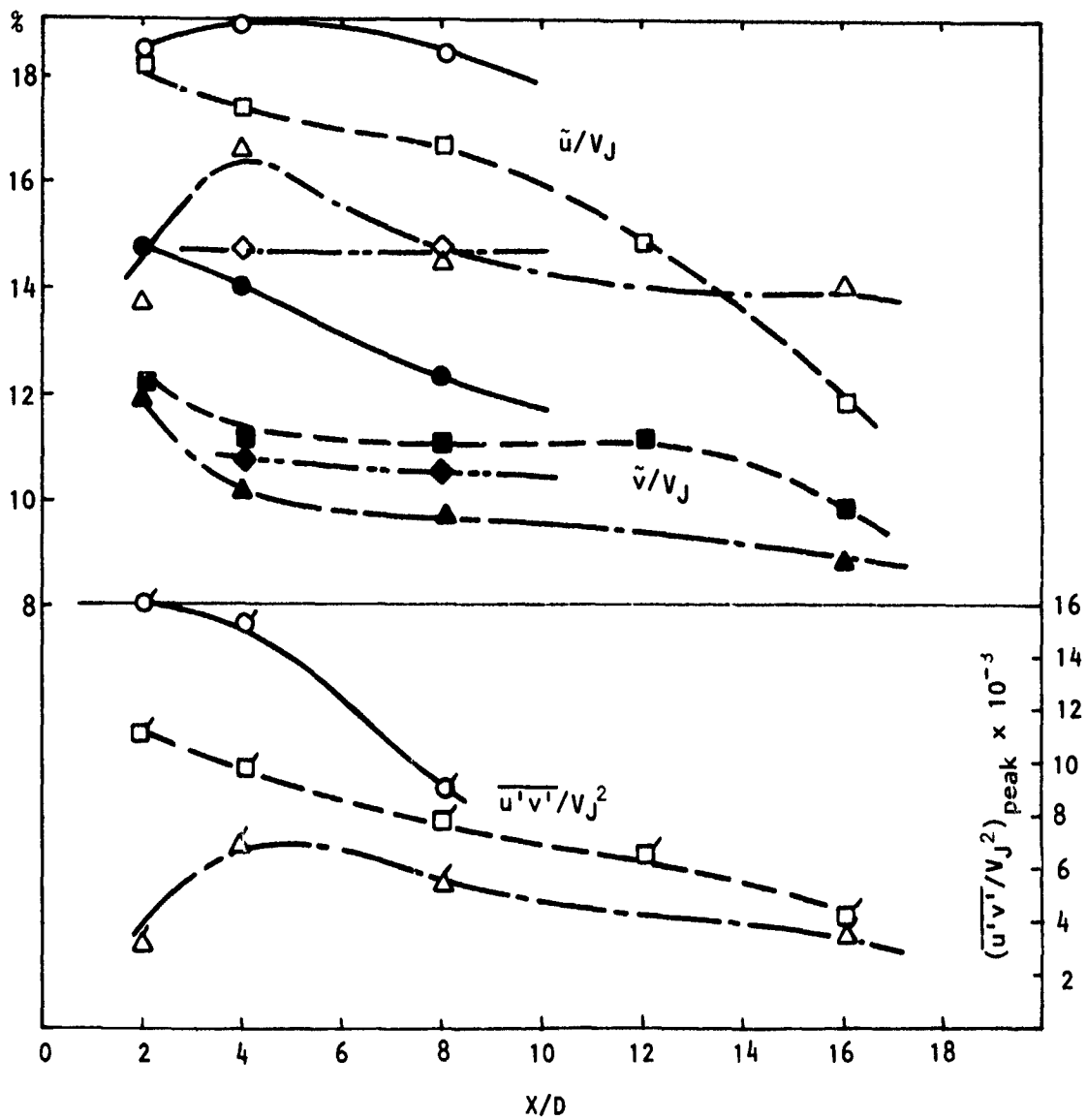
The spreading rate of the mixing layer was observed to decrease with increasing Mach number. This agreed with trends indicated by earlier studies using pitot tubes. The rate of decrease was however more rapid in the present study. Cary⁴² and Knott, et al⁴³ carried out mean flow measurements using respectively, an interferometer and a burst counter type LV. The spreading rates determined from their results agreed with those found in the present study; since they were using remote sensing instruments also, the agreement would suggest that the present results are correct and that the pitot-tube measurements were affected by having the measuring probe inserted into the flow region. An empirical equation was derived, based on the results for jets at ambient temperature ($T_J/T_0 = 1.0$), which related spread rate to Mach number. The equation is given by: $\delta_\eta = 0.165 - 0.045 M_J^2$, where δ_η is the rate of change of vorticity thickness with axial distance.

The decrease in spreading rate of the mixing layer in turn caused an increase in the potential core length (x_c) with increasing Mach number. The relationship is given by: $x_c/D = 4.3 + 1.1 M_J^2$.

Centerline distributions of the mean velocity and the turbulence intensities moved downstream with increasing Mach number. In particular, the axial and radial turbulence intensity peaks were located at progressively greater distance downstream with increasing Mach number. The movement of the curves could be identified directly with the stretching of the potential core, and distributions of the mean velocity were brought to a common curve when the axial distance was normalized by the potential core length. Figure 4.21 shows the collapsed data. However, such a good collapse was not possible with the turbulence intensity distributions because of the general tendency for the normalized turbulence intensities (u'/V_J and v'/V_J) to fall with increasing Mach number. However, all the peaks of the distributions tended to be located close to $x/x_c = 2.0$, thus giving support to the choice of the potential core length as a normalizing factor.

A general equation was derived based on Witze's formulation⁴⁴ of the centerline distribution of the mean velocity. The equation is:

*where $r_{0.5}$ is one-half of the centerline velocity and U is the local velocity.



$(\tilde{u}/V_J)_{\text{peak}}$	$(\tilde{v}/V_J)_{\text{peak}}$	$(\overline{u'v'}/V_J^2)_{\text{peak}}$	M_J	Condition
○	●	⊙	0.28	ISOTHERMAL
□	■	⊠	0.90	ISOTHERMAL
△	▲	⊡	1.37	ISOTHERMAL
◇	◆		0.9	HEATED

Figure 4.20 Peak Values of \tilde{u}/V_J , \tilde{v}/V_J , and $\overline{u'v'}/V_J^2$ vs X/D

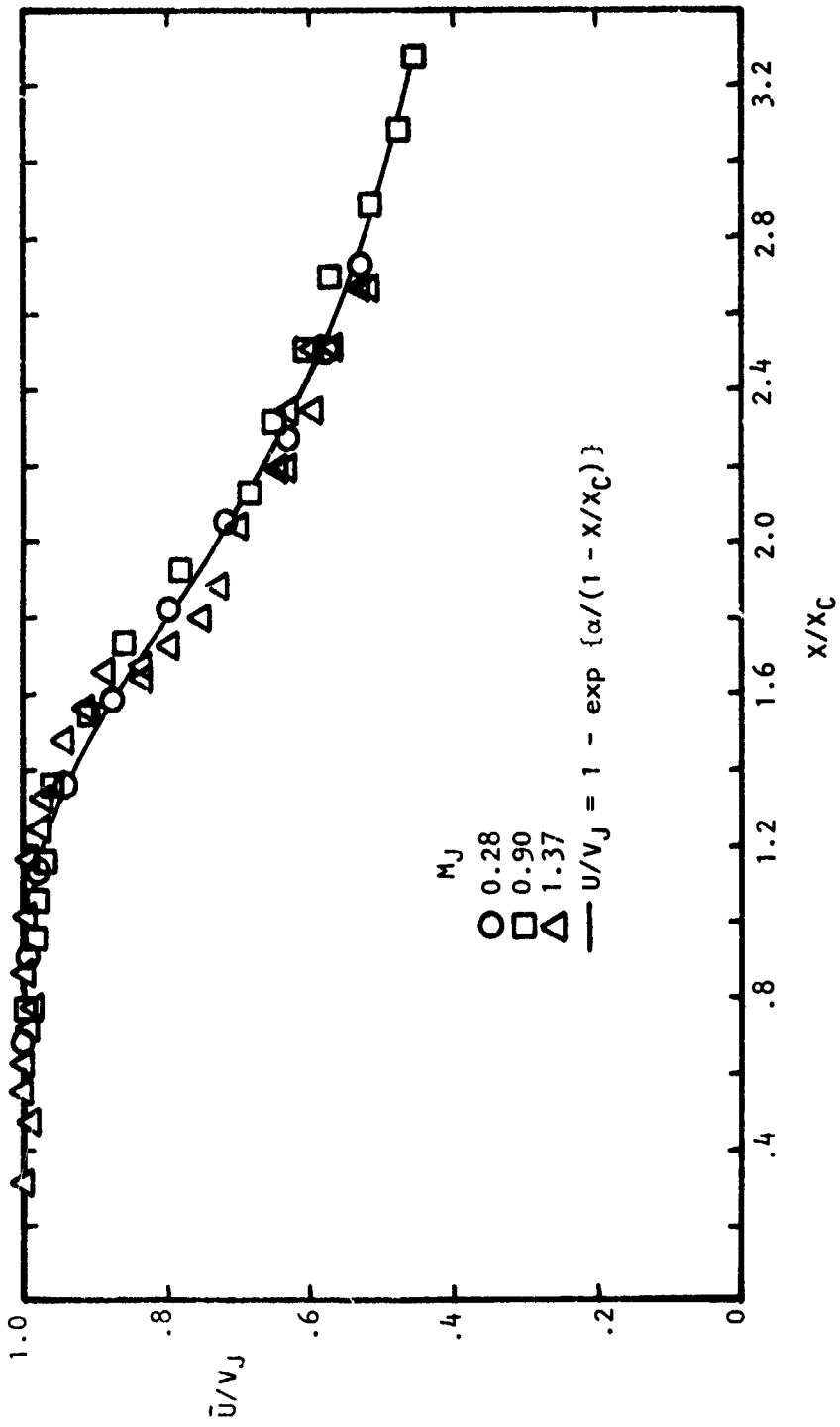


Figure 4.21 \bar{U}/V_J vs X/X_C

$U/V_J = 1 - \exp\{\alpha/(1 - x/x_c)\}$, where x_c is a function of the Mach number as expressed above, and α may be approximated by a constant value of 1.35. The curve for this equation is also shown in Figure 4.21, and it is observed that there is good agreement with the collapsed experimental results.

Radial distributions of the mean velocity at different Mach numbers were found to collapse when the radial distance was expressed in terms of $\sigma_1 \eta^*$ where $\sigma_1 = (0.165 - 0.045 M_J^2)^{-1}$. Since σ_1 is related to the more commonly used spread parameter σ used in Görtler's solution by $\sigma = \sqrt{\pi} \sigma_1$, the results are plotted in terms of $\sigma \eta^*$ in Figure 4.22. The curve for Görtler's error function profile⁴⁵ is also shown. The agreement between the collapsed experimental data and Görtler's error function profile suggests that a general equation for the radial distribution of the mean velocity for jets of varying Mach numbers, may be given by: $U/V_J = 0.5 \{1 + \operatorname{erf} \sigma \eta^*\}$, where $\sigma = 10.7/(1 - 0.27 M_J^2)$.

Radial distributions of the mean radial velocity also collapsed when plotted in terms of $\sigma_1 \eta^*$.

The heated jet was not studied in as great a detail as were the jets at ambient temperature. However, there is sufficient data to throw some light on the effect of heating the jet. It was found that for a constant Mach number of 0.9, the heating of the jet had the tendency of increasing the spreading rate of the jet mixing layer with a consequent reduction in the potential core length. If the jet efflux velocity is kept constant and the jet heated (i.e., a comparison between case 2 and case 4 - $M_J = 0.9$, $T_J/T_0 = 2.32$ and $M_J = 1.37$, $T_J/T_0 = 1.0$; $V_J/a_0 = 1.37$) the increase in spreading rate is greater than the increase observed for heating at fixed jet exit Mach number.

4.1.2.2 Noise scaling at 90° based on turbulence scaling

Returning now to the discussion in Section 4.1.1.1 on noise scaling at 90° for isothermal jets, it was observed that the intensity varied as 7.5 powers of jet velocity, rather than 8, and a dimensional analysis pointed to a slight reduction in the turbulence intensity with Mach number as the most probable reason for this observed effect. The very simplified scaling presented in Section 4.1.1 suggested that for 7.5 powers of jet exit velocity, a peak turbulence intensity functional relationship with jet exit velocity of

$$v' \propto V_J^{0.875}$$

would be required. This type of dimensional analysis assumes that the turbulence intensity peak and radial distributions are constant and similar, respectively, in the annular mixing region. As can be observed from Figure 4.20, this is not true. Thus, to obtain an average peak value of turbulence intensity, the observed peak values from Figure 4.20 are averaged in the region from two diameters to the end of the potential core, which should be a representative region for high frequency noise generation. From this average peak at each isothermal Mach number condition, the following power law behavior between turbulence and jet exit velocity is obtained:

$$u'/V_J = .167 (V_J/a_0)^{-0.085}$$

$$v'/U_J = .111 (V_J/a_0)^{-0.210}$$

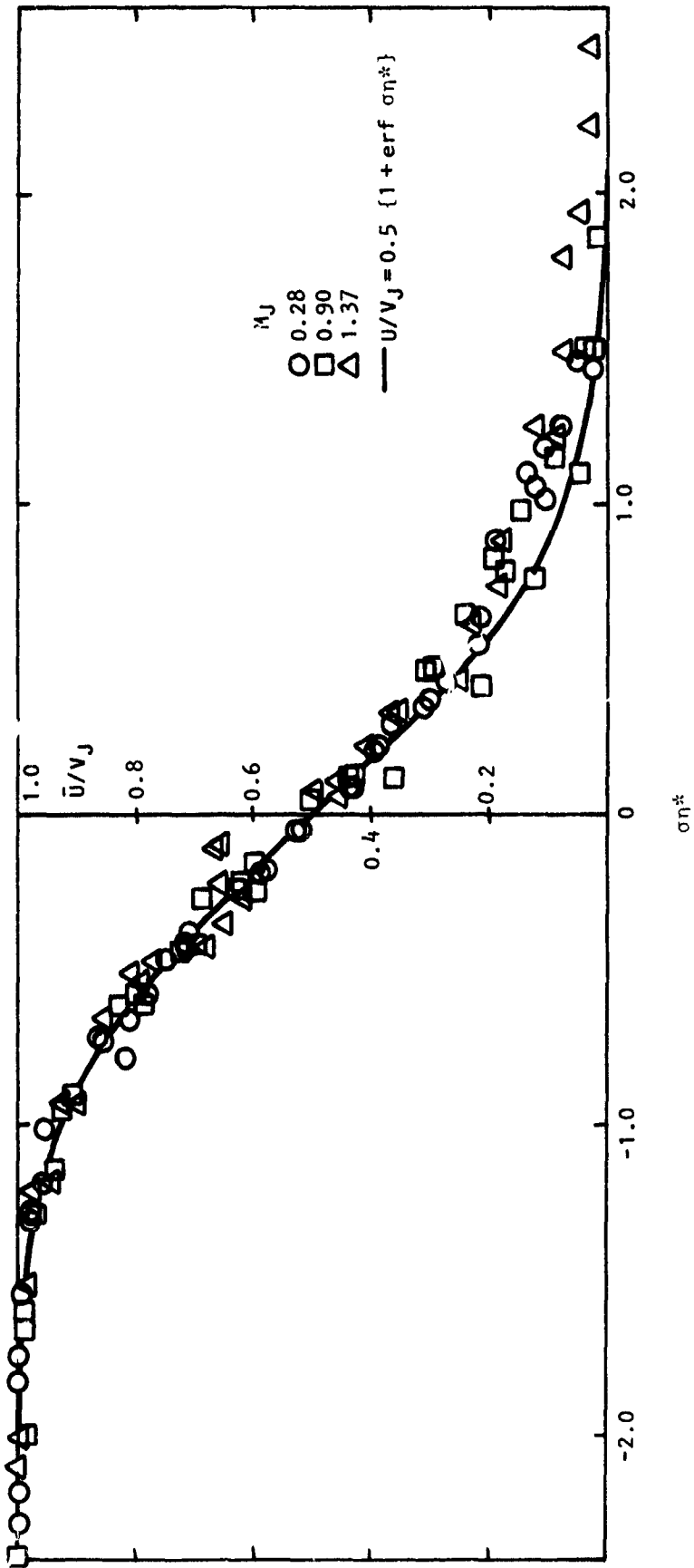


Figure 4.22 U/V_J vs $\sigma\eta^*$

Thus, the variation of peak turbulence intensity with jet exit velocity qualitatively exhibits the trend predicted from observation of the acoustic intensity at 90° .

Based on the actual form of the measured variation with Mach number of both radial and axial turbulence intensity as well as the variations of jet spread rate and potential core length, and their effects on local Strouhal number, a more rational scaling relationship between 90° noise radiation and the turbulence can be derived. In doing this it is still convenient to assume that the jet density is constant and that refraction and source convection effects may be neglected at 90° . For transonic and supersonic velocities, the neglect of refraction is questionable since density gradients are significant even for the isothermal jet exit condition. From this dimensional analysis (based on Lighthill's analysis¹⁰), the following scaling law is derived:

$$I(\theta = 90^\circ, T_J/T_0 = 1) \propto (V_J/a_0)^{6.8} [3.9 + (V_J/a_0)^2].$$

In the region of $0.7 \leq V_J/a_0 \leq 2$, this relationship is most closely approximated by (within ± 0.5 dB)

$$I \propto (V_J/a_0)^{7.5},$$

thus confirming that the modified power law behavior observed in the noise measurements at 90° is directly related to changes in the jet structure due to Mach number. One should be cautioned not to interpret the above result as an indication of two types of sources, since the $a + bM^2$ behavior is a direct result of potential core stretching with increasing Mach number.

This example above is probably the most elementary to which the turbulence data will be applied; however, it is an outstanding demonstration of the usefulness of an instrument which can perform the detailed measurements of the jet structure necessary to identify and validate the origins of jet noise. The potential utility of this instrument will be invaluable in jet noise and turbulence research and it is envisioned that the instrument will be used routinely, within 2-3 years in wind tunnel testing. Thus, what began as a development project on an instrument for studying jet noise generation has opened new vistas in several fields of aerodynamic research, development, and testing.

4.2 TURBULENT MIXING NOISE THEORY AND COMPARISON WITH EXPERIMENT[†]

As discussed in Section 3, Lilley's equation is an exact expression to second order which specifically isolates, on the left-hand side, all the linear fluctuating terms that are associated with sound propagation, including interactions with mean flow and mean temperature gradients (within the restriction of a parallel flow, with only radial gradients), while the right-hand side contains only products of higher order fluctuating terms. The equation is formulated in terms of the primary field variable of interest, acoustic pressure.

[†]This work is described fully in References 28, 38, 46, 47, and 48, as well as Volume II, Section 3.

Lilley's equation can be utilized to study radiation from various types of multipole sources, either fixed or moving and either deterministic or random. It can also be used to study the generation of sound in a turbulent mixing region, provided the major characteristics of the turbulent velocity fluctuations necessary to make up the source function are known. In addition, the transition points of homogeneous Lilley equations are useful in determining regions within the flow field where propagation or else exponential decay occurs. These regions of exponential decay, sometimes called "shadow zones" have been used by Fisher and Szewczyk⁴⁹ to explain the operation of certain types of suppressor nozzles. This phenomenon is referred to as shielding, i.e. of the noise sources from the observer.

Thus, Lilley equation solutions permit identification and separation of source generation effects from acoustic/mean flow interaction effects. It is expected that this type of analysis will ultimately lead to an exact understanding of how various types of suppressor nozzles operate and will also form the basis of a design tool for new suppressor nozzle concepts.

In this phase of the work, there were the major objectives stated in the Introduction to Section 4, as well as several sub-objectives. It had been determined that the Lilley equation solutions would be considered only for turbulent mixing noise studies and that shock-associated noise would be examined via another model, although the Lilley equation does not have this restriction as such. The primary objectives then were to develop numerical solutions to Lilley's equation for assumed turbulent mixing noise source distributions, and to compare these solutions with experiment over as broad a range of velocity and temperature conditions possible. In order to properly evaluate source solutions, it was necessary to devote significant effort to source descriptions. In this regard, a new philosophy was adopted in the turbulent mixing noise quadrupole source model in that particle displacement, rather than particle velocity was the source field variable. Also, new types of temperature source mechanisms were identified and used, along with the Lilley equation propagation characteristics, to explain the effects of temperature on jet noise generation. Finally, as a means of physically characterizing the numerical results, as well as providing a simpler means for obtaining solutions in applicable regions, limiting analytic solutions were developed for both low and high frequencies. In addition to requiring an accurate description of the sources of noise generation, the Lilley equation is fairly sensitive to the mean velocity and temperature distributions and, as such, requires an accurate description of these quantities.

Rather than dwell extensively on the mathematical aspects of the Lilley equation, a brief summary of results achieved during this research will be given, followed by a comparison of relevant solutions with experimental data.

4.2.1 Monopole Source Solutions

The main achievements of the *initial* part of the Lilley equation investigation can be summarized as follows:

4.2.1.1 The solution of Lilley's equation

A method of solving Lilley's equation numerically, based upon the Green function technique, was first carried out in detail for an assumed (volume acceleration) monopole source distribution immersed in a parallel sheared flow of nonuniform velocity and speed of sound. It was felt that these monopole solutions would lead to a better understanding of the major physical characteristics of the Lilley equation solutions and would provide the basis for preliminary comparison with jet noise data as well as with measurements of radiation from "artificial" sources inserted in the jet flow.

4.2.1.2 Preliminary jet noise source model

As a preliminary model for the source of jet mixing noise, the assumed source distribution consisted of a ring of incoherent point sources of *arbitrary* radius, so that the sources could be positioned at realistic locations in relation to the velocity profile (e.g. on the lip-line where the turbulence intensity, and hence the actual source strength, is at or near a maximum in the initial mixing region).

The point source had an arbitrary axial convection velocity and axial coherence; the corresponding convective amplification effect could be calculated with a simple analytic formula, independently of the Lilley equation.

4.2.1.3 Numerical results and comparison with experiment

Numerical solutions to the Lilley equation with the above source model were obtained for a range of jet exit velocities up to and including sonic speed but only at the isothermal condition (i.e. where the speed of sound is uniform throughout the sheared flow and equal to the ambient value). The numerical results were displayed as a function of ring source radius over a wide frequency range and compared with the corresponding *plug* flow results to demonstrate the importance of source location (i.e. ring source radius) and real velocity profile effects.

The error function was used for the velocity profile shape in the potential core/initial mixing region, and its accuracy was verified by comparisons with measured data. In addition, a preliminary comparison of theoretical results with measured isothermal jet noise *directivity* data in the form of "difference spectra" was conducted. For the purposes of that comparison the acoustic-mean flow interactions for the required *quadrupole* jet mixing noise source distribution were assumed to be the same as those predicted by the Lilley equation for the monopole source distribution. Also, no attempt was made to allow for the variation of effective axial source location (and hence for velocity profile variation) with source Strouhal number. Only one axial location, at the end of the potential core, was used for the whole Strouhal number (frequency) range.

Experimental (stationary) point source directivity data were studied in some detail and two forms of the Lilley equation, with a volume *displacement* and a volume *velocity* point monopole source function, were solved to yield theoretical directivity predictions. The results were compared with some of the measured data published by Ribner and his colleagues¹⁵⁻¹⁹.

4.2.2 Jet Noise Source Solutions

During the *main* part of the Lilley equation investigation, the major accomplishments were numerical and analytic solutions for multipole sources, the derivation of a *modified* Lilley equation and detailed comparisons with measured jet mixing noise data, as outlined below.

4.2.2.1 Solutions of Lilley's equation

The Lilley equation numerical solution technique was extended to include radial dipole and radial-radial quadrupole source functions and hence *all* the different quadrupole source types. The theory developed for that purpose allows solutions for multipole source distributions of *any* order to be derived from a single basic numerical solution.

Also, closed-form analytical solutions to the Lilley equation were derived for the limiting cases of high and low frequency.

4.2.2.2 Jet noise source model

One of the major modifications to the Lilley equation was the introduction of a new source function. The reasons for the rejection of the original (volume *acceleration*) source function and the derivation of the new volume *displacement* source function were justified by extensive analytical and numerical work and by appealing to the well-established scaling laws exhibited by measured jet mixing noise data. The volume displacement and volume acceleration quadrupole source functions are both valid second-order approximations to the basic Lilley equation source function, but the corresponding Lilley equation solutions are radically different at low Mach number. The low Mach number asymptotic mean velocity dependence of the radiated intensity is V_j^6 for the volume acceleration quadrupole but is V_j^8 for the volume displacement quadrupole, in agreement with the scaling law exhibited by the measured data. The other major modification was a new (volume *displacement*) dipole source term for nonisothermal jet flows, which is described below under the heading of comparisons with measured data.

4.2.2.3 Numerical results and comparisons with measured data

Following the introduction of the new displacement source, numerical solutions to the Lilley equation were obtained over an extended range of jet exit velocities, up to *twice* the ambient speed of sound, and for a wide range of jet exit temperatures, from one-half to nine times the ambient temperature.

The effects of temperature on the measured noise intensity spectra at 90° to the jet axis were investigated and analyzed first on the basis that the effects might be entirely understood in terms of acoustic-mean flow interactions, that is, interactions between the mixing noise (isothermal) quadrupole sources and the axisymmetric nonuniform mean temperature field, including the mean density gradient. This was followed by a second investigation in which the measured data was correlated on the basis that an *additional* dipole source mechanism appears in nonisothermal jet flows, its radiation intensity being proportional to the sixth power of the jet exit velocity. Distance and angle

calibrations were applied to the measured noise data to allow for the finite distance between the nozzle exit plane and the effective axial source location. The same data calibrations were employed in the following.

Following the early work, the mean velocity profiles for the transition and fully developed regions of the jet mean flow field were chosen and their accuracy verified by comparisons with measured data. In addition, the mean *temperature* profile in each jet flow region was obtained by assuming similarity between velocity and stagnation *temperature* profiles. The speed of sound profile in the original Lilley equation and the mean density profile in the modified version both were related to the mean temperature profile by assuming that the jet fluid is a perfect gas with a constant specific-heat ratio.

A detailed, comprehensive comparison of theoretical results with measured isothermal and heated jet noise *directivity* data was carried out. The variation of effective axial source location, and hence flow profile, with source Strouhal number (frequency) was also incorporated.

Experimental (stationary) point source directivity data recently published by Ribner and his colleagues were re-examined and compared again with our theoretical results after a correction was made to a parameter definition in their work by Ribner⁵⁰. Also, new experimental point source measurements taken at Lockheed-Georgia were compared with Lilley equation theoretical directivity results.

It should be noted that no attempt has been made in general to calculate absolute noise levels with measured or assumed source function data since, strictly speaking, that was *not* part of the original objective. This work has been concerned with the "convective and refractive" effects in a heated jet and these largely control the *directivity* of the radiated noise intensity. For isothermal jets the absolute levels at 90° to the jet axis are mainly determined by the magnitude of the turbulent velocity fluctuations, correlation volumes, etc. However, there *is* a significant refractive influence on noise intensity levels at 90° to the axis of nonisothermal jets; hence, the detailed investigations summarized above.

Finally, the comparisons between *experimental point source* directivity measurements and solutions to appropriate forms of the Lilley equation will not be included in this report, but will be published at a later date. This part of the investigation was curtailed when it was realized that the theoretical results were critically dependent on a correct modeling of the experimental point source. The present investigation was not directly concerned with artificially excited jet exhaust flows. Experiments of this type were originally included to provide an independent check on the validity of the Lilley equation description of the propagation type of acoustic-mean flow interactions. Once the importance and complexity of experimental point source modeling became apparent the exercise was terminated and all the effort was concentrated on the jet mixing noise investigation.

4.2.3 Lilley Data-Theory Comparison

For the purposes of this data-theory comparison, two different types of deviations from the classical theory are introduced and the success of the new theory in accounting for these problems is detailed.

As discussed in Section 4.1.1.1, measured data on hot jets at low Mach numbers ($U_j/a_0 = 0.3$ to 0.6 , where V_j is the jet exit velocity and c_0 is the ambient sound speed) show significant increases in far-field intensity, relative to isothermal jets of the same velocity. At 90° to the jet axis, the measured velocity dependence is V_j^6 in contrast to the V_j^8 Lighthill prediction. Figure 4.23 demonstrates this for a low Strouhal number, $S = 0.1$, where the increase in low velocity noise due to heating is quite pronounced ($S = fd/V_j$, where f is the observed frequency and d is the jet diameter).

The second problem is illustrated in Figure 4.24, where the measured *directivity* of isothermal jet noise at two supersonic jet velocity conditions for a modified Strouhal number $S_m = 0.3$ ($S_m = SD_m$, where D_m is the modified Doppler factor) is compared with the 5th power of Doppler amplification (D_m^{-5}) derived from classical theory. Clearly, there is no real agreement in shape and there are significant deviations at every angle away from 90° .

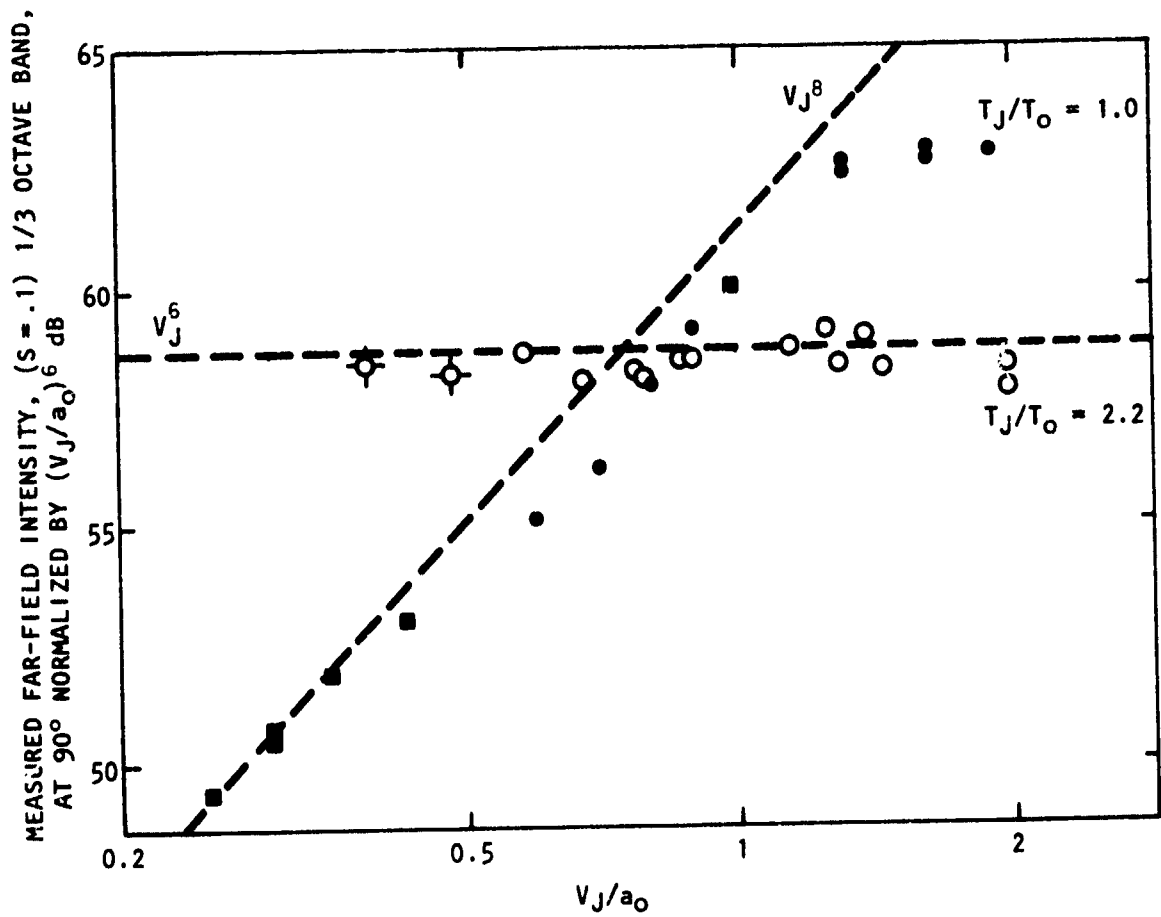
To show how this new work narrows the gap, the main theoretical results on jet mixing noise is given in three parts: (1) the effect of temperature on jet noise at 90° , (2) isothermal jet noise directivity, and (3) hot jet noise directivity. Prior to displaying these solutions, the mean flow assumptions are outlined.

4.2.3.1 Lilley equation flow parameters

In the Lilley equation model the unsteady pressure field of the turbulent jet flow is regarded as a set of small amplitude waves superimposed on a steady, axisymmetric, parallel shear flow (of uniform pressure) with velocity $[U(r), 0, 0]$, sound speed $\bar{c}(r)$ and density $\bar{\rho}(r)$. Realistic profiles for these mean flow quantities are used, as sketched in Figure 4.25; the profiles are characterized by the vorticity thickness δ , the "lip-line radius" r_1 , the center-line values U_1 , c_1 , ρ_1 , and the ambient values $U=0$, a_0 and ρ_0 . In all the *numerical* calculations the fluid is assumed to be a perfect gas with constant specific-heat ratio γ so that the sound speed and density profiles are replaced by a temperature profile $T(r)$ with center-line and ambient values T_1 , T_0 . Hence, the nondimensional flow parameters are δ/r_1 , U_1/a_0 , γ and T_1/T_0 .

The flow parameters are determined by choosing an axial station, X_s , in the jet flow for each modified Strouhal number. The choice is guided by experimental results for the apparent or effective axial distribution of mixing noise sources in real jets. At high frequencies (i.e. large S_m), the axial station is located within the initial mixing/potential core region and then $R_1 = r_0$, where r_0 is the nozzle or actual lip-line radius, $U_1 = V_j$ and $T_1 = T_j$, suffix "j" indicating jet exit conditions. In this region only δ or δ/r_0 varies with axial position. At low frequencies the axial station is downstream of the end of the potential core and all the parameters vary with axial position, although δ/r_1 is constant in the fully developed region.

Within the parallel sheared flow the turbulence mixing sources are represented by a ring of convected, statistically-isotropic point quadrupoles and dipoles (denoted by SIPQ and SIPD) of radius $r = r_s$, where $U = U_s = \phi_s U_1$ and $T = T_s$ (also $\bar{c} = \bar{c}_s$, $\bar{\rho} = \bar{\rho}_s$).



SYMBOL	T_j/T_0	SOURCE
●	1.0	LOCKHEED-GEORGIA
○	2.2	" "
■	1.0	ISVR

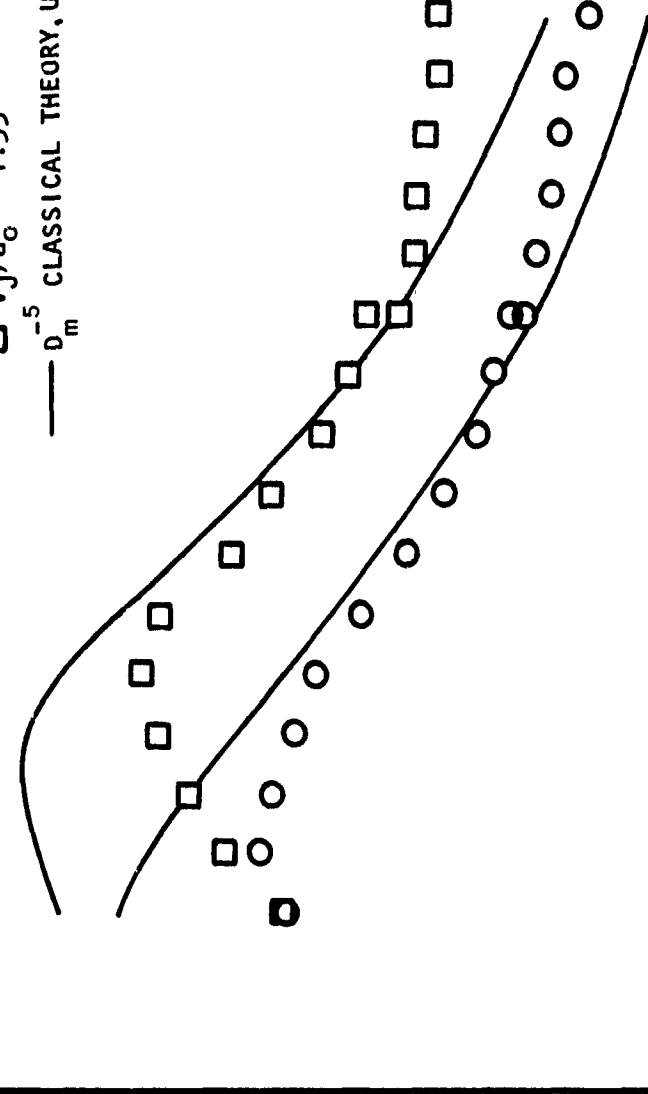
Figure 4.23 Effect of Heating on Jet Noise Measured at 90°: 1/3-Octave Band Centered at $S = 0.1$

SUPERSONIC JET EXHAUST NOISE

MEASURED JET NOISE DATA (LOCKHEED-GEORGIA)

- $V_J/a_0 = 1.33$
- $V_J/a_0 = 1.95$
- D_m^{-5} CLASSICAL THEORY, $U_e = 0.67, V_J \alpha = 0.3$

OVERALL INTENSITY dB (Re 1, 0.0002 dynes/cm²)



DIRECTIVITY ANGLE FROM DOWNSTREAM JET AXIS - θ_0 DEGREES

Figure 4.24 Directivity of Supersonic Isothermal Jet Noise: Comparison of Classical Theory with Measured 1/3-Octave Data at $S_m = 0.3$ ($D_m = \{(1 - U_c \cos \theta_0 / c_0)^2 + \alpha^2 (U_c / c_0)^2\}^{1/2}$)

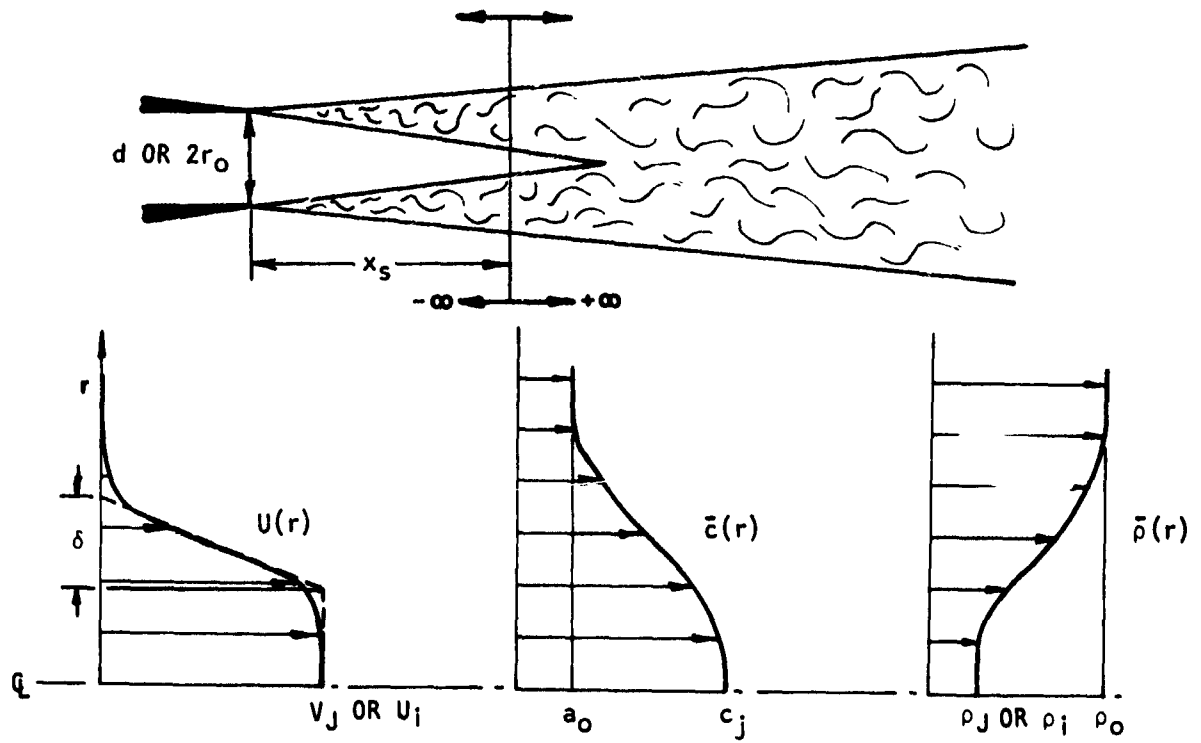


Figure 4.25 Typical Radial Profiles in Basic Cylindrical Flow, Showing Relation to Actual Jet Flow

4.2.3.2 Effect of temperature on jet mixing noise at 90°

To illustrate the theoretical effects of heating on the noise radiation at 90° to the jet axis, some numerical solutions to the Lilley equation for the SIPQ source model are shown in Fig. 4.26 in the form of a *flow factor*.[†] This is defined as the ratio of the far-field intensity to its value without the jet flow, the source strength being held constant. The horizontal scale is the nondimensional frequency parameter, $k_0\delta$, i.e. $2\pi(\delta/\lambda)$ where λ is the wavelength of sound outside the flow. Clearly, $k_0\delta$ is a far more important parameter than the one based on the nozzle radius, k_0r_0 ; the latter is varied over a wide range (specified in Figure 4.26), but the resulting flow factor variation, indicated by the vertical band, is quite small. For small values of $k_0\delta$, these results show that the radiation from the SIPQ source can be *amplified* when those sources are placed within a nonuniform density field. The amplification mechanism is the incomplete cancellation of the radial-radial quadrupole field in the presence of radial density gradients. Failure to cancel at low frequencies is due to the dependence of the radiation from each of the radial dipoles making up the rr -quadrupoles on the local density. The basis for this explanation is the low frequency limit shown in Figure 4.26, which is a new analytical solution to the Lilley equation and is discussed fully in Volume II, section 3.2.5. In that same discussion, the high frequency or geometric acoustics limit is also derived. Clearly, these asymptotic results are useful over a wide range of $k_0\delta$.

Although the low frequency amplification mechanism can be related to the low Mach number condition, since $k_0\delta \propto V_j/a_0$ at constant Strouhal number, it is argued that it *cannot* entirely explain the low Mach number increase in noise levels with heating observed in practice (e.g. see Figure 4.23). The amplification mechanism, which can be referred to as one of scattering by the mean density gradient, is closely related to one of those described by Morfey⁵¹ in his extension of the Lighthill analogy to include the case of flows of non-uniform density. However, that work⁵¹ also uncovered an *unsteady* density field scattering mechanism; when the Lilley equation is modified to include this effect, an additional dipole source is introduced into the source function. That new source is found to explain temperature effects at 90° reasonably well (see Volume II, Appendix 3E) and leads to excellent directivity predictions for hot jet mixing noise (see Volume II, Appendix 3G) as illustrated in the final part of this summary.

4.2.3.3 Isothermal jet mixing noise directivity

A comprehensive study of the *directivity* of isothermal jet mixing noise is described in detail in Volume II (see Appendix 3F). The comparisons between measured data and the corresponding Lilley equation solutions cover a wide range of modified Strouhal numbers (i.e. frequencies), $0.1 \leq S_m \leq 3.0$, Mach numbers, $0.5 \leq V_j/a_0 \leq 1.95$ and polar angles, $22\frac{1}{2}^\circ \leq \theta_0 \leq 135^\circ$. The study clearly demonstrates that outside the cone of silence, i.e. when $\cos\theta_0$ is in the range

[†]In these results the error function temperature profile has been used [Volume II, equation (2-53)]; it is independent of Mach number, unlike the general case when similarity is assumed between velocity and stagnation temperature profiles.

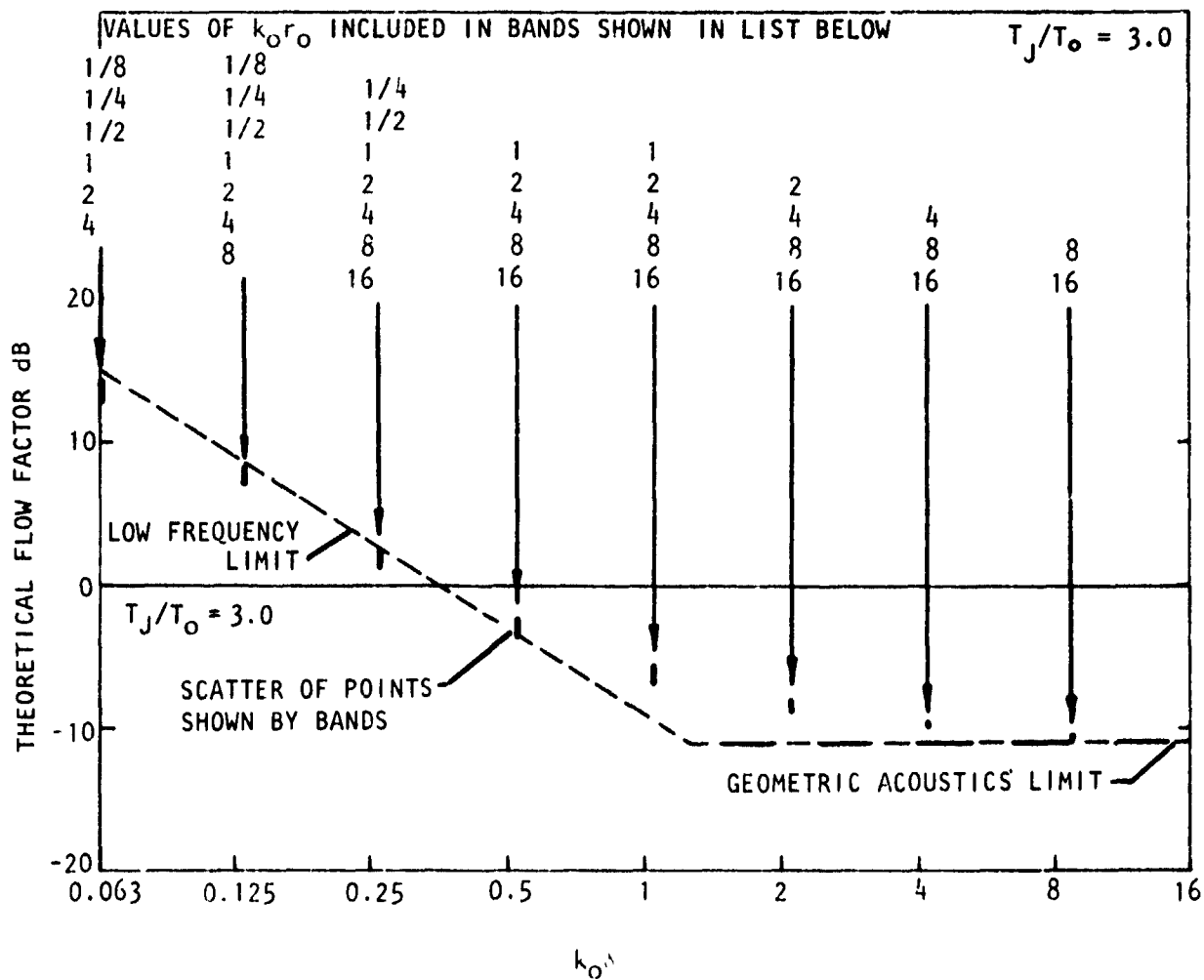


Figure 4.26 Lilley Equation Flow Factor for a Quadrupole (SIPQ) Ring Source in an Axisymmetric Shear Flow. Hot Case, $T_J/T_0 = 3.0$; Radiation Angle 90° ; Radial Source Location (Ring Radius) Corresponds to $\phi_s = 0.663$. Bars on Graph Indicate $k_0 r_0$ (or δ/r_0) Dependence of Results

$$- a_0/(\bar{c}_s - U_s) < \cos\theta_0 < a_0/(\bar{c}_s + U_s), \quad (U_s/\bar{c}_s < 1^\dagger)$$

the directivity shapes can be predicted from the Lilley equation solutions with considerable accuracy. This major achievement is illustrated in Figures 4.27 and 4.28 for the same examples given previously in Figure 4.24. The improved agreement involves only a small change at some angles but the *consistent* accuracy of the new prediction and the large changes from the classical D_m^{-5} law in the forward arc demonstrate the validity of the new Lilley equation results.

In order to achieve this agreement outside the cone of silence, it has been necessary to process the measured data so that the polar origin for the directivity angle is located at the effective axial source location (as in the theoretical model) *and* to use an eddy convection velocity that varies with S_m in a realistic way, that is, decreasing with decreasing S_m .

Inside the cone of silence the over-prediction by the D_m^{-5} law is contrasted with an under-prediction by the Lilley equation solutions, as in Figure 4.27 and 4.28. The most likely reason for this large discrepancy is that the direct radiation from the large-scale turbulence structure, the subject of a parallel investigation described in Section 4.3 is *not* included in the comparisons presented here. At the lowest Strouhal number considered, $S_m = 0.1$, this must be an important source of acoustic radiation inside the cone of silence. Almost of equal importance though, particularly for higher Strouhal numbers, $S_m \geq 0.3$, is a lack of realism in the present, assumed source function model; the actual source distribution in the radial-azimuthal plane has been modeled by a *ring* source, that is, radially it is a point source. At angles well inside the cone of silence the ring source of a given radius may be very effectively shielded by the flow, giving rise to low predicted levels. In reality, however, other parts of the actual source distribution nearer the outer edge of the sheared flow are less well shielded and if their contributions to the radiation levels were included, a significant increase in predicted level would result. Thus, there is an urgent need to replace the present ring source model with a radially distributed source, in order to evaluate the relative importance of the two most likely causes for the large discrepancies inside the cone of silence, the unrealistic source model and large-scale turbulent structure radiation.

4.2.3.4 Hot jet mixing noise directivity

A theoretical model for the variation of jet mixing noise with jet exit velocity and temperature at 90° to the jet axis has been evaluated and found to be in reasonable agreement with the measured data, although there are some significant deviations occurring at high velocities (see Volume II, Appendix 3E). The model is based upon a source function made up of quadrupoles *and* dipoles, i.e. on a *modified* right-hand side of the Lilley equation. The dipole sources result from the scattering of turbulent pressure fluctuations by unsteady density fluctuations within nonisothermal jet flows. The relative

[†]When $U_s \geq \bar{c}_s$ the lower bound is replaced by -1 .

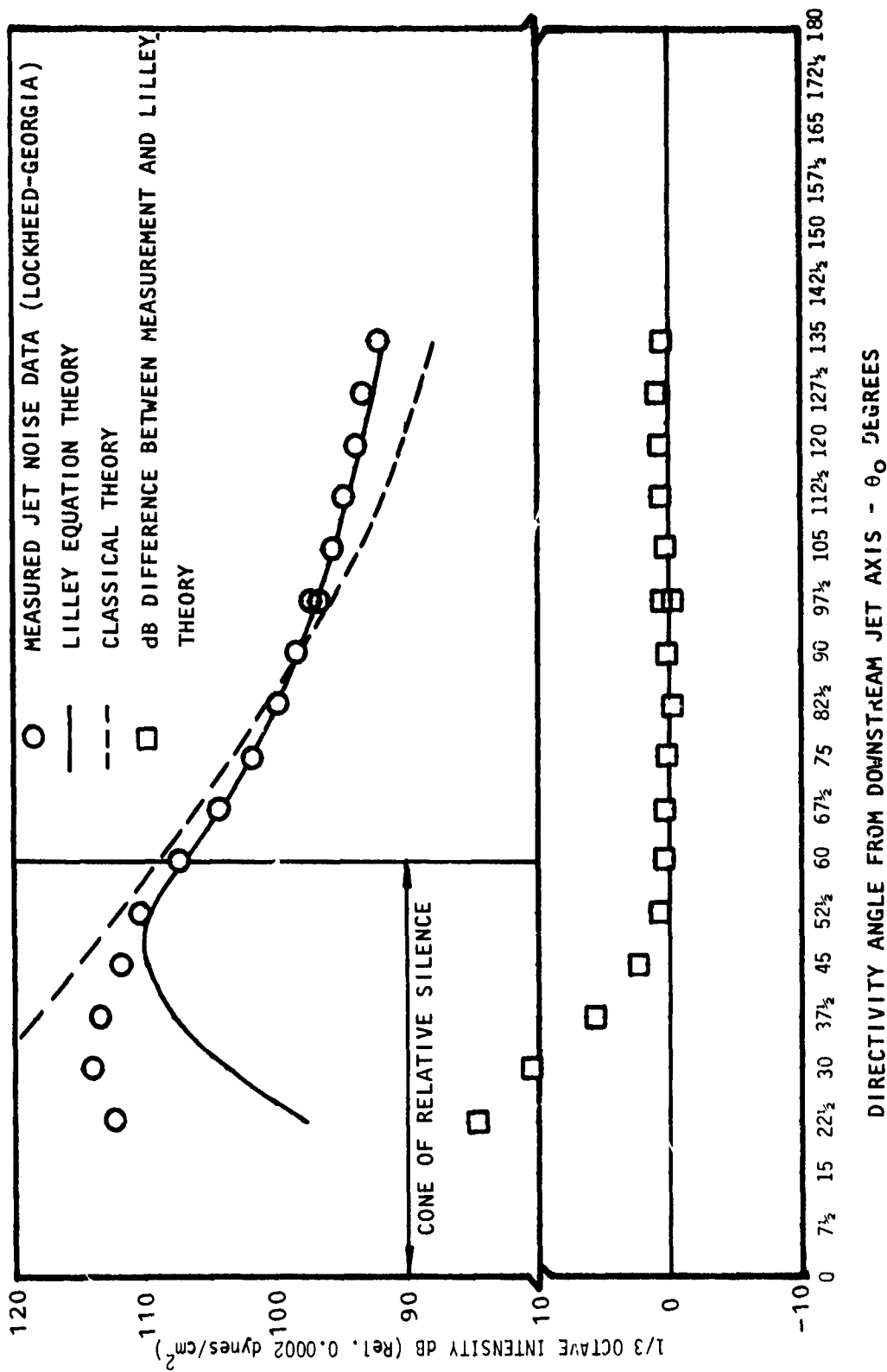


Figure 4.27 Directivity of Supersonic Isothermal Jet Noise: Comparison of Lilley Equation and Classical Theoretical Models with Measured 1/3-Octave Data, for $S_m = 0.3$, $V_J/a_0 \approx 1.33$

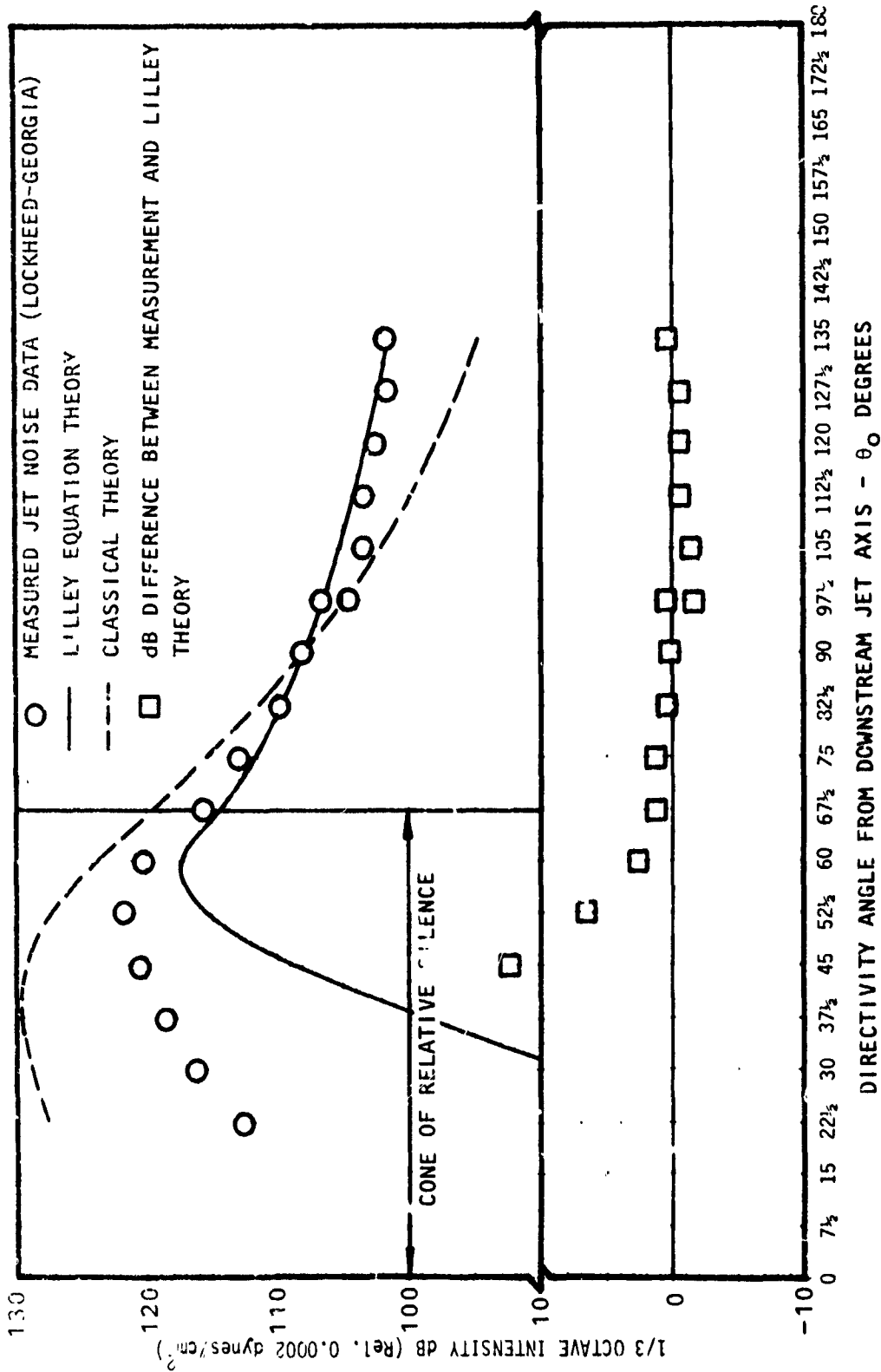


Figure 4.28 Directivity of Supersonic Isothermal Jet Noise: Comparison of Lilley Equation and Classical Theoretical Models with Measured 1/3-Octave Data, for $S_m = 0.3$, $V_j/a_0 \approx 1.33$

weighting of this source combination is determined mainly from the measured isothermal and hot jet noise spectral data at 90° to the jet axis.

The Lilley equation can then be used to predict the *directivity* of hot or nonisothermal jet noise, given that weighted source combination. However, in the preliminary study described in Volume II (Appendix 3G), an attempt has been made to separate out temperature effects from those that cause disagreement between measurement and theory at isothermal conditions, in order to test the complete theoretical model specifically with regard to temperature effects. This was accomplished by comparing calculated and measured *changes* with temperature in the radiation directivity. Thus, in Figure 4.30, for example, heating the jet to an exit temperature of $\sim 3\text{-}1/3$ times the ambient temperatures reduces the level at 90° by ~ 3 dB (relative to isothermal conditions). This determines the quadrupole/dipole relative weighting and also allows a Lilley equation directivity to be calculated for this jet temperature. The *difference* between it and the calculated isothermal directivity is then compared with the corresponding-measured difference.

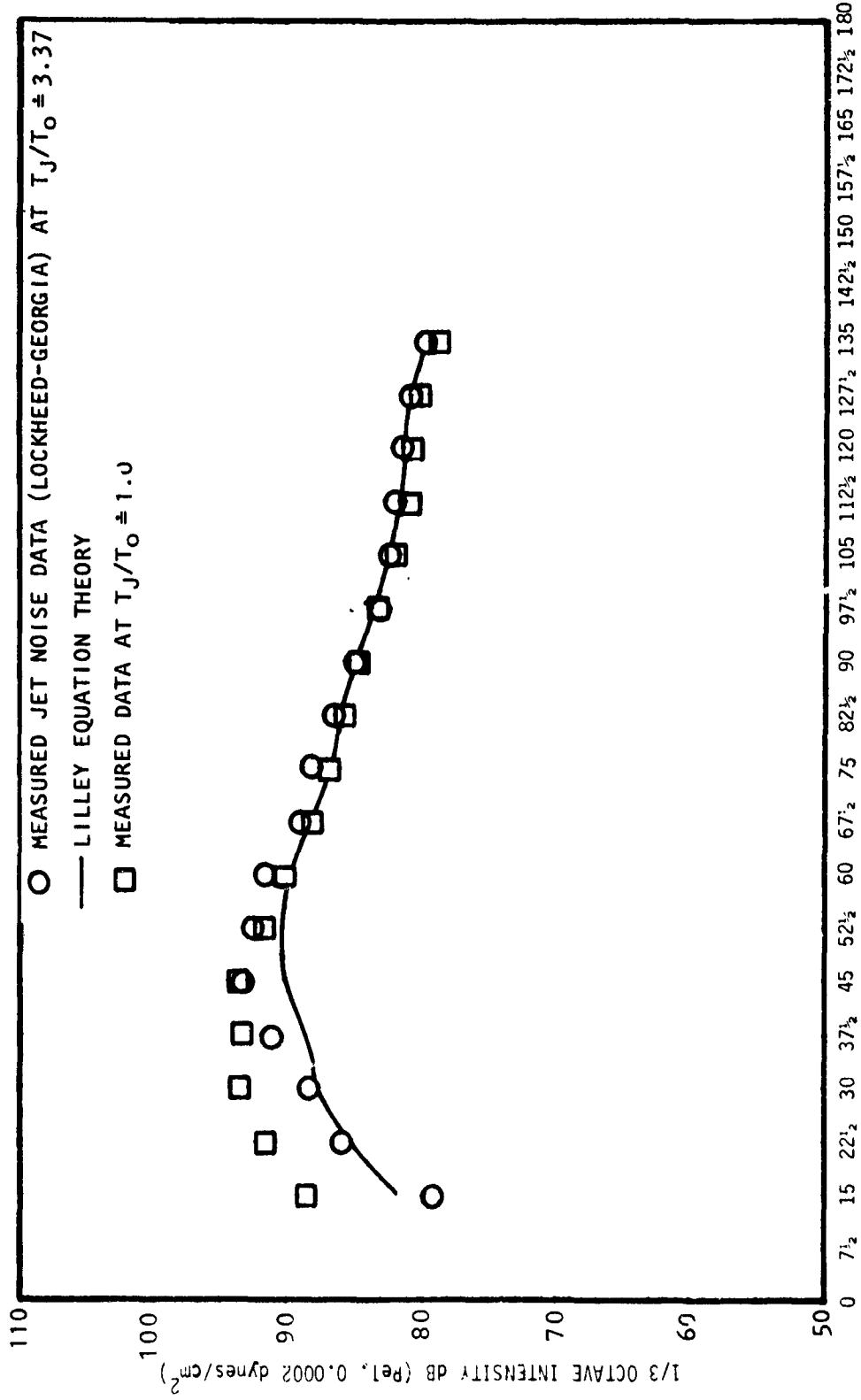
Rather than present predicted and measured differences for comparison, absolute levels are recovered by adding both to the measured isothermal levels, as in the examples of Figures 4.29, 4.30, and 4.31; the Lilley equation prediction is shown as a continuous line. The agreement with the measured hot jet data is remarkably good at this jet exit condition (that is, a velocity ratio $V_J/a_0 \approx 0.9$ and a temperature ratio $T_J/T_0 \approx 3.3$). In Figures 4.29 through 4.31 the frequency parameter S_m takes the values 0.3, 1.0, and 3.0. At $S_m = 0.1$ (Figure 4.29), despite the negligible change in measured levels at 90° , the theory reproduces the trend of lower measured levels at small angles. At the higher frequencies, the measured changes at 90° of ~ 3 dB and ~ 6 dB (Figures 4.30 and 4.31) remain about the same in the forward arc but both widen to ~ 15 dB at the smallest angles; both features are accurately reproduced by the Lilley equation-based predictions.

Clearly in those examples and others included in Volume II, the modified Lilley equation model (with the new dipole sources) must contain an adequate description of all temperature dependent flow-acoustic interactions within a heated or nonisothermal (shock-free) turbulent jet.

4.3 THEORY FOR NOISE FROM LARGE-SCALE TURBULENT STRUCTURE[†]

In Phase I, Lilley²⁸ proposed a model for the generation and radiation of sound in a turbulent mixing region. The central feature of the radiation model was the derivation of Lilley's equation which explicitly included mean flow/acoustic interactions as previously discussed. The model proposed for the turbulence was based on a decomposition of the fluctuating flow field into Fourier components and the proposition of a dominant wave motion. It was proposed to use this model of the turbulent structure to generate the source function in Lilley's equation and then proceed to calculate the radiated noise from this turbulence model. Thus, the objective of this part of the program

[†]This is a summary of results which appear in References 38, 54, and 55, and Volume II, Section 4.



DIRECTIVITY ANGLE FROM DOWNSTREAM JET AXIS - θ_0 or θ_m DEGREES

Figure 4.29 Directivity of Hot Jet Noise: Comparison of Lilley Equation Theoretical Model with Measured 1/3-Octave Data, for $S_m = 0.3$, $V_J/a_0 \approx 0.9$, $T_J/T_0 \approx 3.37$

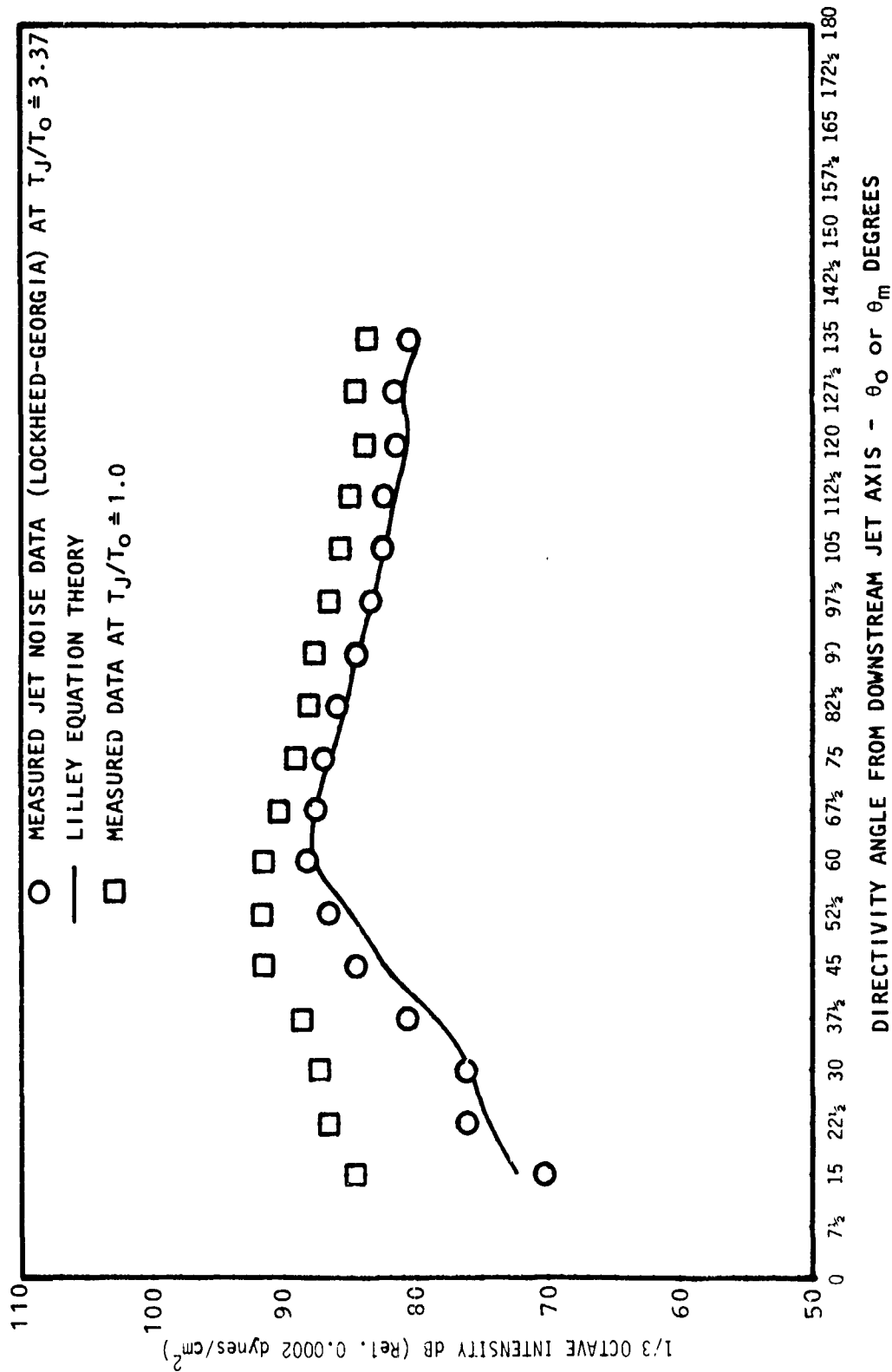


Figure 4.30 Directivity of Hot Jet Noise: Comparison of Lilley Equation
 Theoretical Model with Measured 1/3-Octave Data, for $S_m = 1.0$,
 $V_J/a_0 \approx 0.9$, $T_J/T_0 \approx 3.37$

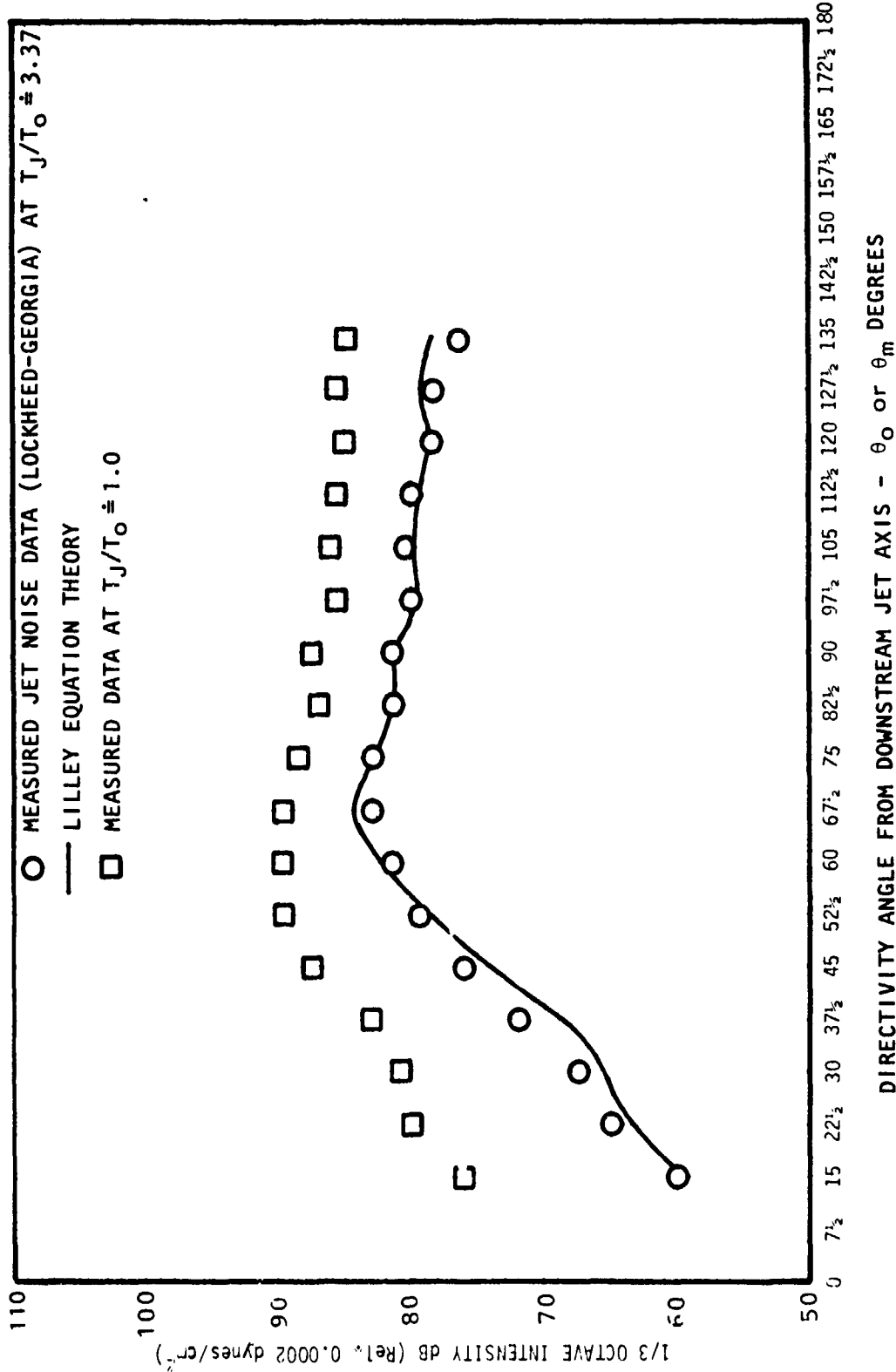


Figure 4.31 Directivity of Hot Jet Noise: Comparison of Lilley Equation
 Theoretical Model with Measured 1/3-Octave Data, for $S_m = 3.0$,
 $V_j/a_0 \approx 0.9$, $T_J/T_0 \approx 3.37$

was to define and calculate a wave-like structure for the turbulence. In the Phase II research, it was assumed that the time-dependent component of the turbulence was composed of two parts: a large-scale wave-like component and a fine-scale random component. In the work to follow, only noise radiation from the large-scale component will be considered, whereas the work summarized in Section 4.2 was concerned with noise radiation from small-scale turbulence.

In this summary a general introduction to the wave-model will be given and some of the results of the calculations will be discussed. The reader is referred to Volume II for details of the analysis and numerical techniques.

4.3.1 Method of Approach

The ideas for modeling the turbulence proposed by Lilley²⁸ had been pursued by Sharma⁵² and Morris⁵³. The former study considered the boundary layer and the latter considered a two-dimensional mixing layer. The concepts proposed in these models were used as a starting point and it was intended to sequentially study the incompressible axisymmetric jet, the compressible two-dimensional mixing layer, the compressible subsonic axisymmetric jet and the compressible supersonic axisymmetric jet. The first two of these cases were reported in 1974 by Morris⁵⁴ and Kapur and Morris⁵⁵. These turbulence models were essentially different to the final model used though the ideas expressed are relevant to turbulence modeling. For the purposes of determining the radiated noise, a modified approach was developed and the compressible axisymmetric jet was modeled in this fashion. This model is described in the next section.

4.3.2 The Turbulence Model

A laminar flow, whether it is bounded or free is known to exhibit certain characteristic modes when it is perturbed. These fluctuations may represent the first stages of transition from laminar to turbulent flow. Measurements of fluctuations in both naturally and artificially excited flows have shown that these fluctuations are wave-like in both space and time. Thus, it was natural to perform a decomposition of the unsteady equations of motion assuming a wave-like form for the fluctuations. Since these fluctuations were also very small in relation to the magnitude of the mean flow, it was also natural to linearize the resulting equations. An analysis of this kind for a viscous fluid leads to the classic Orr-Sommerfeld equation for a parallel mean flow. This equation is homogeneous and introduction of boundary conditions relevant to the flow being considered leads to a two-point boundary value problem. The order of the homogeneous differential equation depends on the geometry of the problem and whether the flow is compressible or incompressible. The parameters in this eigenvalue problem are the Reynolds number, the Mach number, the wavenumbers in two dimensions and the frequency of the fluctuation. Various combinations of these parameters enable the boundary conditions to be satisfied and are hence eigenvalues. The Reynolds number and Mach number are real quantities by definition, however, some physical reasoning must be used if either the frequency or wavenumber are taken to be wholly real rather than complex. For various reasons, early analytical and subsequently numerical solutions of this boundary-value problem chose to keep the wavenumber real. This implied that variation in amplitude of the fluctuation took place in time. However, most established flows develop spatially and most good agreement of theory and experiment has occurred when the frequency is made real and the wavenumber is complex. This provides variation in amplitude with space rather than time.

The essential difference between the boundary layer equations for laminar and turbulent flows is the existence of extra terms which are nonlinear in the fluctuations. These terms include the shear and normal stresses. The modeling of these stresses has been the consuming interest of researchers and has led to the development of such concepts as the mixing length and eddy viscosity. In this latter case the motion of the fluctuations is assumed to provide one extra viscosity to the fluid which, in most cases, is far in excess of the fluid viscosity. When this assumption is made, the boundary layer equations reduce to an equivalent laminar boundary layer form, with an added viscosity whose behavior has to be determined. This concept has led to considerable success in predicting the development of a turbulent flow and the assumption of an eddy viscosity will be used in the present model.

With this obvious link between laminar and turbulent flows, a model of the flow may be proposed which consists of three components; a time-independent component, a wave-like periodic component, and a random time dependent component. All three of these components may be obtained from experiment by techniques such as time-averaging and phase-averaging. The equations and boundary conditions for the wave-like component are identical to those of the assumed periodic fluctuation in a laminar flow except for the presence of terms which represent the fluctuating random stresses. If an assumption is made as to the value of the eddy viscosity, this turbulent flow eigenvalue problem may be solved in an identical fashion to the laminar flow case. There are two further physical assumptions to be made before the linear wave model is complete. Firstly, it will be assumed that in spite of the axial variation of the mean flow properties, the characteristic oscillations at any axial location may be approximated by making a locally parallel flow assumption. Secondly, because of the dynamic nature of the instability process in a jet flow, the local fluctuations may be determined by an inviscid stability analysis; that is to say that even the turbulent Reynolds number is sufficiently high to render the problem essentially inviscid.

The fundamental flow model may now be summarized. A disturbance of a fixed frequency is generated in the flow. This could be an oscillation in the jet-pipe boundary layer, some fluctuating mass flow, or an infinitesimal exterior influence. As this wave propagates downstream its rate of growth is determined by the characteristics of the local flow profile. In fact, the wave will encounter regions of growth, neutrality and decay. The maximum amplitude of the fluctuation will occur at the axial station where it is a locally neutral disturbance. This process of growth and decay is found to be confined to the nozzle exit region for high frequencies and is spread over a longer axial extent for low frequencies.

Calculations are performed for an isothermal jet with a jet exit Mach number of 1.4. Though the axial development of the wave is described by an integral analysis, some aspects of the wave behavior can be determined from the local stability analysis. The phase velocity as a function of jet width for the helical, $n=1$ mode is shown in Figure 4.32. If the phase velocity predicted by linear theory is supersonic with respect to the ambient speed of sound, then a linear coupling of the propagating wave and the acoustic field occurs leading to direct far-field radiation.

Since the small-scale random fluctuations have been included through an assumption of an eddy viscosity, they are confined to regions of non-zero

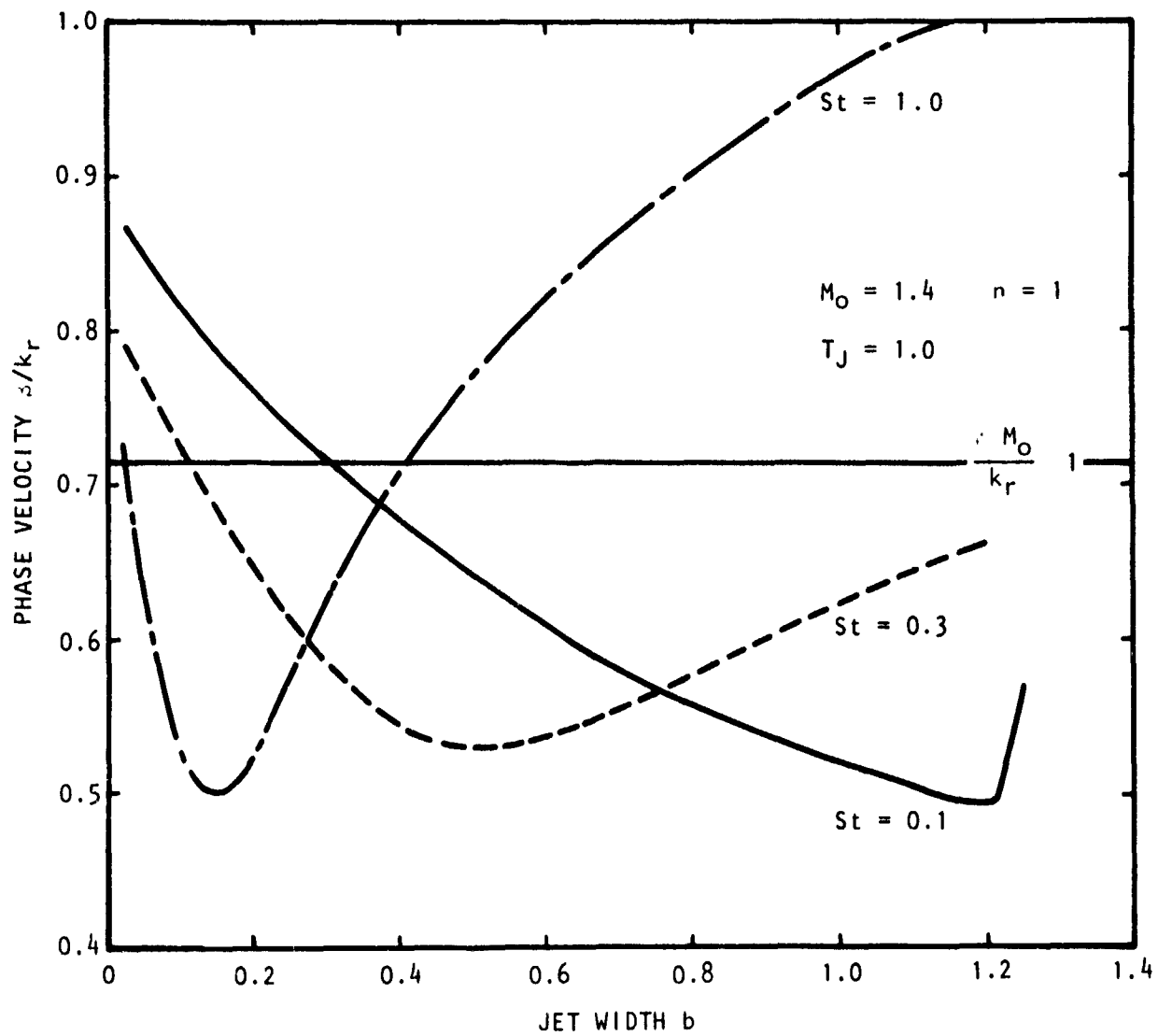


Figure 4.32 Variation of Phase Velocity with Jet Width: $n = 1$

mean flow gradients. However, the wave-like components of the flow-field extend beyond the edges of the jet flow decaying as Hankel functions of the first kind. Thus, the near-field pressure fluctuations in the jet may be associated with the wave-like structure so long as the distance from the edge of the shear layer is not sufficiently large to make the locally parallel flow eigensolutions invalid. Examples of the near-field contours of equal SPL are shown in Figure 4.33 and 4.34 for an axisymmetric mode and Strouhal numbers of 1.0 and 0.3 and an isothermal jet Mach number of 1.4. The higher frequency case peaks close to the jet exit and the $St=0.3$ peaks further downstream. This behavior is characteristic of near-field pressure measurements.

4.3.3 The Radiation Model

With the flow field apparently well defined, the mechanism by which these wave-like motions radiate noise to the far-field must be examined.

In order for a wave to radiate in some direction to the far-field, it must have a sonic phase velocity in that direction. In the locally parallel flow analysis used above to calculate the near-field, it is found that the local phase velocity never exceeds the jet centerline velocity. Thus, it might appear that the dominant near-field structure can only radiate noise for supersonic jet exit velocities. However, as the fixed frequency wave propagates downstream, its amplitude varies and the Fourier transform in the axial direction provides a spectrum of wavenumber components. Some portion of this one-dimensional energy spectrum can lead to far-field radiation. Clearly, the peak in the spectrum will occur close to these values of wavenumber calculated in the local flow analysis, and the higher the jet exit velocity, the closer this wavenumber peak will come to the band of wavenumbers that can radiate. However, in spite of the discreteness of the frequency fixed in the analysis, the wavenumber spectrum is continuous and hence the far-field noise is not confined to a single direction. Also, all frequencies are permissible though the calculations may show some range of frequencies to radiate dominantly in certain directions.

The variation of the amplitude of the $n=1$ mode, which is characterized by the relative wave kinetic energy flux, is shown in Figure 4.35. As discussed above it is this variation of amplitude with axial distance that is found to provide the mechanism by which a wave which has a subsonic phase velocity, calculated from local linear stability theory, may radiate noise to the far field. The Strouhal number 0.3 wave is seen to reach the greatest amplitude.

In spite of the essential simplicity of this noise generation and radiation model, the actual calculation of far-field noise is not straightforward. Two approaches are open. In the first the flow-field and hence the source term in a Lighthill or Lilley equation is defined and the analysis may proceed accordingly. However, there is some question in the use of these models as to the convergence of various integrals and to the true physical meaning of 'near' and 'far' field when the flow model is essentially the inner solution in a matched asymptotic method. The second technique is easier to use numerically, but has certain physical limitations which will be described below. In this approach a control surface is constructed in the ambient medium around the jet. The fluctuations on this surface can be obtained from the

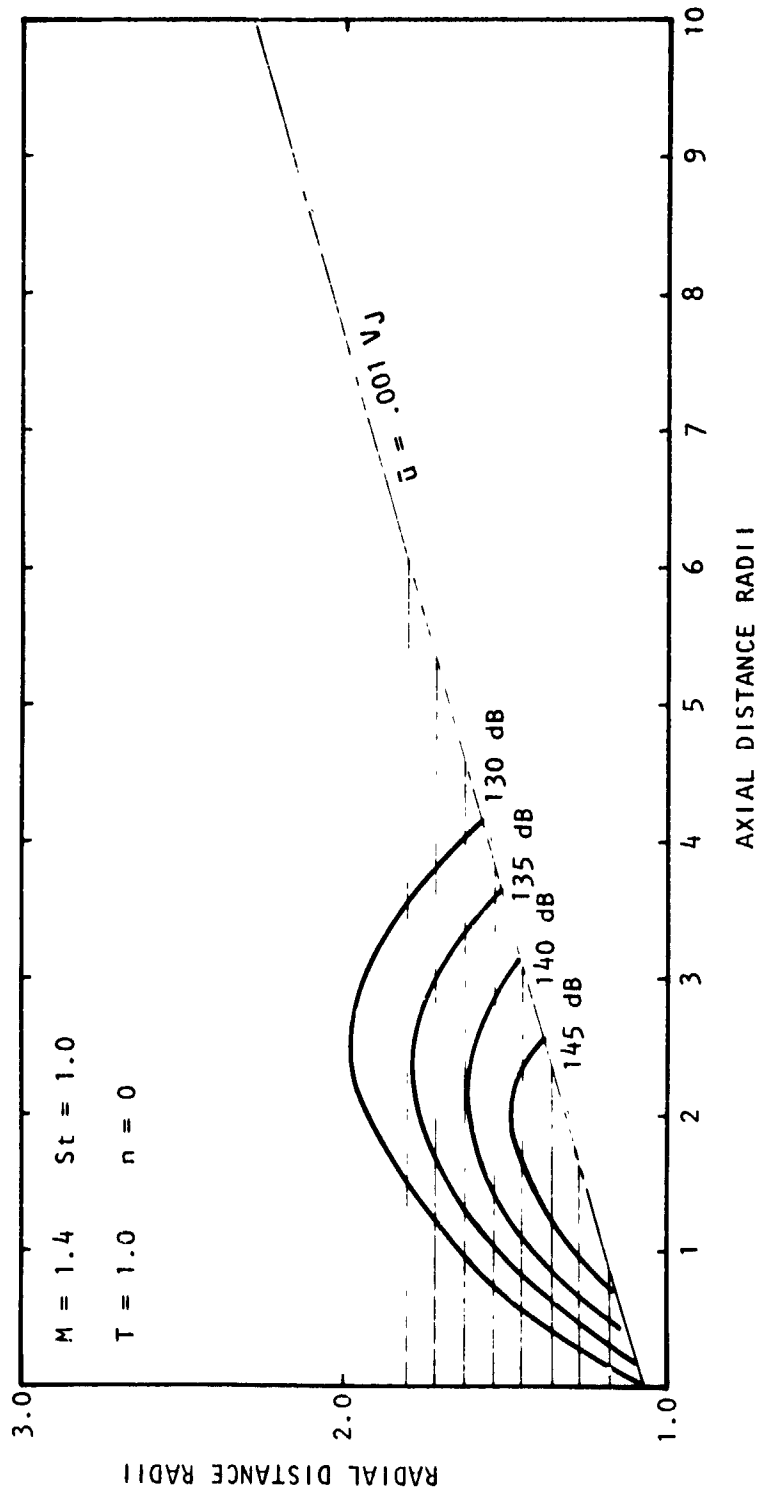


Figure 4.33 Contours of Sound Pressure Level in the Near Field: $St = 1.0$

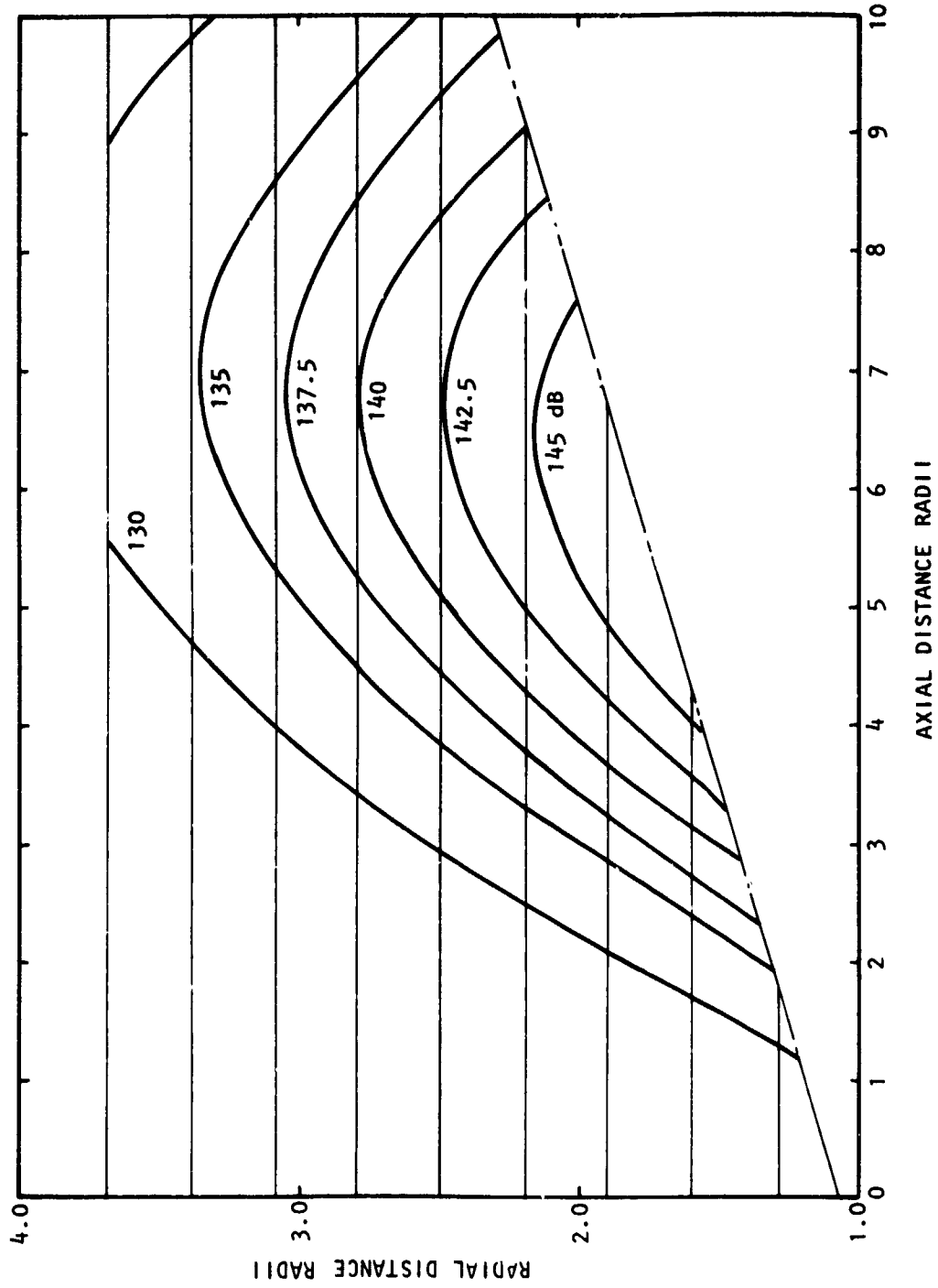


Figure 4.34 Contours of Sound Pressure Level in the Near Field: $St = .3$

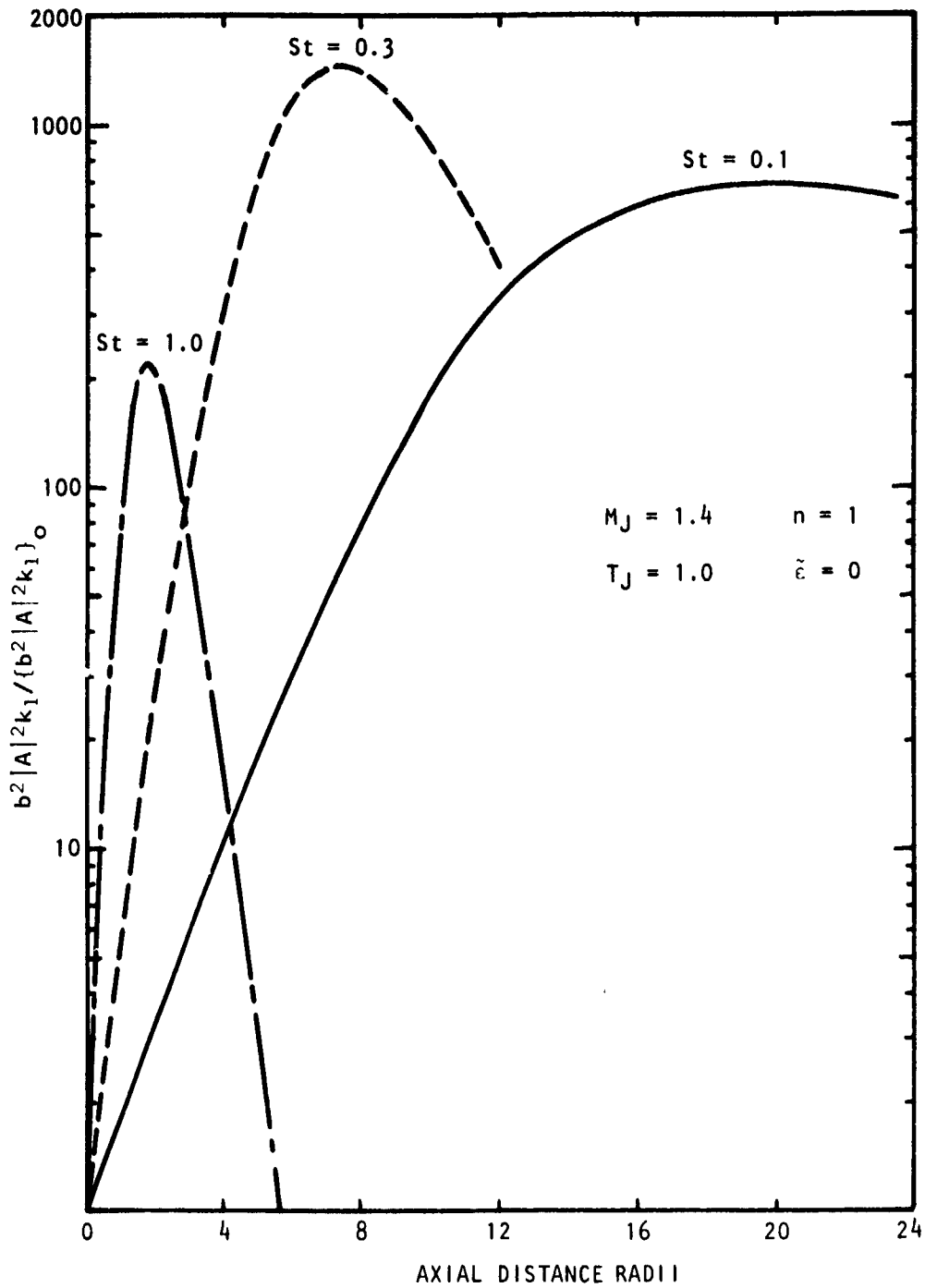


Figure 4.35 Axial Variation of Relative Kinetic Energy Flux
Integral Amplitude: $n = 1$

near-field solution and the far-field noise may then be calculated by classical methods.

This latter model is used in the present work. The control surface is cylindrical and its radius is chosen so that the diverging jet flow does not intersect it until downstream of the region where the frequency fluctuation of interest dominates the near-field. A correction to the locally parallel flow solutions is applied so that they locally satisfy continuity and momentum in a diverging flow. This correction is shown to render the problem independent of control surface radius. The wavenumber component spectrum of axisymmetric radial velocity fluctuations on a control surface of nondimensional radius $(1 + \lambda/2)$, where λ is the acoustic wavelength, and Strouhal number 0.3 is shown in figure 4.36. At this Strouhal number sound is radiated to the far-field for $-St M_0/\pi \leq k \leq St M_0/\pi$ ($-\pi \leq \theta \leq \pi$, where θ is the direction in the far-field). The corresponding far-field directivity is shown in figure 4.37. The peak radiation angle occurs close to the jet axis. A complete set of results for various frequencies and mode numbers is given in Volume II. These results indicate certain differences between the predicted and the measured far-field noise. This leads to the conclusion that this conceptually simple technique has physical deficiencies. The major criterion lies in the assumption that the axial distribution of a single frequency wave on the control surface may be expressed in terms of locally corrected parallel-flow eigensolutions. The analysis does not allow for either upstream or downstream propagation of fluctuations from one station to the next except by means of a piecewise locally parallel flow approximation. This leads to major discrepancies where the control surface is far from the edge of the jet such as in the case for low frequencies close to the plane of the jet exit. However, the calculations do demonstrate that the basic mechanism described above is capable of radiating noise to the far-field even when the local near-field solution has a subsonic phase velocity and it is the method of calculating the far-field not the basic generation mechanism which is in question.

The reader is referred to Section 4, Volume II for further discussion of this last problem. Also given in more detail are the mathematical derivations, a discussion of the role of eddy viscosity in the model, the effect of finite amplitude forced oscillations and the analysis for local corrections for the effects of flow divergence.

4.4 SHOCK-ASSOCIATED NOISE THEORY

While the evaluation of existing theories for turbulent mixing noise generation revealed distinct inadequacies with regard to source definition and flow acoustic interactions, the existing theory for shock-associated noise was in a somewhat better situation. While the existing theory depended to a great extent on modeling concepts, rather than on solution of field equations, the model included a rather specific definition of the source characteristics. Thus, unlike the Lighthill model, one is delving into the actual characteristics of the shock-turbulence interactions when defining the source of broadband noise. However, like the Lighthill analysis, only the Doppler features of the flow/acoustic interactions are included in the model. Refraction and diffraction by the jet flow are not included, however, this is not considered to be nearly as serious an omission as it was for the turbulent mixing noise.

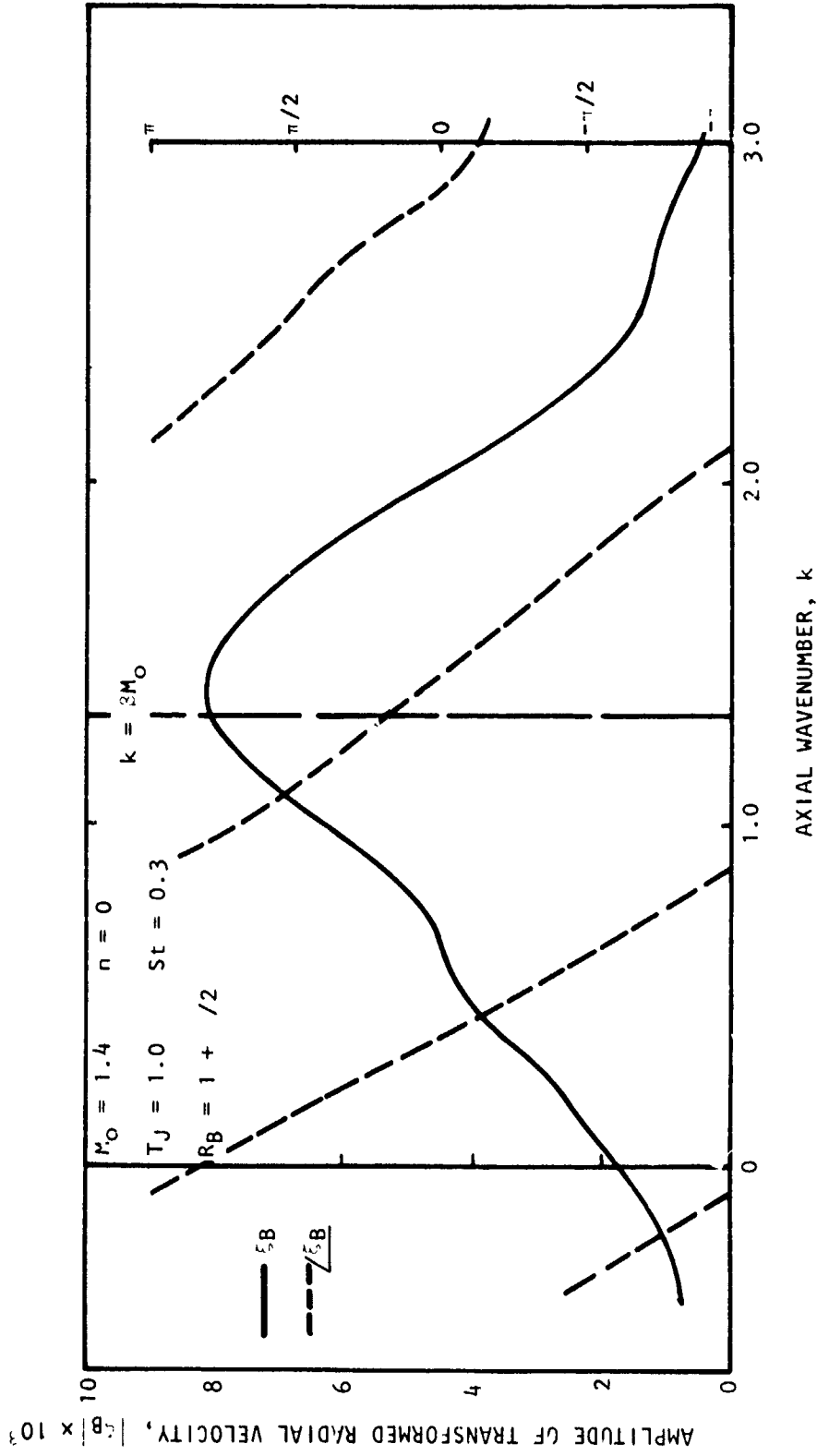


Figure 4.36 Wavenumber Component Spectrum of Radial Velocity Fluctuation

RELATIVE PHASE OF TRANSFORMED RADIAL VELOCITY, ϕ_B

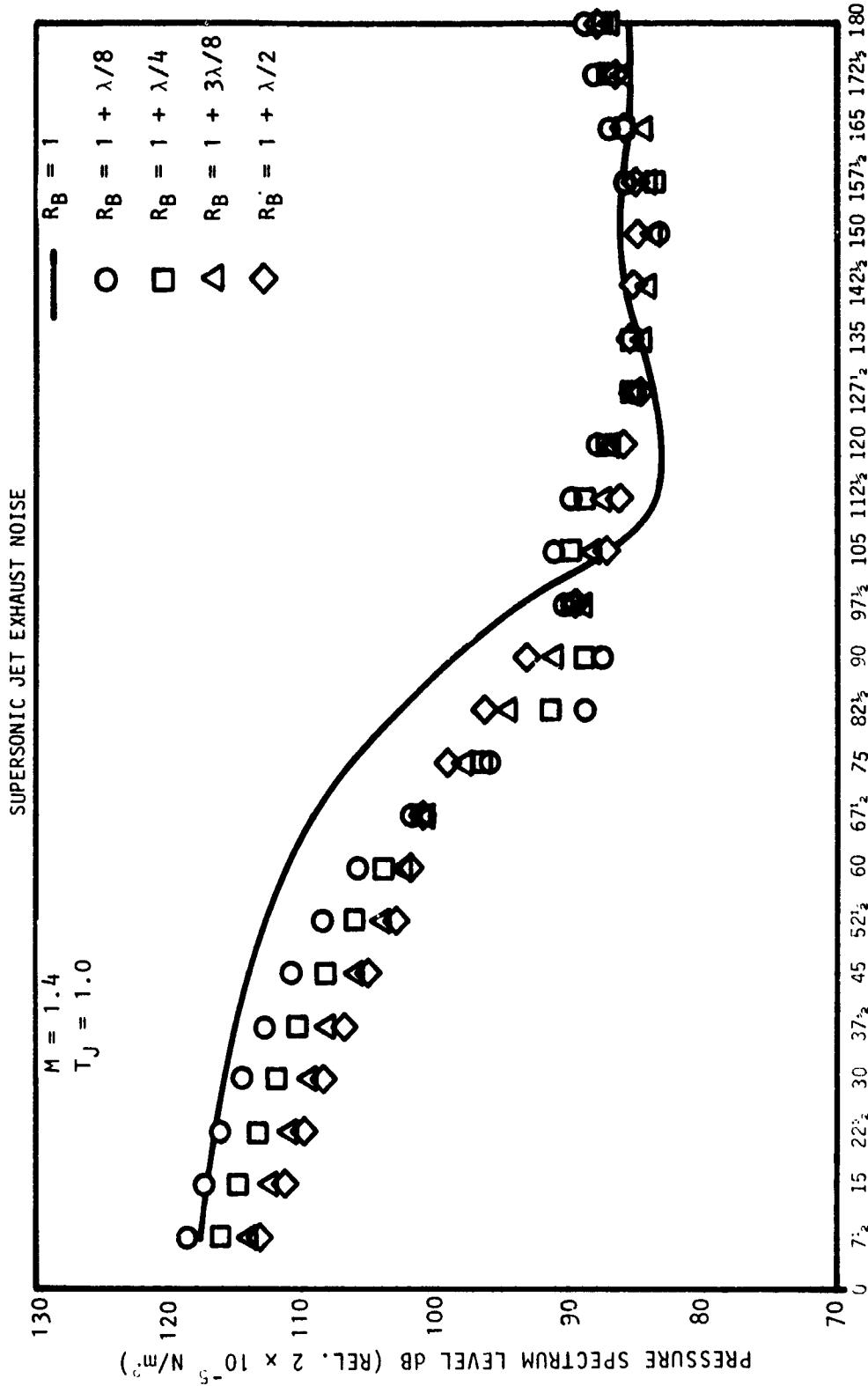


Figure 4.37 Predicted Far-Field Directivity Pattern: $n = 0$, $St = .3$

since shock-associated noise for predicted engine operating conditions normally dominates only in the forward arc, where these effects can be expected to be small.

The existing shock-associated noise model of Harper-Bourne and Fisher⁴¹ was evolved by extending Powell's original model⁵² for the discrete components, but without the feedback mechanism between the nozzle lip and the first shock. In this model the end of each shock cell is taken as a compact source of sound and the relative phasing between the sources is determined by the convection of turbulent eddies between them. The model therefore consists of an array of shock-turbulence interaction sources in line with the nozzle lip and almost equally spaced with separation L . It is assumed that the convection of turbulent eddies along this line of sources causes each to emit sound at the time of arrival of the eddy.

The model considered the far-field sound pressure to be the sum of contributions from each correlated point source located at the shock positions. Also, even though the shock locations are stationary, it was shown by an extensive investigation of the flow characteristics that the source has the convective characteristic of the turbulence, thus justifying the Doppler frequency dependence.

The theoretical model gives the far-field spectral density of sound pressure, $G_{pp}(R, \theta, \omega)$, as a product of three terms in the following manner:

$$\underbrace{\text{Far-Field Intensity Spectrum}} = \underbrace{\text{Mach Number Dependence}} \times \underbrace{\text{Group Source Spectrum}} \times \underbrace{\text{Interference Weighting}}$$

$$G_{pp}(r, \theta, \omega) \quad \left(\frac{D}{R}\right)^2 \left(\frac{D}{a_0}\right) \beta^5 \quad H_0(\sigma) \quad f\{N, L_n, \theta, C_{m-n}(\sigma), \omega, V_c\}$$

where

$H_0(\sigma)$ = group source strength spectrum

$C_{m-n}(\sigma)$ = correlation coefficient spectrum between fluctuations at m^{th} and n^{th} shocks

N = number of shocks

L_n = shock spacing for n^{th} shock

V_c = turbulence or eddy convection velocity

and σ = Strouhal number, $\omega L/a_0$.

The first term includes the basic Mach number or pressure ratio dependence discussed previously for the overall intensity results. The second term is defined as the normalized group source strength spectrum, and it effectively represents the combined strength of the shock-turbulence interactions occurring

at several shock locations. The final term represents the magnitude of the constructive or destructive interference that occurs when sound waves emitted from various sources arrive simultaneously at the observation point (R, θ) . This interference function is dependent on the number of shocks, N , the shock spacing, L_n , the angle of radiation, θ , the correlation coefficient spectrum between fluctuations at various shock locations, C_{m-n} , and the frequency. Harper-Bourne and Fisher determined the strength of the correlation coefficient spectrum by making detailed measurements with a crossed-beam Schlieren system.

In our program of examining and verifying the theory, the following was accomplished.

The peak frequencies of shock-associated noise were examined in light of the theoretical model. The presence of Doppler shift with angle in the measured peak frequencies, and the variations of measured peak frequencies with pressure ratio and temperature ratio, are all found to be in good qualitative agreement with the theoretical model. Further comparison of measured peak frequencies with theoretical scaling formulae provide several useful implications regarding the characteristics of shock-containing jet flows. It is inferred that the average value of turbulence or eddy convection speed in a jet flow is approximately 0.7 times the jet efflux velocity, and this fraction remains nominally independent of the pressure ratio. This observation therefore agrees with the measured value of V_c , obtained mainly from unheated jets by several investigators. The values of a shock spacing constant, K (shock cell length, $L = K\beta D$) are also calculated, and it is inferred that this increases with pressure ratio parameter β . It remains to be seen whether this trend can be verified experimentally.

A computer program for the prediction of shock-associated noise, based on the model, was developed, and a preliminary comparison of measured and predicted spectra was conducted. An example is given in Figure 4.38. Although the predicted spectra are found to be in good agreement with the measured spectra, it has not been possible to derive any specific conclusion. There are significant quantitative differences since the comparison was not extensive. Furthermore, it is suggested that such a comparison will become more meaningful if values of various jet flow parameters, required for input to the prediction scheme, are obtained experimentally. A considerable amount of future effort is therefore required on various specific aspects of shock-associated noise, and this is discussed in Section 7 of Volume II.

SUPERSONIC JET EXHAUST NOISE

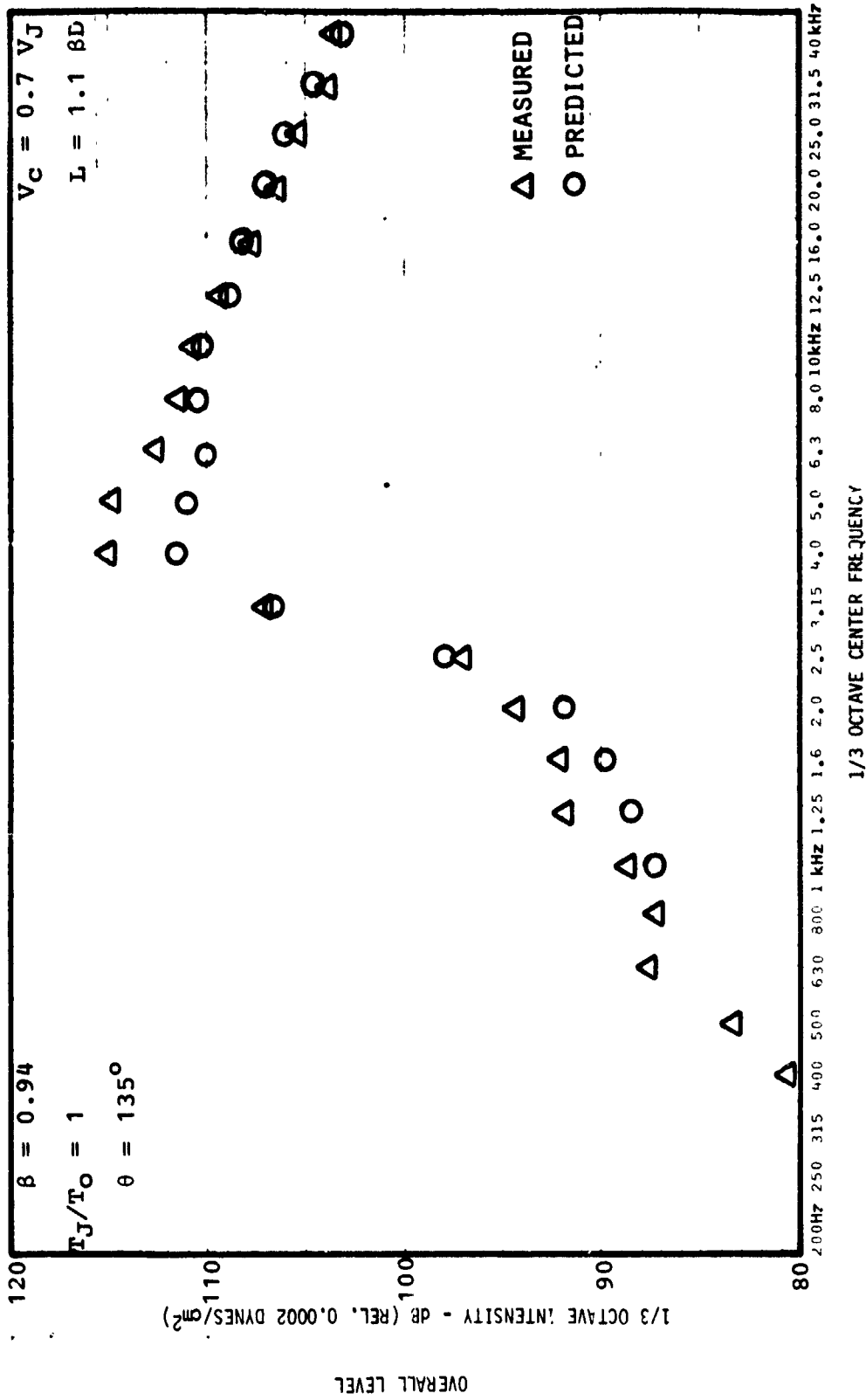


Figure 4.38 Comparison of Measured and Predicted Spectra

5. CONCLUSIONS

This program of research on supersonic jet noise has produced several fundamental advances in the physical understanding and quantification of both the noise generating mechanisms within the jet flow and the radiation out to the far field. The total sound field from a heated supersonic jet exhaust was taken to be comprised of contributions from three types of noise sources (or noise generating processes). These were (i) the sound generated by small-scale turbulence associated with the mixing of the jet exhaust flow with ambient air, (ii) the sound generated by large-scale orderly structure within the jet flow, and (iii) the sound generated by the interaction between convected turbulence and stationary shocks at supercritical conditions. Each noise source has been examined independently as far as possible, and both acoustic as well as flow characteristics have been investigated in order to link the noise generation processes with the far-field propagation phenomena.

The theoretical studies on turbulent mixing noise were centered around the Lilley equation. These studies (i) have successfully explained all the features of subsonic isothermal jet noise directivity variations with velocity and frequency, (ii) have explained the relevant features of supersonic isothermal jet noise outside the so-called cone of silence, and (iii) have explained the effects of jet temperature at subsonic and supersonic velocities, and in the process have identified new dipole sources of noise in heated jets. These dipole sources arise from (a) an imbalance of the turbulent mixing noise lateral-lateral quadrupoles across temperature gradients and (b) scattering of turbulent pressure fluctuations by unsteady density fluctuations in heated jets. It was also shown how the jet temperature field affects propagation to the far field. In these Lilley theory studies, it was also discovered that, rather than the Lighthill "volume acceleration" quadrupole, the jet mixing noise is generated from a "volume displacement" quadrupole. In addition to the numerical solutions, low and high frequency analytic solutions were developed, which will ultimately provide the foundation for a prediction program.

The Lilley theory solutions have also shed light on what may be termed one of the additional sources of supersonic jet noise generation. The present solutions do not match experiment within the cone of silence (i.e., a conical volume with axis along the jet exhaust and whose half-angle is given by the angle at which rays, parallel to the jet axis within the flow, are emitted in the ambient atmosphere) for supersonic conditions. Instead, it appears from examination of the experimental data that another source of sound exists with a strong directivity in the vicinity of the exhaust axis, whose strength increases with jet velocity. All evidence suggests that this sound is the result of radiation from large scale helical instabilities in the jet mixing region. A theory which describes the development of these instabilities and the associated jet structure development has been completed for the case of a compressible axisymmetric supersonic jet. A model for the noise radiation from this large-scale motion was also presented and qualitative agreement with experiment was achieved in the preliminary numerical calculations. However, future calculations of the far-field noise will define the large-scale source function in Lilley's equation which will take account of the finite extent of the source region and flow-acoustic interaction effects, both of which were not accounted for in the work completed.

The third source of supersonic jet noise, mentioned above, arises only in shock-containing jets. When present, it usually dominates the sound field in the forward arc. It is referred to as the broadband shock-associated noise. A theoretical model had been developed by Harper-Bourne and Fisher for this noise source, and this theory was shown to provide good agreement with the experimental results obtained in the present program.

The success of the theoretical results hinged on close interaction with the experimental program. Since some of the effects predicted by theory exhibit only small, but in terms of the generating mechanisms involved physically significant variations from the primary V_J^8 dependence for turbulent mixing noise, it was necessary to acquire precise acoustic and jet flow data.

In the acoustic experimental program, after carefully removing all significant external contaminations, a series of tests was conducted which effectively separated turbulent mixing noise from broadband shock-associated noise. Furthermore, within each of these two categories, the experiments provided independent isolation of the effects of temperature and velocity (or Mach number) on the radiated sound. From these tests, the following conclusions were drawn:

- (i) Based on the 90° noise data for isothermal exit conditions in the range $0.35 \leq V_J \leq 2.0$, a $V_J^{7.5}$ velocity dependence was observed, leading to the inference, subsequently verified by flow measurements, that turbulence does not scale linearly with jet mean velocity at high velocity.
- (ii) At low velocity and high temperature, an increase in noise was observed, based on the isothermal reference levels, in support of the theoretical predictions of additional dipole sources resulting from temperature gradients and scattering from density fluctuations. Later correlations with the theory showed detailed quantitative agreement.
- (iii) Data from convergent-divergent shock-free nozzles at supersonic conditions provided proof that turbulent mixing noise could effectively be separated from shock-associated noise. Temperature effects at high velocity were reversed from those observed at low velocity.
- (iv) Broadband shock-associated noise data confirmed the validity of the theoretical model of Harper-Bourne and Fisher over a wide range of Mach number and jet temperature.

In general, the acoustic experimental data have confirmed the new predictions of the theory relative to flow/acoustic interactions, source strength modifications, and new sources, and have provided an accurate data base for use in future jet noise research.

In addition to acoustic data, it was necessary to have accurate data on the turbulence and mean velocity behavior with jet velocity and efflux temperature. This required the development of a sophisticated laser velocimeter, which was finally accomplished although somewhat late in the Phase II program. The LV was successfully calibrated against a hot-wire in a low velocity

environment. Upon conclusion of this calibration, a limited but very useful experimental program was conducted. From these experiments it was found that:

- (i) In progressing from low subsonic to supersonic speed, the jet structure did not suffer drastic changes.
- (ii) Increase in Mach number caused the spread rate to decrease and the potential core length to increase. Useful relationships expressing this behavior were derived. In addition, the mean velocity profiles, up to the end of the potential core, were shown to correlate universally on specific parameters.
- (iii) Turbulence level was shown to scale with mean velocity raised to a power less than unity, and similarity was not observed in the turbulence data.
- (iv) Based on dimensional analysis, the turbulence data confirmed the 90° noise observations, i.e. that the observed $V_j^{7.5}$ behavior is a consequence of reduced turbulence scaling with jet velocity.
- (v) Limited experimental data with heated jets showed a drastic increase in spread rate and a decrease in potential core length.

It can finally be concluded that this program of jet noise research has provided a theoretical explanation of most of the previously recognized problems with the old jet noise theory. However, a few specific areas of work need to be completed before a unified supersonic jet noise prediction scheme, which would calculate the sound field from all types of noise based on fundamental principles, can be completed. One major problem is a positive confirmation that the discrepancy at supersonic velocity inside the cone of silence is due to large-scale noise radiating eddies and that this noise is accurately predicted by the large-scale turbulence noise theory developed during this program. It is also essential to the ultimate development of a general supersonic jet noise prediction capability to provide a unified turbulence and jet noise source prediction capability for the small-scale turbulence. This capability hinges on precise experimental evaluation of the turbulence properties including the fourth order correlations.

A Phase III program, due for completion at the end of 1977, is designed to provide a jet noise prediction capability for arbitrary, but axisymmetric jet exhaust conditions. In order to accomplish this, theoretical work described in this report is being continued and experimental work on turbulence and acoustics is underway. Flow field measurements will be accomplished with a new four-channel, two-point LV for measuring the convected properties of turbulence as well as for extending the available turbulence and mean velocity measurements.

APPENDIX I

ANECHOIC JET NOISE TEST FACILITY CALIBRATION[†]

[†]*The results to follow are summarized from data published by Tanna, Dean, and Fisher³⁹ and Burrin, Dean, and Tanna⁵⁷, as well as information in Reference 38.*

Much confusion about jet noise has arisen in the past as a direct result of inadequate facilities and insufficient knowledge and control of test conditions. The present facility was carefully designed to avoid, insofar as possible, other facilities' shortcomings, the design being guided by the stringent demands of on-going jet noise research at Lockheed. Prior to the design and construction of the facility, a one-sixth scale model of the anechoic room was constructed and a comprehensive series of flow visualization and temperature mapping experiments was conducted. The results of this model study dictated the design of the exhaust collector/muffler to provide entrainment and room cooling air in the quantities demanded by the jet operating conditions. The choice of acoustic wedge material and design was optimized by conducting an extensive series of performance evaluation tests in a specially built impedance tube. A plan view of the complete hot jet noise facility is shown in Figure 1-1. The major points are summarized below.

The anechoic room measures 22 ft. (long) x 20 ft. (wide) x 28 ft. (high) between concrete walls and the flame-retardant wedges are 18 in. long. The room is anechoic at all frequencies above 200 Hz as can be observed from Figure 1-2, which is a typical intensity-distance result obtained in the room with a point source with 1/3-octave broadband excitation. The facility is capable of testing model jets of 2 in. diameter at stagnation temperatures up to 2000°F and pressure ratios as high as 8. The hot air is supplied by the Sudden Expansion (SUE) Propane Burner, with afterheating by an electric heater between the muffler and the plenum.

Three special features of the facility are:

- (a) an acoustically treated exhaust collector that sucks entrainment air through the outer channel in quantities dictated by the particular jet operating condition with no special forced-air injection or fan installation;
- (b) an air gap between the concrete wall and the false wall on the collector side of the room to distribute this entrainment air symmetrically around the jet axis, as well as to keep the room air-flow circulation velocities to a minimum; and
- (c) a "cherry-picker" crane used to gain access to instrumentation, etc. for maintenance, calibration and set-up, thus eliminating the need for access platforms. The crane is stowed by remote control under an anechoic cover during all test operations.

ANECHOIC ROOM PERFORMANCE EVALUATION TESTS

In order to confirm the design criteria and to ensure the accuracy of the subsequent jet noise measurements, the facility was subjected to rigorous performance evaluation tests at appropriate stages. The major findings are as follows:

- (a) The overall SPL of background (or ambient) noise in the anechoic room is 45 dB.

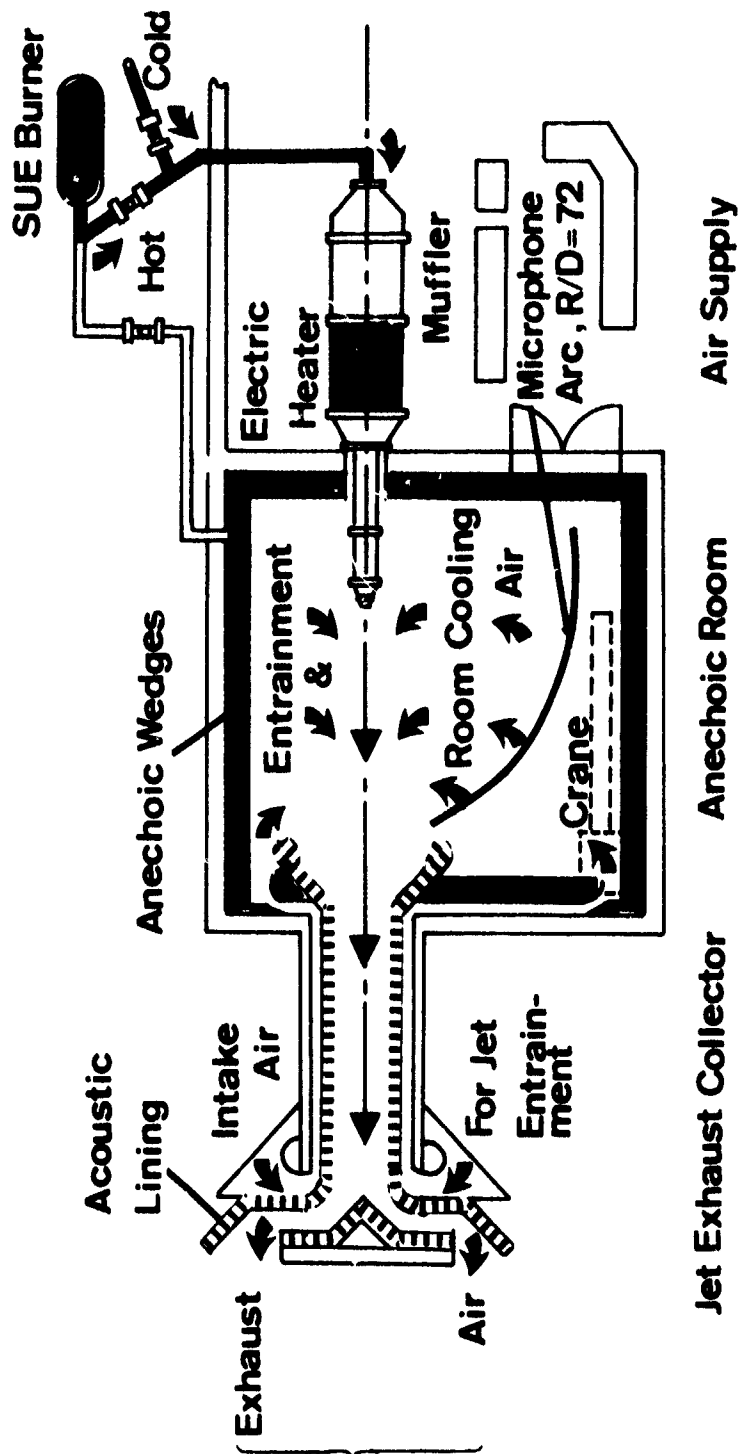


Figure 1-1 Plan View Schematic of Supersonic Hot Jet Noise Facility

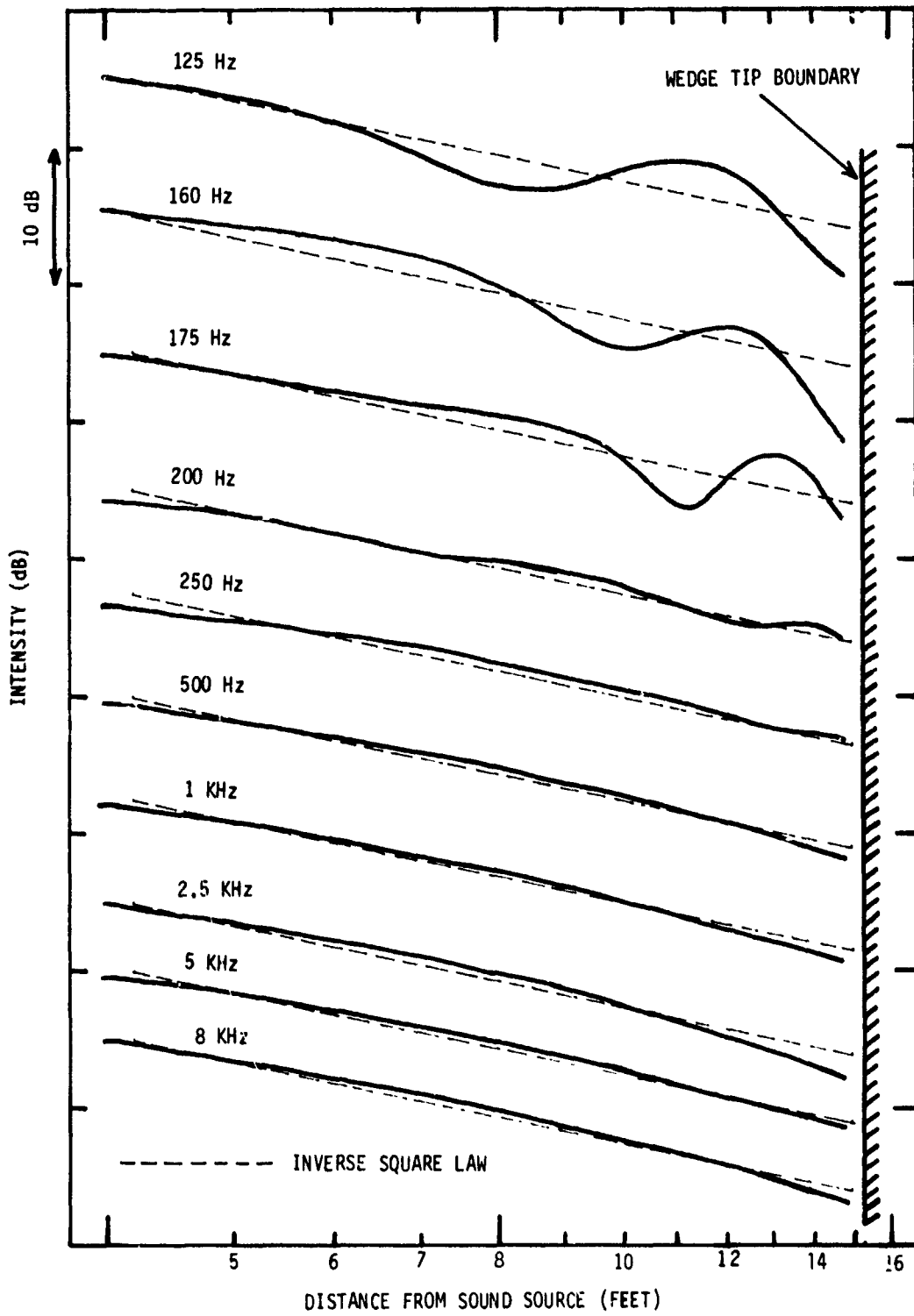


Figure 1-2 Intensity-Distance Plots with Point Sound Source

- (b) The attenuation produced by the lined exhaust collector was determined approximately by subjecting the outside end of the collector tunnel to a broadband noise and measuring the 1/3-octave SPL spectrum at the entrance to the tunnel. The measured noise reduction of the collector was 47 dBA, being 20 dB in the 200 Hz band and increasing to approximately 60 dB in the 10 kHz band.
- (c) In order to evaluate the anechoic quality of the room and to ensure that the proposed microphone distance of 12 ft. (72 D) is in the *acoustic* far-field, an audio driver unit placed at the nozzle exit location was used as the sound source (i.e., point source), and the intensity vs. distance plots at various 1/3-octave frequencies were obtained with a traversing microphone arrangement. These plots established that the cut-off frequency of the room was 200 Hz and that at a distance of 12 ft. the observer was in the *acoustic* far-field at all frequencies (above 200 Hz) of interest, as shown in Figure 1-2.
- (d) With the same traversing microphone arrangement, a cold jet ($V_j/a_0 = 0.85$) was used as the sound source in a second series of tests and the intensity-distance plots at various 1/3-octave frequencies were measured at four angles to the jet axis. At distances greater than 9 ft. from the nozzle exit plane, the intensity conformed to "inverse-square law," except at frequencies above 8 kHz, where the decay was somewhat sharper because of the increasing atmospheric attenuation with frequency, as shown in Figure 1-3. Hence, it was established that for frequencies above 200 Hz, the acoustic interference produced by sources distributed over a finite region of the jet exhaust flow does not affect the "inverse-square law" decay of intensity for observer distances greater than approximately 54 nozzle diameters.

"ACOUSTIC CLEANLINESS" TESTS

The "acoustic cleanliness" or internal noise aspect of the rig was examined in the first instance by employing the usual method of measuring the noise from a cold convergent nozzle at 90° to the jet axis and studying its velocity dependence. It was found that the overall SPL followed a V_j^8 law within 1 dB between the velocities of 400 and 1000 fps, whereas at velocities outside this range, the levels were higher. At velocities above 1000 fps, it was clear that the levels were higher because of the presence of shock-associated noise. At velocities below 400 fps, however, a careful examination of the 1/3-octave spectra, together with the combined spectrum of background and instrumentation noise of the complete measuring system as shown in Figure 1-4, revealed that, at these low jet velocities, the low and high frequency ends of the spectra were being lifted by the instrumentation noise.

In order to further substantiate this observation and quantify the extent of the instrumentation noise contamination, the same series of mixing noise data were measured, this time with a minimum amount of instrumentation: i.e., a 1/2-in. Brüel and Kjaer (B&K) microphone, a 1/3-octave analyzer and a level recorder. The corresponding spectra at jet efflux velocities from 300 to 1240

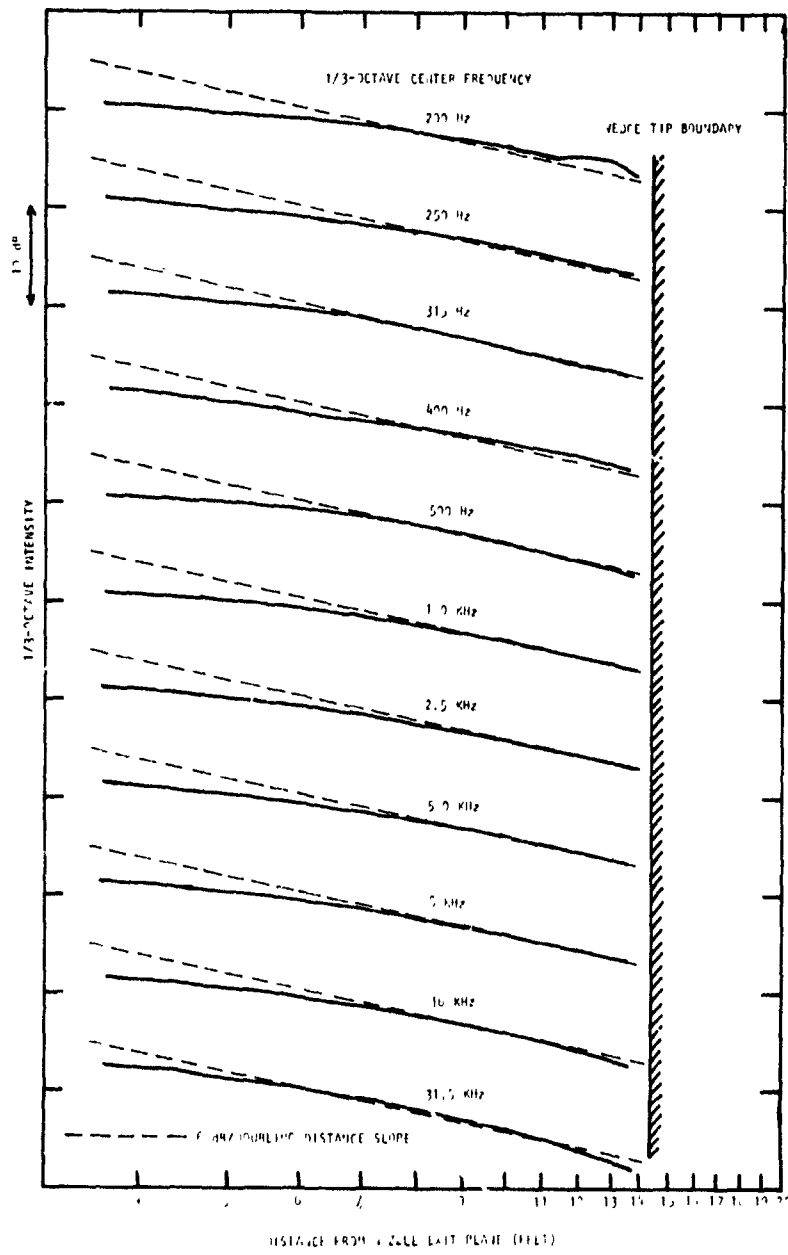


Figure 1-3 Intensity-Distance Plots with Cold Jet: $D = 2$ in.,
 $V_J/a_0 = 0.85$, $\theta = 90^\circ$

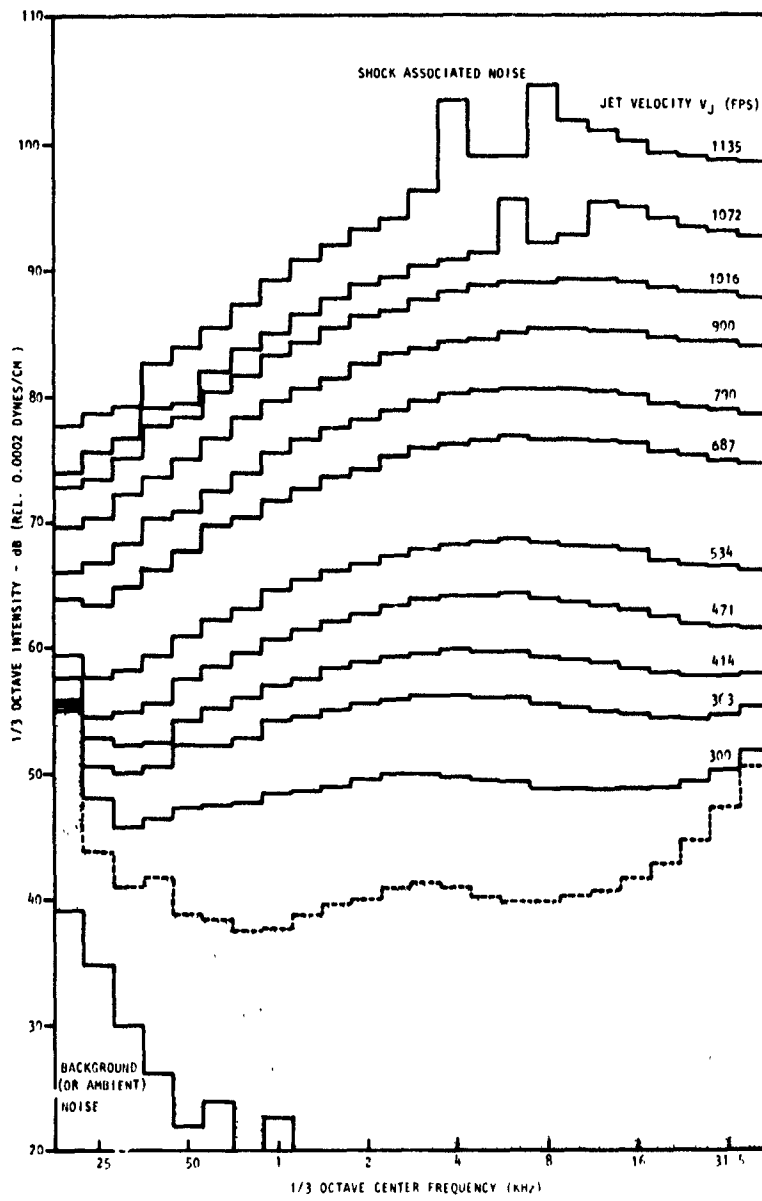


Figure 1.4 Jet Noise Spectra at $\theta = 90^\circ$ for Various Jet Velocities

fps, together with the new background/instrumentation noise spectrum, are presented in Figure 1-5. It can be seen that the instrumentation noise spectrum is much lower in level this time and hence the mixing noise spectrum for $V_J = 300$ fps is no longer contaminated by the instrumentation noise, except at the lower frequency end due to the presence of a.c. line frequency and its harmonics. At this stage, therefore, it appears that the acoustic cleanliness for cold operation of the rig is not affected by internal noise, at least down to 300 fps, where the tests were terminated.

Having established the influence of the measuring instrumentation noise on low velocity jet noise measurements, we could proceed to produce additional evidence for the lack of any significant internal noise levels. Once again, the tests described below were carried out with the basic instrumentation system, consisting of 1/2-in. B&K microphones, a 1/3-octave analyzer and a level recorder, so that the instrumentation noise was kept to a minimum.

In order to establish the magnitude of the internally generated noise at a low value of jet exit velocity ratio ($V_J/a_0 = 0.32$), both cold and hot, a systematic study was carried out and a typical set of results at 45° to the jet axis is presented in Figure 1-6. The background/instrumentation noise is given by spectrum A in this figure. Spectrum B represents the turbulent mixing noise for the 2-in. diameter cold jet at $V_J/a_0 = 0.32$. The internal noise for this jet operation condition was determined by increasing the nozzle diameter to 4 inches and keeping the mass flow through the pipework constant. The jet velocity therefore is reduced by a factor of 4, and from the relationship $I \propto D^2 V_J^8$ for the turbulent mixing noise, it can be calculated that the mixing noise will be 42 dB down in this case, while the internal noise will be essentially unaltered. The resulting spectrum C shown in Figure 1-6, therefore, represents the combined background/instrumentation/internal noise contribution and it will be observed that it is much lower in magnitude than the corresponding mixing noise spectrum B.

Once the internal noise had been estimated for the cold jet, it was necessary to repeat the exercise for the heated case, since the internal noise spectrum then would be different due to presence of combustion noise. The mixing noise from the heated 2 in. diameter jet ($T_J/T_0 = 2.8$, $V_J/a_0 = 0.32$) is given as spectrum D in Figure 1-6. This spectrum exhibits the characteristic increase over the corresponding cold jet spectrum B. In order to confirm that this increase is a genuine effect of heating, and not a direct result of the increase in internal noise, the nozzle diameter was increased to 4 inches as before and the mass flow through the pipework was kept constant. The resulting spectrum E therefore represents the combined background/instrumentation/internal noise contribution for this heated jet, and once again it is much lower in magnitude than the corresponding mixing noise spectrum D. In order to further establish that the result D above was not affected by the type of heating (heating in Figure 1-6 was achieved with the propane burner), the test was repeated with the electric heater with the observed temperature effect above being repeated. This establishes the independence of the result from the heater system.

In conclusion, therefore, it has been established that the internally generated noise, for cold as well as hot operation of the facility, is not significant, at least down to $V_J/a_0 = 0.32$. All data for $V_J/a_0 > 0.32$ obtained from this jet noise rig represent true turbulent mixing noise, unadulterated

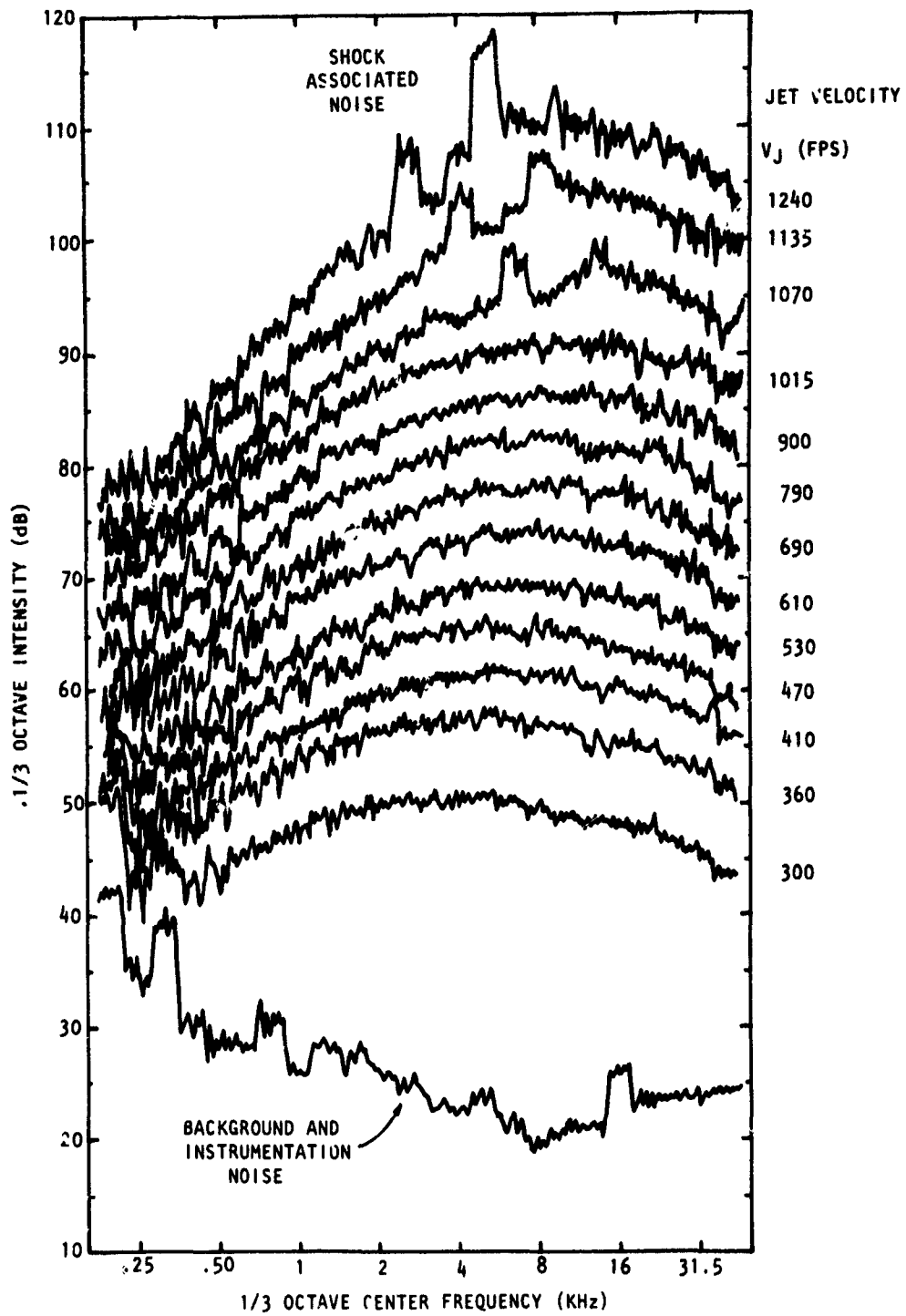


Figure 1.5 Jet Noise Spectra at $\theta = 90^\circ$ for Various Jet Velocities - Cold

	V_J/a_0	T_J/T_0
A BACKGROUND + INSTRUMENTATION NOISE		
B MIXING NOISE, COLD	0.32	1.0
C BACKGROUND + INSTRUMENTATION + INTERNAL NOISE, COLD	0.32 (Effective)	1.0
D MIXING NOISE, HOT	0.32	2.8
E BACKGROUND + INSTRUMENTATION + INTERNAL NOISE, HOT	0.32 (Effective)	2.8

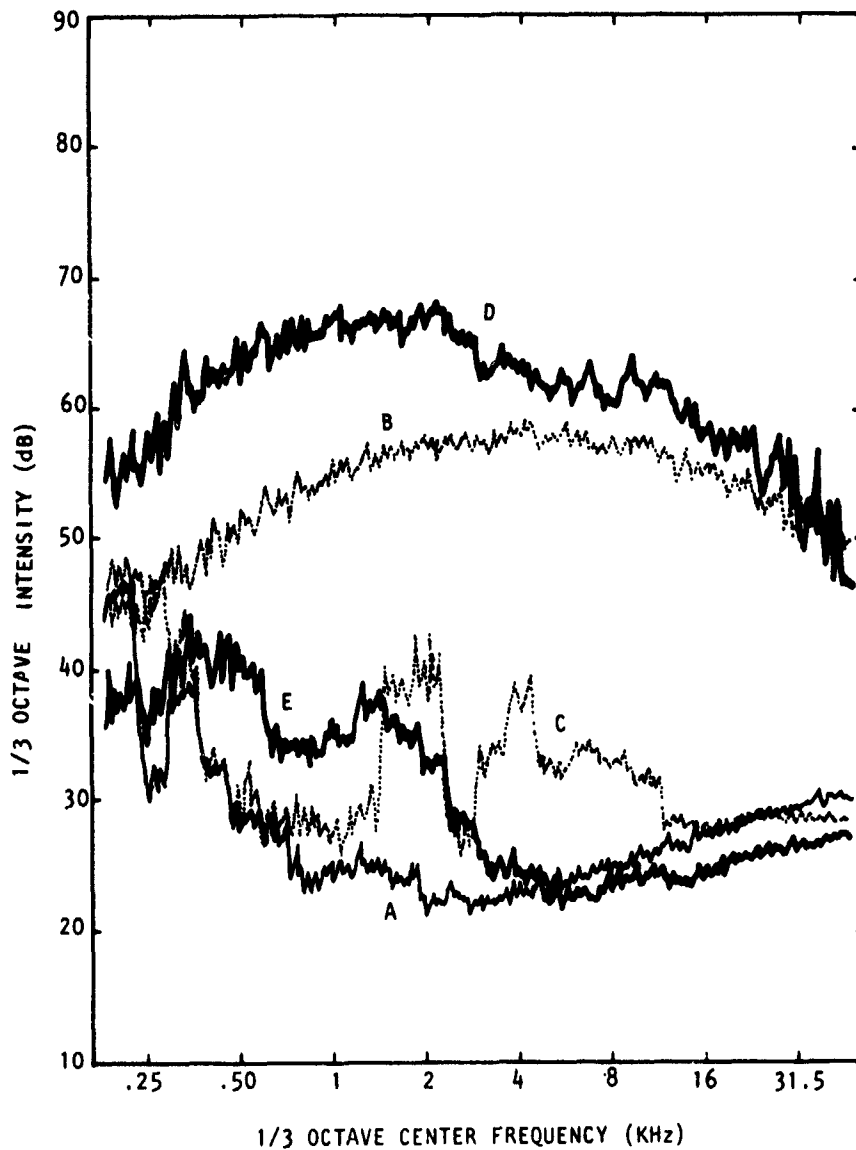


Figure 1-6 Turbulent Mixing Noise and Internal Noise Spectra
at $\theta = 45^\circ$, Cold and Hot

by internal noise. Due to limitations imposed by the background and instrumentation noise, however, the lower limit of V_J/a_0 in the jet noise experimental programs was restricted to 0.35.

DATA ACQUISITION

In the present experimental program, twelve 1/2 in. B&K microphones Type 4133 with FET cathode followers Type 2619 were mounted on the microphone arc at $7\frac{1}{2}^\circ$ intervals from 15° to $97\frac{1}{2}^\circ$. The responses were recorded simultaneously on a 14-channel Honeywell FM tape recorder at 120 inches per second (ips). In order to obtain the 1/3-octave spectrum from 200 Hz to 40 kHz by using a Hewlett-Packard real time 1/3-octave audio spectrum analyzer, the tape speed was reduced to 30 ips on playback. The 1/3-octave levels then were recorded on an incremental tape recorder for subsequent detailed analysis by means of a data reduction program developed for use on the Univac 418 digital computer. This program incorporates the microphone frequency response corrections and atmospheric absorption corrections. The results finally are displayed to include test conditions and computed jet flow parameters, 1/3-octave acoustic spectra, and computed overall sound pressure levels. The day-to-day repeatability of the complete measurement and analysis system is ± 0.5 dB.

APPENDIX II
THE LOCKHEED LASER VELOCIMETER[†]

[†]*This is a summary of material appearing in References 38, 58, 59, and 60
Volume II, Section 5.*

Preceding page blank

At the beginning of this Phase II program, the requirement was established for the development of a Laser Velocimeter (LV) system for the measurement of mean and turbulence velocity characteristics. Specifically, it was required that an LV system be developed for accurate measurements in heated supersonic flows with maximum velocities up to 3000 fps. For mean velocity measurement, radial and axial distributions were required for both the axial and transverse components. For turbulence measurements, in addition to the radial and axial intensity distributions, it was necessary to determine the turbulence spectrum, correlation and convection information.

After extensive research into optical flow measurement systems in the Phase I contract, it was concluded that the burst counter type of laser velocimeter showed the greatest potential as a versatile instrument for turbulence research. Effort was therefore concentrated on developing such an LV. This has resulted in an instrument which is capable of performing most of the measurements at subsonic and supersonic speeds which can now be carried out with the hot-wire anemometer at low subsonic speeds.

The laser shown in the LV Block Diagram, Figure II-1, generates an intense beam of coherent light which is divided into two beams. The two beams are projected to an intersection in the flow where a fringe pattern is formed by the coherent structure of the beams. The fringe pattern consists of many parallel sheets of light separated by 10 to 20 microns. The fringe volume is about 300 microns in diameter and 1 mm long. Particles of 0.5 to 1.0 microns diameter are injected into the flow and are rapidly accelerated to the flow velocity. When these particles pass through the fringe volume, they scatter light at each fringe crossing. The scattered light is focused by the collecting optics onto a photomultiplier tube where the light bursts are converted to electrical signals. Since the spacing of the fringes is accurately known, the frequency of the electrical signal is a linear function of the particle velocity normal to the fringe plane. The processor converts the frequency to digital form and transmits it to a computer where thousands of such measurements may be accumulated and processed. Details of the design and construction of the burst counter LV may be found in Reference 38.

The Lockheed LV, developed as part of this program, is somewhat more sophisticated than the basic system just described. There are three major differences; it measures two orthogonal vectors of velocity, includes a velocity bias to allow reverse flow measurements and includes the time information necessary to determine flow velocity frequency spectrum.

It was necessary in this study to define both the axial and radial components of velocity. In order to accomplish this, two basic systems were designed with their fringe planes superimposed, but orthogonal to each other. This involved the development of unique beam splitter and color separator optics to extract two sets of beams of different color from the multicolor argon laser. The beams, shown in Figure II-1, were oriented at right angles to each other and projected by a lens to the same intersection point in the flow. The light scattered by a passing particle is separated by filters and each color is focused on a separate photomultiplier tube. The PMT signals then constitute separate velocity vector data. The processor is designed for two-channel operation and thereby provides separate digital data for each velocity vector.

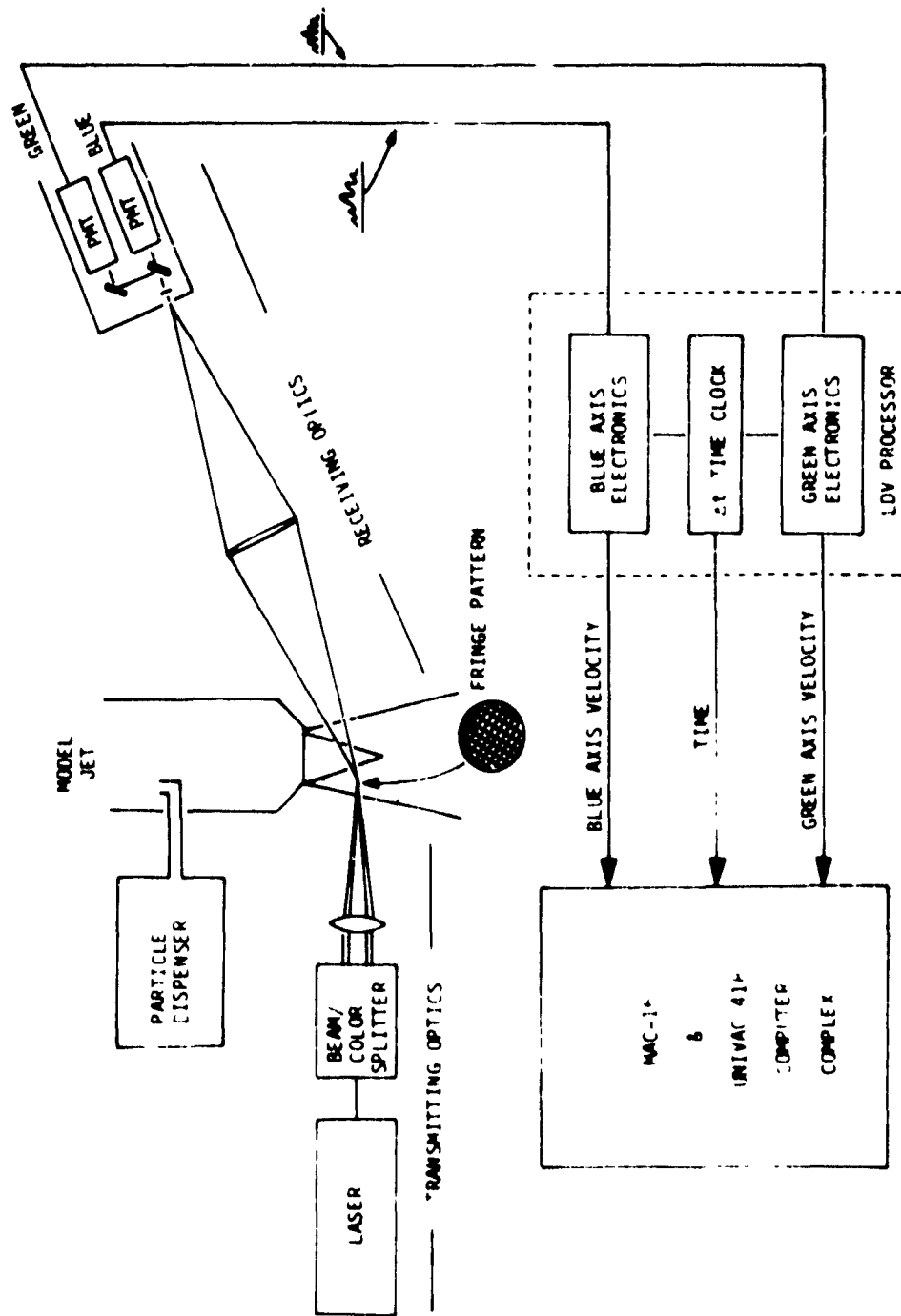


Figure 11.1 Laser System Block Diagram

The second refinement of the Lockheed LV is the addition of a velocity bias to the measurement volume. This was accomplished by introducing an acousto-optic modulation into one of the two laser beams prior to their intersection in the flow. The modulator shifts the light frequency of the beam by an amount determined by the modulation frequency, Figure 11-2. It can be shown that the fringe pattern resulting from this process moves through the fringe volume at a velocity determined by the fringe spacing and the modulation frequency. The result is that particles travelling in both forward and reverse directions with respect to the fringe vector produce unique frequencies thereby allowing subsequent resolution of particle direction.

The data processing techniques necessary to determine the velocity frequency spectrum required the addition of a time interval measurement to the processor electronics. Frequency spectrum is obtained by estimating the velocity auto-correlation function from the random (in time) velocity measurements. Fast Fourier transform software techniques transform the auto-correlation to frequency spectrum. When the two separate channels have the fringes oriented parallel and are located at points separated in space, the cross-correlation information produces cross-spectra and convection speeds. Cross-correlation of the two-channel information at a single point produces a parameter related to Reynolds stress. Thus, in its current configuration, the LV is an extremely versatile instrument.

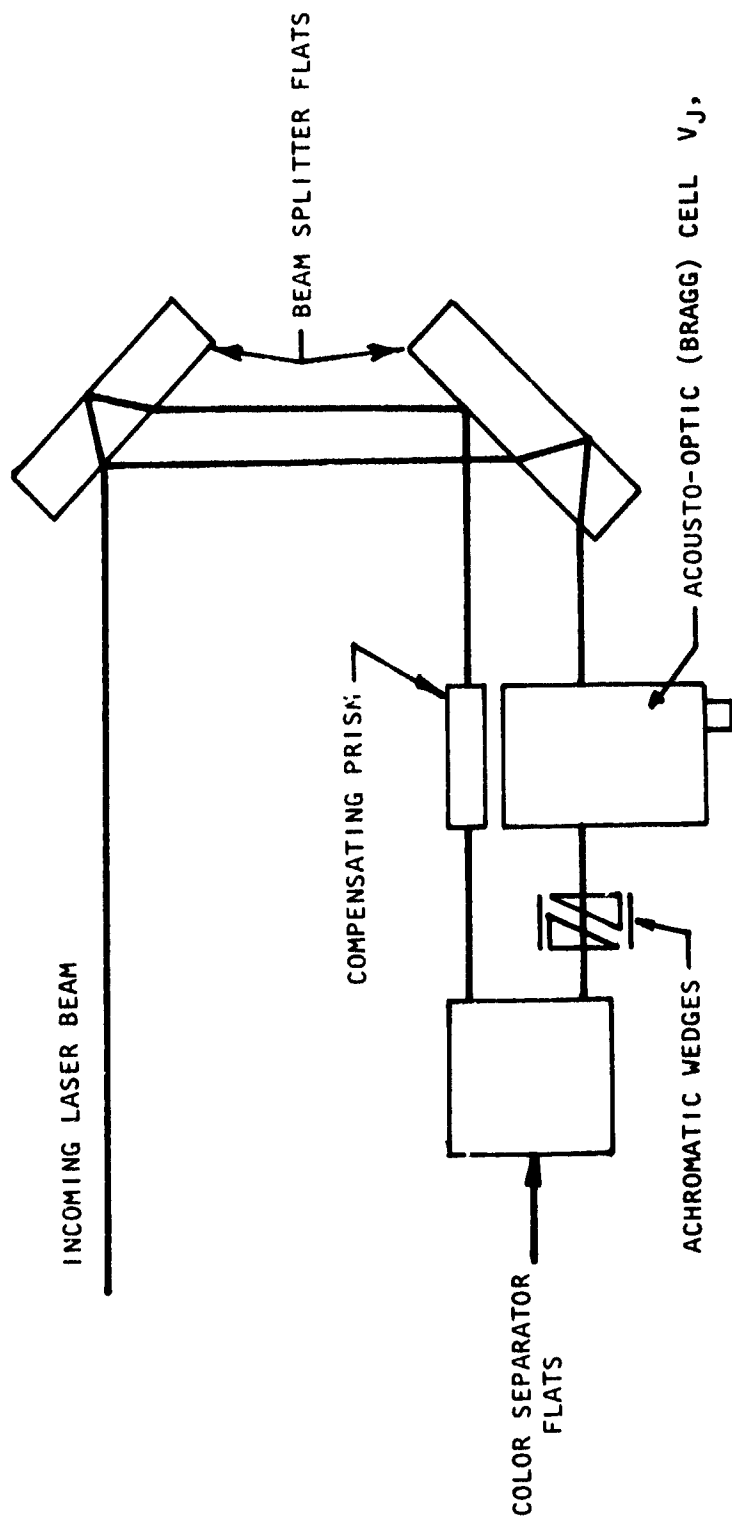


Figure 11.2 Beam Splitter/Color Separator and Acousto-optic Cell Arrangement

APPENDIX III

COMPARISON OF LV AND HOT-WIRE DATA[†]

[†] *This is a summary of work appearing in Reference 61 and Volume II, Section 6.*

Once the LV development was completed, it was necessary to establish the validity of the LV measurements. Since the hot-wire anemometer has been the standard instrument for turbulence measurements it was chosen as the standard for comparison. A test program was carried out to produce a series of LV and hot-wire measurements from the same test rig at the same test conditions. The tests were conducted at low jet velocity (Mach 0.28). Mean and turbulence velocity radial and axial distributions, turbulence spectra, turbulence auto-correlation coefficients, Reynolds stress, and velocity histogram data were obtained. The following brief discussion relates the success of this comparison. A more detailed discussion may be found in Volume II.

Figure III-1 shows the radial distribution of the mean axial velocity obtained with the LV and the hot-wire. The velocity is normalized by the jet efflux velocity, V_j , and the radial distance is normalized by the nozzle radius, r_0 . The agreement between the two sets of results is good. Experience has shown, however, that LV measurements of mean velocity are strongly influenced by the region from which the predominant portion of the seeds reaching the measurement volume originate. Results are presented in Volume II, which illustrate this influence. However, when the jet was seeded evenly from the inside and the outside, data were obtained which compared well with hot-wire results.

The distinctive advantage of the LV in being able to distinguish between forward and reversed flows may be seen in the histograms of Figure III-2. The LV data show that there is a high probability of negative velocities in the mixing region of the jet. However, the hot-wire data do not show this as a result of the inherent rectification of the negative velocity values by the hot-wire.

Figure III-3 shows radial distributions of the axial turbulence intensity. The LV data tend to be higher than those of the hot-wire across the cross-section of the jet. After taking account of the known corrections to both the LV and the hot-wire data, it appears that there is a nearly constant difference of about 2% in turbulence intensity between the two sets of data across the whole jet. The origin of the net discrepancy is still not clear. However, on the evidence of work with hot-wires⁶², it would appear that this may be due to a misinterpretation of hot-wire measurements.

Figure III-4 shows a family of curves of spectra of the axial velocity fluctuations obtained at a number of radial positions using an LV. Similar spectra have been obtained in other studies using hot-wires, and direct comparison between LV and hot-wire spectra obtained under the same jet flow conditions appears in Volume II.

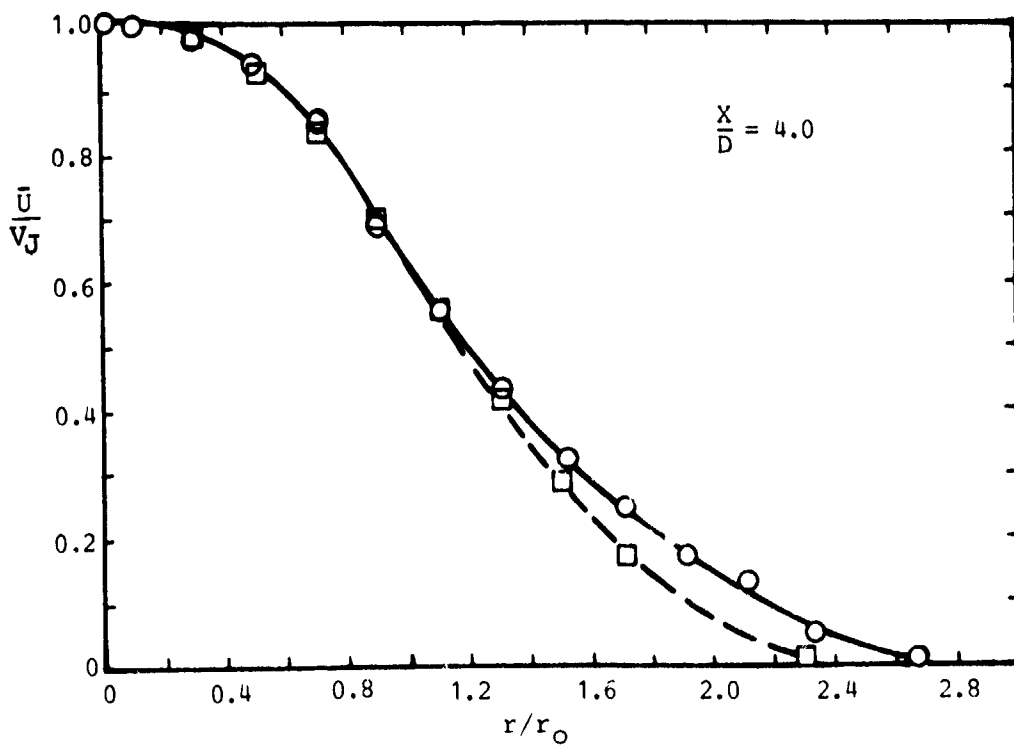
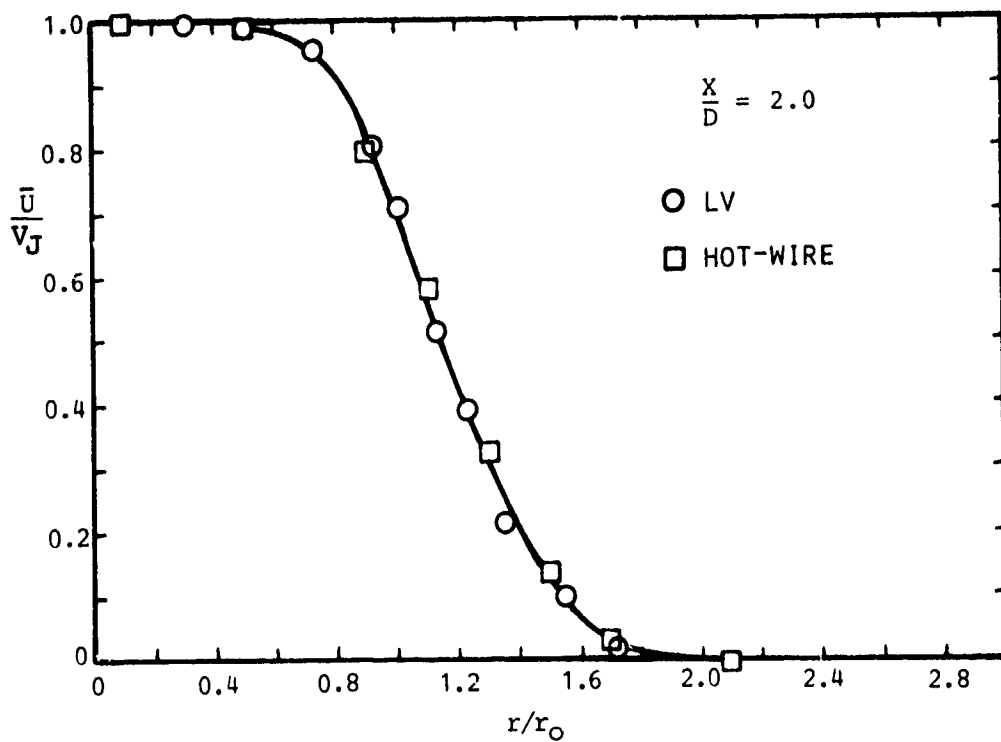


Figure III-1 Comparison Between LV and Hot-Wire Results: \bar{U}/v_J , ($M_J = 0.28$)

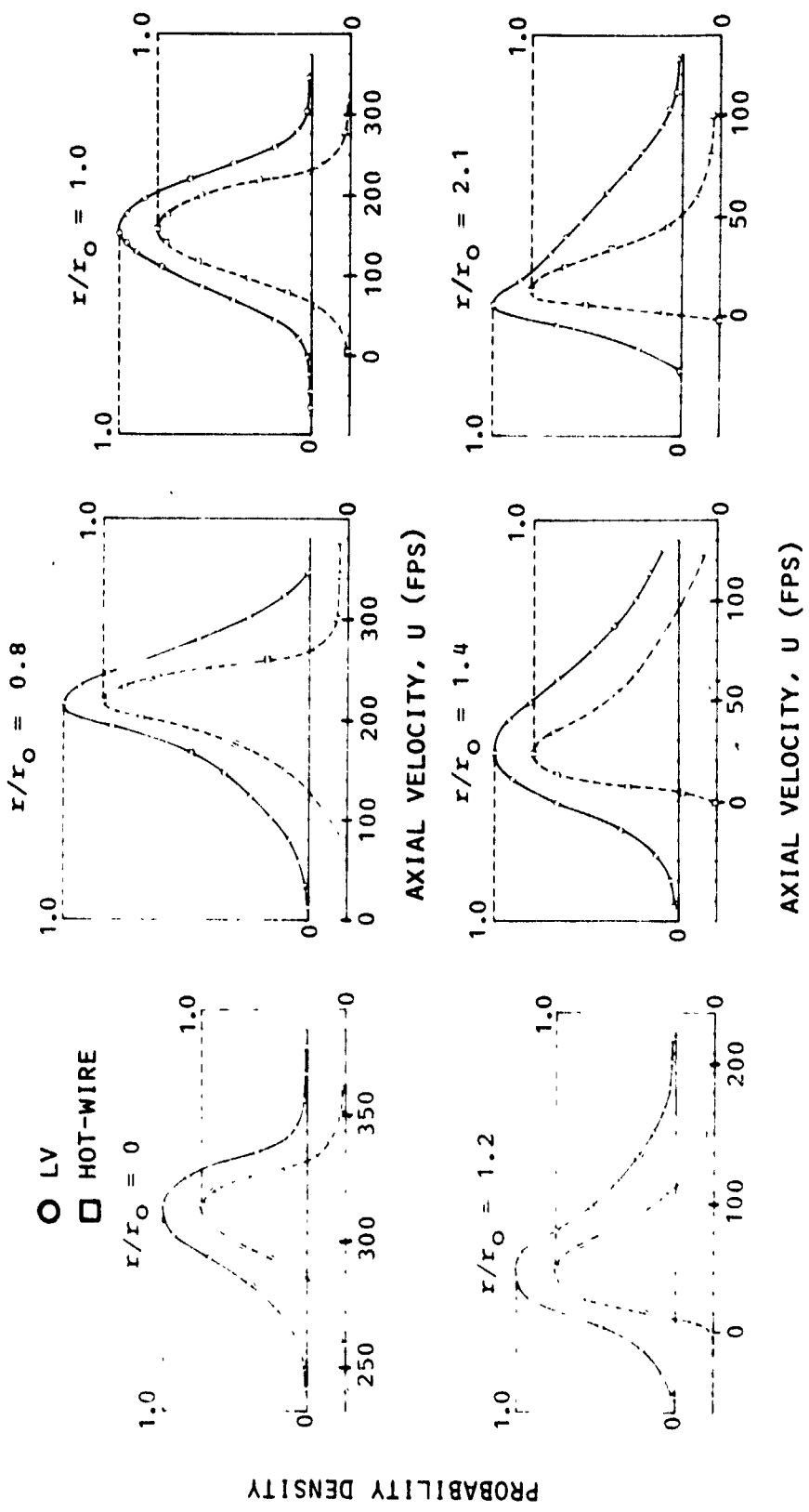


Figure 111-2 Probability Density of Axial Velocity Fluctuations

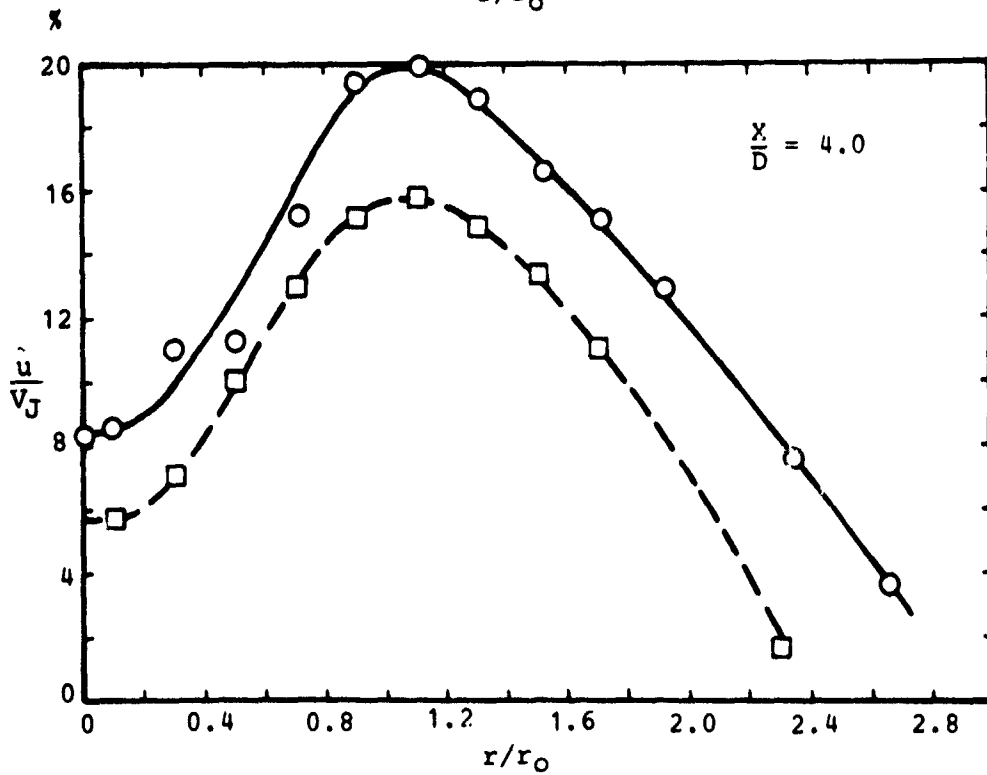
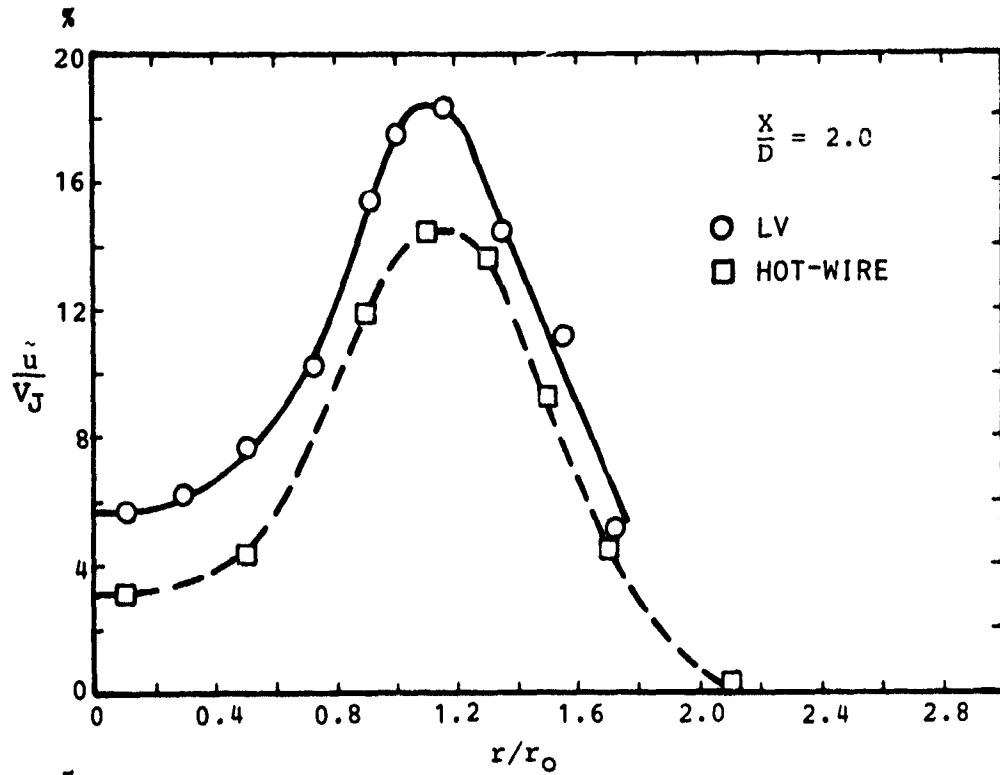


Figure 111-3 Comparison Between LV and Hot-Wire Results: \tilde{u}/V_J , ($M_J = 0.28$)

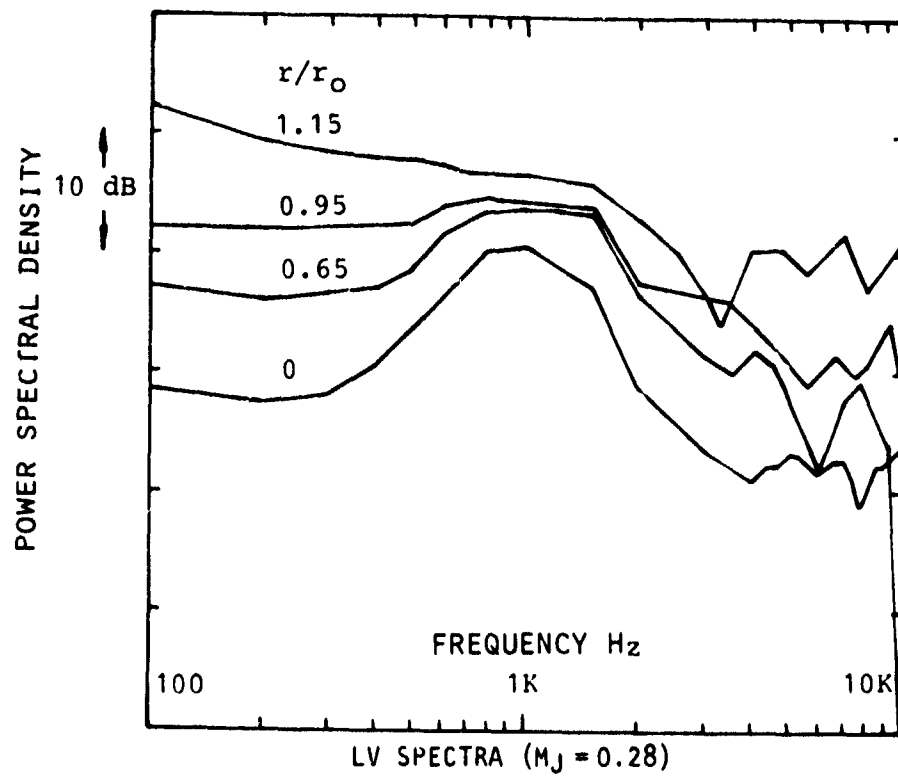


Figure III-4 Spectra at Various Radial Positions ($X/D = 2.0$)

APPENDIX IV

LV-MICROPHONE AND LV-LV CORRELATION

The potential of the LV as a device for locating sources of sound generation and for defining statistical quantities directly related to the noise generation process has long been realized. As a part of this Phase II work, two specific correlation techniques were assessed. These were correlation between one LV channel and a far-field microphone and correlation between two LV channels, located either at a single-point or at separated points.

LV-MICROPHONE CORRELATION

It is shown in Proudman's⁶³ work based on Lighthill's theory that the radiated far-field pressure can be directly related to the component of fluctuating velocity in the turbulent mixing region in the direction of the observer location. Several source location techniques have been discussed in the past based on this method of approach. Basically, the far-field sound pressure is correlated with the oriented velocity fluctuation in the source region.

As part of our instrumentation development program with the LV, the software and hardware were developed to enable this in-jet/far-field correlation to be made. The LV processor electronics were modified as shown in Figure IV-1. An analog-to-digital converter was substituted for the input circuitry of the blue LV channel. The triggering pulse for the A/D sample was obtained from every particle arrival event attempted by the Green LV channel. When the LV data was properly validated, both the digitized word from the acoustic signal and the LV velocity word were transmitted to the computer.

With two very minor exceptions, the software required to reduce the LV-microphone correlation data was identical to that used for all LV experiments. One minor exception was in handling the analog data, since the inversion normally applied to LV measurements to convert from 8-fringe period to velocity was inhibited. The software to perform the correlation was identical to that used to compute power spectra. The data management portion was extended to allow extra data sets to be included at the end of one data set, thus enabling an apparently endless amount of data to be added to the correlation process.

Since the reported correlation measurements between hot-wires and microphones show quite small amplitudes, a system checkout situation was chosen such that one of the jet instability modes was excited. This should give an artificially high correlation. The set-up is illustrated in Figure IV-2. A 1 KHz acoustic signal was present in the jet plenum. This sound radiated to the far-field from the jet exit plane and also triggered one of the jet instability modes. Correlation between the velocity signal and the microphone showed a very high value, with the peak occurring at the time delay expected (being the difference between the propagation time from the exit plane to the observer point and the convection time from the exit plane to the in-jet point.) This example, however, illustrates the major objection to this type of test, whereas the reported correlation between the LV and microphone is high; without a rather complete knowledge of the physics of the situation, there is no way of determining if this correlation is between a source region and a field point or between two points in a propagating wave field. In the example situation, the correlation must be high since the sound field radiating

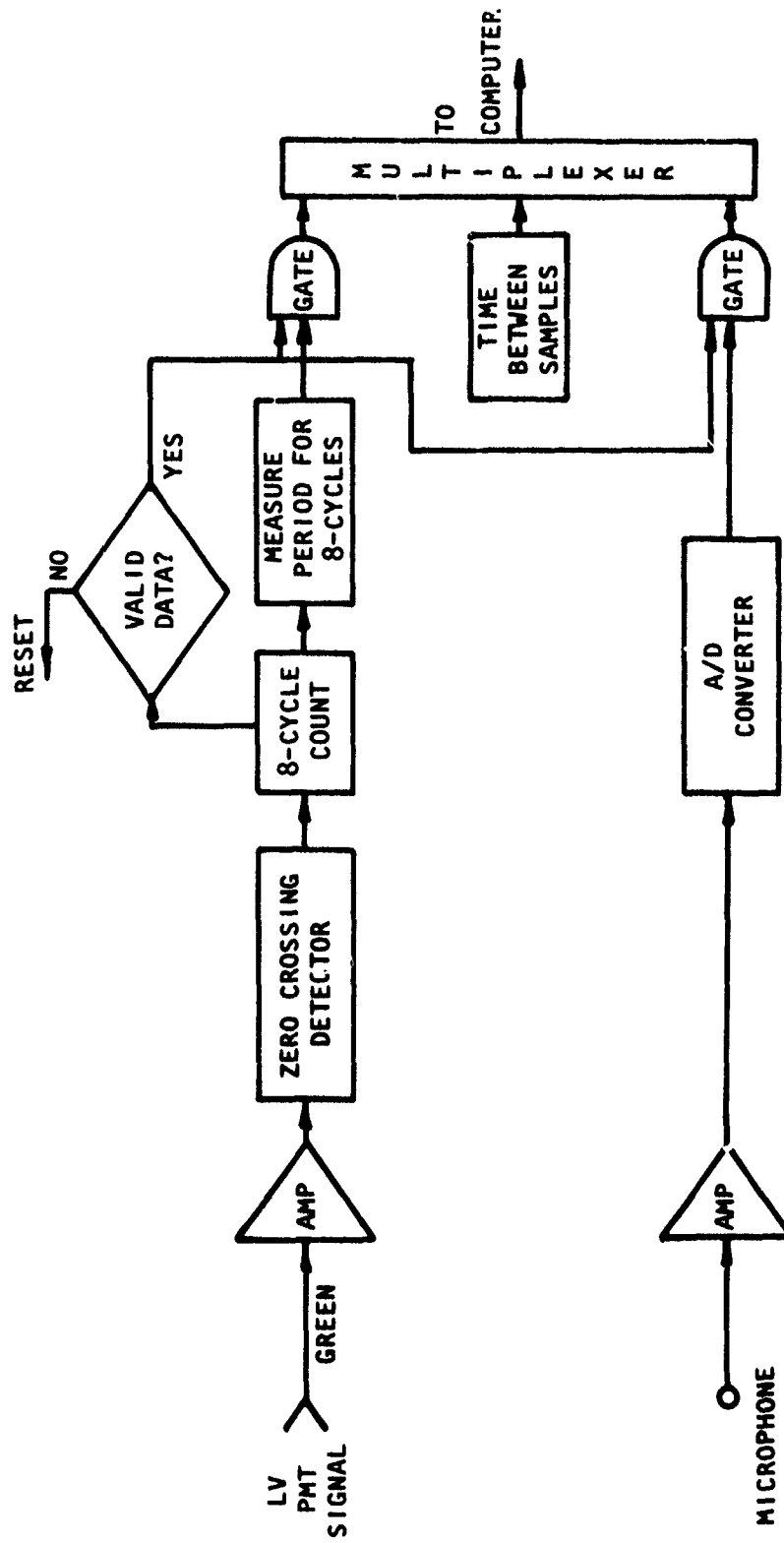


Figure IV-1 Microphone/LV Correlation Block Diagram

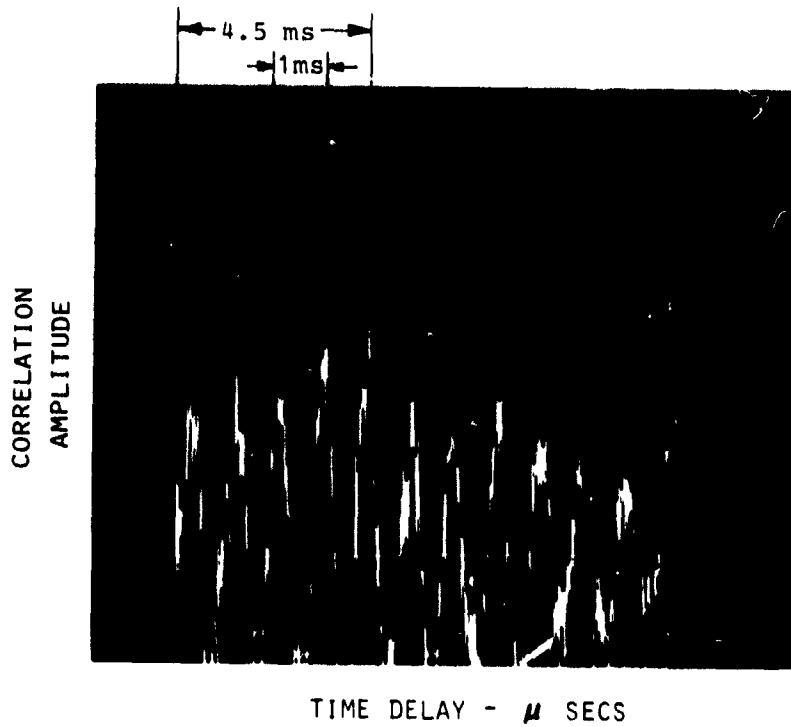
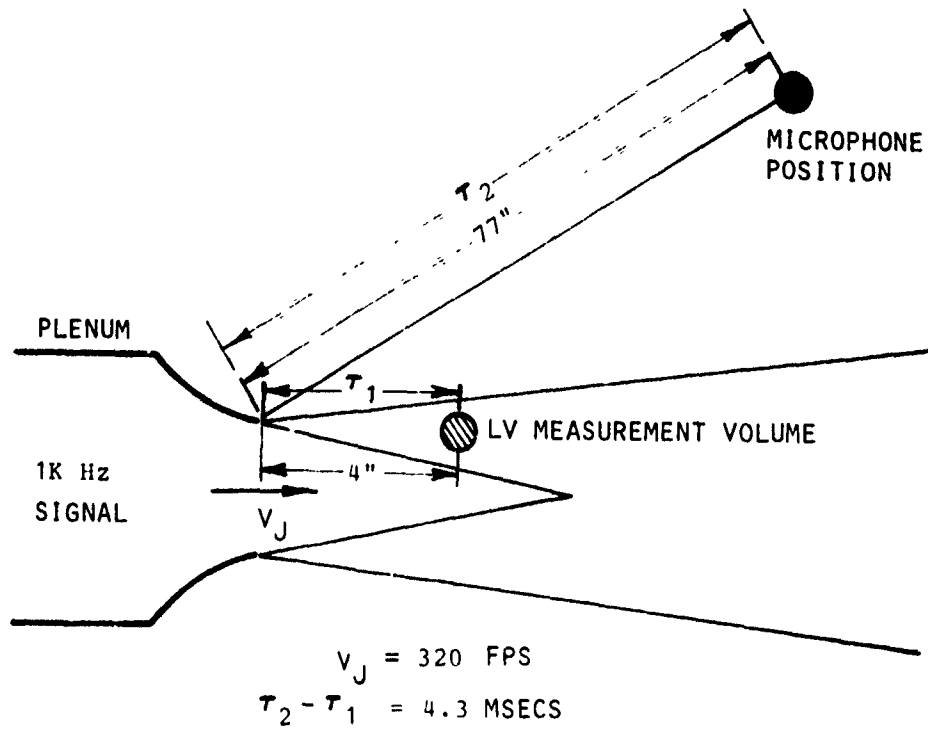


Figure IV-2 LV-Microphone Correlation - Test Description and Example Result

to the far field from the duct also drives the jet velocity field. In most practical situations, it would be difficult to determine which situation occurs.

Thus, the major significance of this particular system checkout experiment is not in the details of the result, but that the correlation could be performed, if a practical application arises in the future. It was demonstrated that the technique was mechanically practical and that the time to acquire the data was not excessive. In this particular test, approximately 100,000 sample pairs were obtained in about 10 seconds. As stated above, this was accomplished by triggering the microphone data acquisition circuit every time LV data was obtained. The cross-correlation function was then obtained directly from these data.

As a result of the difficulties in application as a source location tool, this method was not used further. Instead, it was determined that in-jet cross-correlations provide the most useful information relevant to source definition. The following section outlines our efforts to develop this technique in the Phase II program.

TWO-POINT VELOCITY CROSS-CORRELATION EXPERIMENTS

Single-point measurements in turbulent flows do provide considerable useful information of importance from the aero-acoustic viewpoint. Such data include mean velocity profiles which govern flow acoustic interactions and turbulence intensities which control the absolute source strength. However, the radiation of noise depends on the statistical relationship between fluctuations at separate points in the flow. In order to determine such properties as phase velocities and length scales, it is necessary to generate two-point statistics of the flow field such as spatial correlations and the related cross-spectral density fluctuations. An attempt to measure these functions is detailed below.

A series of measurements of two-point axial cross-correlations of turbulent velocity fluctuations were performed in a jet mounted in a low-speed wind tunnel. This configuration was chosen to minimize the "angular window" required by the laser velocimeter since at the time of the measurements no frequency shifting was available. It was felt that the deviations of instantaneous velocity fluctuations from the axial direction would be less for a jet exhausting into a moving stream rather than exhausting into still air.

An existing backscatter laser velocimeter was modified to perform the single-vector two-point spatial correlations. This optical system was different to the forward-scatter system used in the single-point jet measurements. A second set of beam transmitting and signal collecting optics was fabricated and together with the original optics the system constituted two separate LV systems utilizing the same laser. The existing system was a two-vector, that is, two color system. These colors were separated by a special mirror and each was directed to the separate optical systems. The blue optics were arranged so that they could be rotated and moved vertically with respect to the green optics which were fixed to the laser assembly. A drawing of the system is shown in Figure IV-3. The two blue beams were aligned exactly on

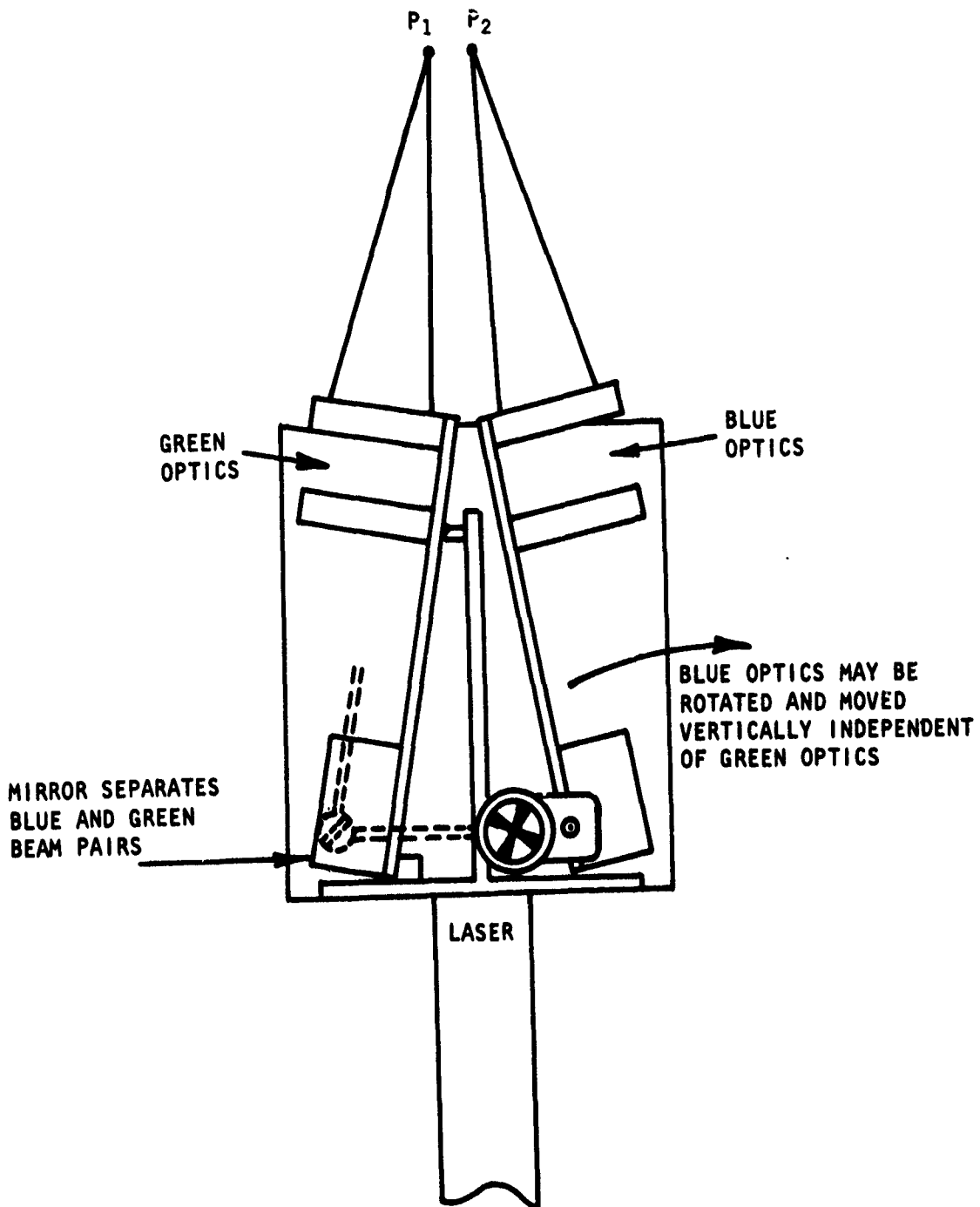


Figure IV-3 Single Vector - Two-Point Optics

the rotational and vertical axes of the optics to prevent the necessity of realignment when the blue measurement point, P_2 , was moved with respect to the green measurement point, P_1 .

A photograph of the wind tunnel working section showing the jet nozzle, the transparent working section wall and the laser velocimeter optics is shown in Figure IV-4. Since, as can be seen in Figure IV-3, neither set of beams entered the tunnel normal to the tunnel wall, or the axis of the jet, the two point cross-correlation contained some components of transverse velocity.

In spite of the deficiency in the system (namely, backscatter optics, no frequency-shifting, non-parallel optical systems and an early error detection circuit design), some correlation was evidenced in the data analysis. Because of the very low data rates and general unsuitability of the system for this kind of experiment, this data was not considered satisfactory for inclusion in the report.* The reason for this unsuitability is discussed below.

Since the light scattered by particles of the order of one micron in the forward direction is at least ten times greater than the intensity of the backscattered light, the signal-to-noise ratio of the backscatter LV is inherently lower than a forward scatter system. As the signal-to-noise ratio increases, so does the probability of double zero-crossing counts. If the PMT signal is attenuated so that only larger particles are counted, this noise problem is reduced but the sampling rate is also reduced. However, in order to obtain good correlation data, a high sample rate is required. These opposing requirements are felt to be the major reason for the unsuccessful experiment. These difficulties are reduced by using a forward-scatter system and improving the counting and error detection circuitry.

A new four-channel laser velocimeter system, designed especially for the measurement of two-point spatial correlations, is under construction and will be operational during 1976. The optics will be an augmentation of the present frame-mounted, two-color system which provides both forward and backscatter capabilities. A second set of two-color optics will be mounted on a separate frame so that the measurement volume can be moved independently of the first set under computer control. A completely new, four-channel set of electronics, which will incorporate frequency shifting on all four channels and the latest

**Coincidence.* In the early LV systems, before Bragg cell frequency shifting was used, the transverse velocity component was measured by using the fringe patterns oriented at 45° to the mean flow direction. This required coincidence between channels for every data point recorded so that the axial and transverse components could be resolved. Since the introduction of frequency shifting, the fringes have been oriented in the direction of the required measurements. Coincidence between channels is, therefore, no longer a requirement unless the experimenter is considering a statistic such as Reynolds stress, instantaneous particle direction or velocity vector magnitude. The new four-channel system will have options which will enable the experimenter to request coincidence at either measurement volume. Since the data correlation is entirely statistical, it is neither necessary nor desirable to require coincidence between one measurement volume and the other.

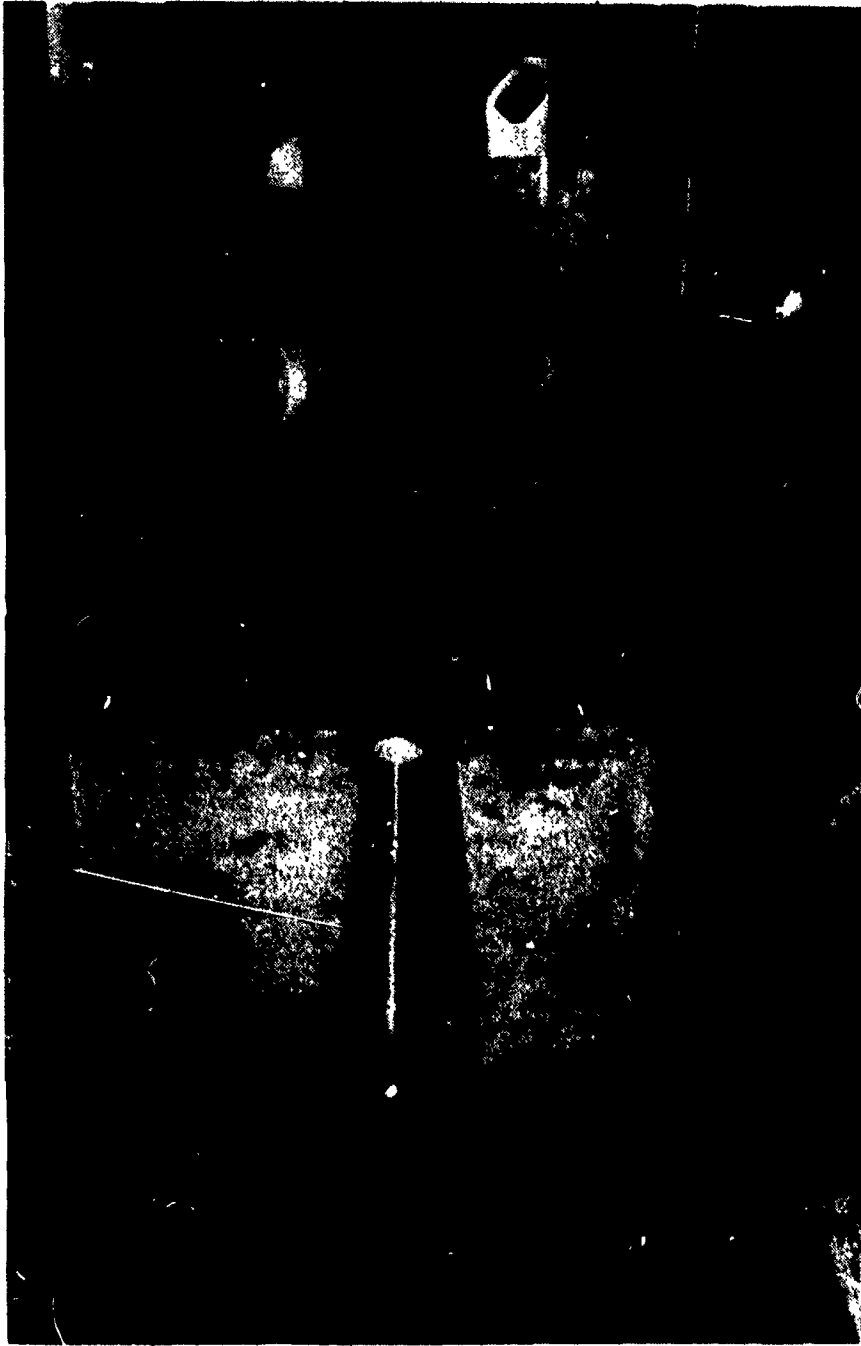


Figure IV-4 LV-LV Correlation Test Setup in Wind Tunnel

advances in data validation circuits, is also being made. The computer interface has also been redesigned to allow up to four simultaneous particle velocity measurements to be transferred to the computer. A block diagram of the new four-channel system is shown in Figure IV-5.

The data reduction software will be augmented to allow a large range of different studies to be performed using the data from the new electronics. It is anticipated that with the improved signal quality and data rate expected and computerized measurement volume positioning the generation of spatial correlation functions and their associated wave number spectra will become a practical reality for the first time.

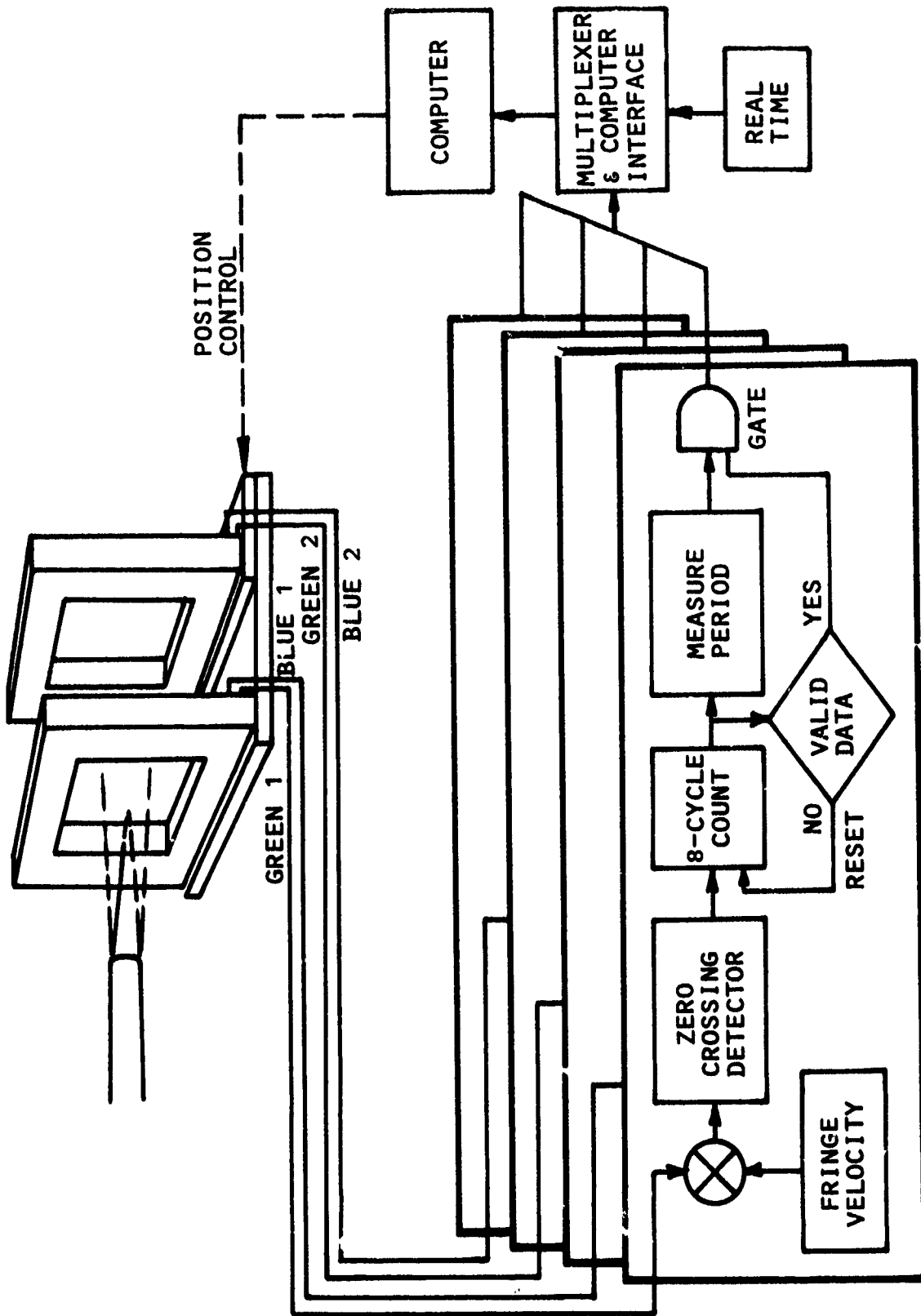


Figure IV-5 Block Diagram of Four-Channel LV System

REFERENCES

1. Lighthill, M. J.: On Sound Generated Aerodynamically. I. General Theory. *Proc. Roy. Soc. (London)*, Vol. A211, 1952, pp. 564-587.
2. Lighthill, M. J.: On Sound Generated Aerodynamically. II. Turbulence as a Source of Sound. *Proc. Roy. Soc. (London)*, Vol. A222, 1954, pp. 1-32.
3. Ribner, H. S.: A Theory of the Sound from Jets and Other Flows in Terms of Simple Sources. UTIAS Report No. 67, AFOSR TN 60-950, July 1960
4. Ffowcs Williams, J. E.: Noise from Turbulence Convected at High Speed. *Phil. Trans. Roy. Soc.*, Vol. A255, 1963, pp. 469-503.
5. Lush, P. A.: Measurements of Subsonic Jet Noise and Comparison with Theory. *J. Fluid Mech.*, Vol. 46, pp. 477-500, 1971.
6. Bushell, K. W.: A Survey of Low Velocity and Coaxial Jet Noise with Application to Prediction. *J. Sound Vib.*, Vol. 17, No. 2, pp. 271-1971.
7. Lilley, G. M.: On the Noise from Airjets. ARC Report 20, 1958, p. 376.
8. Ribner, H. S.: The Generation of Sound by Turbulent Jets. *Adv. in Applied Mech.*, Vol. 8, pp. 103-182, 1964.
9. Doak, P. E.: Progress Toward a Unified Theory of Jet Engine Noise, Vol. III. The Generation and Radiation of Supersonic Jet Noise. AFAPL-TR-72-53, July 1972.
10. Lighthill, M. J.: The Bakerian Lecture, Sound Generated Aerodynamically. *Proc. Roy. Soc.*, Vol. A267, 1962, pp. 147-182.
11. Ffowcs Williams, J. E.: Some Thoughts on the Effect of Aircraft Motion and Eddy Convection on the Noise from Air Jets. Univ. of Southampton, Aero. Astr. Report No. 155, 1960.
12. Ribner, H. S.: On the Strength Distribution of Noise Sources Along a Jet. UTIA Report No. 51, 1958.
13. Ribner, H. S.: Aerodynamic Sound from Fluid Dilatations - A Theory of Sound from Jets and Other Flows. Univ. of Toronto, UTIA Report 86, 1962.
14. Ribner, H. S.: Quadrupole Correlations Governing the Patterns of Jet Noise. *J. Fluid Mech.*, Vol. 38, Pt. 1, 1969.
15. Atvars, J.; Schubert, L. K.; Grande, E.; and Ribner, H. S.: Refraction of Sound by Jet Flow or Jet Temperature. Univ. of Toronto, Institute for Aerospace Studies, TN 109, NASA CR-494, 1966.
16. Grande, E.: Refraction of Sound by Jet Flow and Jet Temperature, II. Univ. of Toronto, Institute for Aerospace Studies; TN 110, 1966; NASA CR-840, 1967.

17. Schubert, L. K.: Numerical Study of Sound Refraction by a Jet Flow. Vol. I, Ray Acoustics. *J. Acous. Soc. Amer.*, Vol. 51, Pt. 1, 1972.
18. Schubert, L. K.: Numerical Study of Sound Refraction by a Jet Flow, Vol. II, Wave Acoustics. *J. Acous. Soc. Am.*, Vol. 51, Pt. 1, 1972.
19. MacGregor, G. R.; Ribner, H. S.; and Lam, H.: Basic Jet Noise Patterns After convection and Refraction Effects. Experiment vs. Theory. Presented at the 83rd Meeting of the Acoust. Soc. Amer., Buffalo, April 1972.
20. Bschorr, O.: Analyses of Jet and Boundary Layer Noise. Proceedings of 6th International Council of the Aeronautical Sciences, 1968.
21. Meecham, W. C.: A Fluid Mechanics View of Aerodynamic Sound Theory. Proceedings of British Acoustical Society/Royal Aeronautical Society Symposium on Aerodynamic Noise, Loughborough, September 1970.
22. Crow, S. C.: Aerodynamic Sound Emission as a Singular Perturbation Problem. *Stud. in Appl. Maths.* XLIX, 1970.
23. Phillips, O. M.: On the Generation of Sound by Supersonic Shear Layers. *J. Fluid Mech.*, Vol. 9, 1960.
24. Pridmore-Brown, D. C.: Sound Propagation in a Fluid Flowing through an Attenuating Duct. *J. Fluid. Mech.*, Vol. 4, p. 393, 1958.
25. Mungur, P.; and Gladwell, G. M. L.: Acoustic Wave Propagation in a Sheared Fluid Contained in a Duct. *J. Sound Vib.*, Vol. 9, pp. 28-48, 1969.
26. Mungur, P.; and Plumblee, H. E.: Propagation and Attenuation of Sound in a Soft-Walled Annular Duct Containing a Sheared Flow. *Basic Aerodynamic Noise Research*, pp. 305-327, 1969.
27. Plumblee, H. E.; Dean, P. D.; Wynne, G. A.; and Burrin, R. H.: Sound Propagation in and Radiation from Acoustically Lined Flow Ducts: A Comparison of Experiment and Theory. NASA CR-2306, October 1973.
28. Lilley, G. M. et al: Theory of Turbulence Generated Jet Noise, Noise Radiation from Upstream Sources, and Combustion Noise. Vol. IV, Generation and Radiation of Supersonic Jet Noise. AFAPL-TR-72-53, July 1972.
29. Doak, P. E.: Acoustic Radiation from a Turbulent Fluid Containing Foreign Bodies. Proceedings of the Royal Society (London), Vol. A254, pp. 129-145, 1960.
30. Doak, P. E.: Vorticity Generated by Sound. Proceedings of the Royal Society, Vol. A226, pp. 7-16, 1954.
31. Doak, P. E.: Analysis of Internally Generated Sound in Continuous Materials: (1) Inhomogeneous Acoustic Wave Equations. Vol. 2, p. 53, 1965.

32. Doak, P. E.: On the Identification of Acoustic, Turbulent, and Thermal Components of Fluctuating Motion in Fluid Flows. Lockheed-Georgia Company Aerospace Sciences Laboratory Research Memorandum ER-10464, February 1970.
33. Doak, P. E.: On the Interdependence Between Acoustic and Turbulent Fluctuating Motions in a Moving Fluid, *J. Sound Vib.*, Vol. 19, pp. 211-225, 1971.
34. Tack, D. H.; and Lambert, R. F.: Influence of Shear Flow on Sound Attenuation in Lined Ducts. *J. Acous. Soc. Am.*, Vol. 38, p. 655, 1965.
35. Chu, B. T.; and Kovaszny, L. S. G.: Nonlinear Interactions in a Viscous Heat-Conducting Compressible Gas. *J. Fluid Mech.*, Vol. 3, p. 454, 1958.
36. Morfey, C. L.: Theory of Sound Generation in Ducted Compressible Flows with Applications to Turbomachinery. Ph.D. Thesis, Univ. of Southampton, 1970.
37. Doak, P. E.: The Momentum Potential Field Description of Fluctuating Fluid Motion as a Basis for a Unified Theory of Internally Generated Sound. AIAA 1st Aero-Acoustics Conference, AIAA Paper 73-1000, October 1973.
38. Plumblee, H. E. Jr.(Ed.): A Progress Report on Studies of Jet Noise Generation and Radiation, Turbulence Structure, and Laser Velocimetry, AFAPL TR 74-24, June 1974.
39. Tanna, H. K.; Dean, P. D.; and Fisher, M. J.: The Influence of Temperature on Shock-Free Supersonic Jet Noise. *J. Sound Vib.*, Vol. 39, No. 4, 1975, pp. 429-460.
40. Tanna, H. K.; and Dean, P. D.: An Experimental Study of Shock-Free Supersonic Jet Noise. AIAA Paper No. 75-480, 1975.
41. Harper-Bourne, M.; and Fisher, M. J.: The Noise from Shock Waves in Supersonic Jets. Proceedings of the AGARD Conference on Noise Mechanisms; Brussels, Belgium; September 1973.
42. Cary, B. B. Jr.: An Optical Study of Two-Dimensional Jet Mixing. Ph.D. Thesis, Univ. of Maryland, 1954.
43. Knott, P. R. et al: Supersonic Jet Exhaust Noise Investigations. AFAPL TR- (to be assigned), 1976.
44. Witze, P. O.: Centerline Velocity Decay of Compressible Free Jets. *AIAA Journal*, Vol. 12, 1974, pp. 417-418.
45. Görtler, H.: Berechnung von Aufgaben der Freien Turbulenz auf Grund eines Neuen Näherungsanstazes. *ZAMM*, Vol. 22, pt. 5, 1942, p. 244.
46. Lilley, G. M.; Morris, P. J.; Tester, B. J.: On the Theory of Jet Noise and Its Application. AIAA Paper No. 73-987, 1973.

47. Tester, B. J.; Burrin, R. H.: On Sound Radiation from Sources in Parallel Sheared Jet Flows. AIAA Paper No. 74-57, 1974.
48. Tester, B. J.; and Morfey, C. L.: Developments in Jet Noise Modeling - Theoretical Predictions and Comparisons with Measured Data. AIAA Paper No. 75-477, 1975.
49. Fisher, M. J.; and Szewczyk, V. M.: Flow Acoustic Interaction Effects in Jet Noise. ARC Paper No. 35 212 N897, 1974.
50. Ribner, H. S.: Personal communication to B. J. Tester.
51. Morfey, C. L.: Amplification of Aerodynamic Noise by Convected Flow Inhomogeneities. *J. Sound Vib.*, Vol. 31, 1973, pp. 391-397.
52. Sharma, R.: The Structure of Turbulent Shear Flow. Ph.D. Thesis. Univ. of Southampton, 1968.
53. Morris, P. J.: The Structure of Turbulent Shear Flow. Ph.D. Thesis, Univ. of Southampton, 1971.
54. Morris, P. J.: A Model for the Structure of Jet Turbulence as a Source of Noise. AIAA Paper No. 74-1, 1974.
55. Kapur, S. S.; and Morris, P. J.: A Model for the Orderly Structure of Turbulence in a Two-Dimensional Shear Layer. Appendix 1-6, AFAPL TR 74-24, June 1974.
56. Powell, A.: On the Mechanism of Choked Jet Noise. *Proc. Phys. Soc. B.*, Vol. 66, 1953, pp. 1039-1056.
57. Burrin, R. H.; Dean, P. D.; and Tanna, H. K.: A New Anechoic Facility for Supersonic Hot Jet Noise Research at Lockheed-Georgia. In The Generation and Radiation of Supersonic Jet Noise. U. S. Air Force Aero Propulsion Laboratory Technical Report, AFAPL TR 74-24, 1974.
58. Whiffen, M. C.; and Meadows, D. M.: Two Axis, Single Particle Laser Velocimeter System for Turbulence Spectral Analysis. Proceedings of the Second International Workshop on Laser Velocimetry, Vol. 1, March 1974, pp. 1-12.
59. Smith, D. M.; and Meadows, D. M.: Power Spectra from Random-Time Samples for Turbulence Measurements with a Laser Velocimeter. Proceedings of the Second International Workshop on Laser Velocimetry, Vol. 1, March 1974, pp. 27-44.
60. Whiffen, M. C.: Polar Response of an LV Measurement Volume. Proceedings of the Minnesota Symposium on Laser Anemometry, October 1975, pp. 589-590.
61. Lau, J. C.; Morris, P. J.; and Fisher, M. J.: Turbulence Measurements in Subsonic and Supersonic Jets Using a Laser Velocimeter. AIAA paper No. 76-348, July 1976.

62. Proudman, I.: The Generation of Noise by Isotropic Turbulence. *Proc. Roy. Soc.*, Vol. A214, 1952.
63. Perry, A. E.; and Morrison, G. L.: Static and Dynamic Calibration of Constant-Temperature Hot-Wire Systems. *J. Fluid Mech.*, Vol. 47, 1971, pp. 765-777.